

Università di Pisa

Facoltà di Ingegneria

Dipartimento di Ingegneria Meccanica, Nucleare e della Produzione

**Dottorato di Ricerca in
Sicurezza Nucleare e Industriale**

A Multiple Cell Proportional Counter for
Continuous Airborne Radon Assessment

Ph.D. THESIS

in

Nuclear and Industrial Safety



Candidate :

Supervisor :

Dahmane MAZED

Prof. Giorgio Curzio

Inizio Tesi : **2003**



To my wife Nacéra and our children : Cyria, Daniel and Maria-Luisa,
who shared with me hard sacrifices during the performing of this work

To my father and mother who permitted
me to get instructed

To all of our mindful Italian friends met here, during our stay
in Pisa,
Italy.



ACKNOWLEDGEMENTS



I would like to acknowledge the thoughtful, constant and patient help provided by my supervisor Prof. Giorgio Curzio since hosting me at the Nuclear Instrumentation and Measurements Laboratory of DIMNP/University of Pisa, within the framework of the present Ph.D. thesis research.

I would like to express also my grateful thanks to Prof. Marino Mazzini, president of the Nuclear and Industrial Safety doctorate council and also my thesis director for putting upon me his confidence and for all his valuable guidance remarks, assigned to me during the execution of herein reported research work.

Finally, would all of the staff of the LSMN/DIMNP laboratory find here my sincerely thanks for their kind and grateful help, permitting me to perform this work in perfect conditions. I would like to cite namely: Prof. Francesco d'Errico, Dr. Riccardo Ciolini, Dr. Valerio Giusti and Sig. Aldo Del Gratta, who made my joyful stay among them really unforgettable.



Abstract :

A new proportional counter type, baptized Multiple Cell Proportional Counter (MCPC), intended for continuous airborne radon activity measurements is described and its operation principle presented. This gas-flow proportional counter, consisting in a pile-up of 20 separate proportional counters elements, uses an argon-propane (1%) as a binary gas mixture to which is admixed an appropriate fraction of ambient air, in which radon activity concentration has to be continuously measured through a periodic counting of the α particles emitted by ^{222}Rn and its short-lived decay products within the sensitive volume. A Monte Carlo simulation code, RADON-MCPC, which takes into account the major physical processes that determine directly the detector performances, has been written and used for design optimization purposes. According to preliminary design calculations the MCPC model, should achieve a radon counting efficiency greater than 100 %. The simulation results show that the admixture of 10 % of ambient air seems to be sufficient to continuously assess radon concentration levels ranging from about 15 Bq/m^3 up to $1.5 \cdot 10^5 \text{ kBq/m}^3$ for an integral counting period of 10 minutes, when setting the energy discrimination at 250 keV. The expected radon sensitivity is about $11 \text{ cpm} / 100 \text{ Bq}\cdot\text{m}^{-3}$, achieving thus a measurement accuracy of $\pm 10 \text{ Bq/m}^3$ at a mean radon concentration level of 100 Bq/m^3 with a detector time response of 10 min. The preliminary experimental α spectra registered show a great agreement with those obtained through the simulation code.



INTRODUCTION

It is well known that the earth's crust contains radionuclides which constitute the major source of naturally occurring radioactive material (NORM) in the environment. Most of these radionuclides are members of the radioactive decay chains beginning with ^{238}U , ^{235}U and ^{232}Th . There are also many human activities that lead to the production of NORM. These include activities which can enhance NORM levels directly. The technologically enhanced NORM (TENORM) radioactivity arises in many industrial areas, such as the mining, milling and processing of uranium containing ores and also mineral sands.

Since radon (^{222}Rn) and its progenies have come to be recognized as the largest source of radiation dose received by the general public, a great deal of interest is devoted to the assessment of the radon activity concentration in air, water and soils.

Indeed, radon is a radioactive noble gas, produced in the decay chain of the primordial elements uranium which are found in different concentrations in the soil worldwide. For example, as a mean value one metric ton of the earth's crust contains about 3 g of uranium (and 9 g of thorium). Radon presents thus very particular properties: being a radioactive noble gas, it diffuses easily out of soils or building materials, spreading out in the environment. Consequently, different concentrations of radon and its progenies can be found everywhere around us. For this reason radon is really an inescapable radiation exposure source both at home and at work. Since it

is an inert gas, ^{222}Rn does not react chemically with other atoms or molecules, making its chemical separation impossible and its physical trapping often difficult.

Since its short-lived alpha emitting decay products, ^{218}Po and ^{214}Po , can have a so pronounced adverse effect on lung tissues, leading to lung cancer in many cases as reported recently in numerous biological and epidemiological studies, it was shown that approximately 12 % of annual lung cancers reported worldwide can be linked to radon gas exposure from the environment [1,2]. For this reason it has been recognized by various international health organizations as a major lung carcinogen [3-9].

Concerning the regulatory requirements and normative policies in radiation protection, the U. S. Environment Protection Agency (EPA) has defined the so-called action level guideline to be 148 Bq/m^3 (4 pCi/liter) [10]. For the European Union, there seems exist urgent requirements to challenge and very abroad deadlines are scheduled by the entering in vigour of the European Community recommendations [11-13]. What concerns specifically the Italian policies, it has been reported [14] that one of the most important objectives of the 1989 italian survey was to promote ad hoc policies to reduce radon exposure of the population, and the annual mean value that was recorded that time (1989) was 81.5 Bq/m^3 , which was found somewhat higher than the reported for other industrialised countries. Thus, concerning such requirements, it is stated [15] that the required operative levels, on which the so-called action levels are defined consist in the annual average levels. But, taking into account the fact of the extreme variability of radon concentration in air, along days and seasons, the relevant need recommends long-termed measurements (3 to 6 months or even more) of average radon concentration levels or otherwise, by continuous radon monitoring along the whole effective period. We shall emphasis however, that if the required kind of measurements have though many advantages (more likely to indicate accurate average radiation level and exposure), they are in contrary too penalized by many other practical limitations : the results are delayed by up to 1 year and cannot inform us adequately about the time variation of the radon concentration.

Although there is too many radon monitor devices commonly available in the market, there remains however a huge matter of further development that has to be carried out in order to challenge these newly defined regulatory requirements and also to improve the general skills and performances of those existing devices, letting

them to operate within special conditions and to fulfil more and more constraining requirements.

Within this scope, the main purpose aimed through this PhD research work consists in the elaboration of extended studies which would bring in a profound insight into the monitoring, the analyses and the assessment of some NORM type radiations, especially, those arising from radon and its progenies. The main objective precisely relays in the contribution to the development of a new active method which enables the assessment of sudden variations of airborne radon activity concentration. This also includes, the examination of the possibility to monitor those common low-level activities of alpha emitters that would be present in the air as a result of the presence of TENORM in consummation products or in the rejected waste residues, produced or enhanced through various industrial processes, within diverse practical situations commonly encountered in several production and industrial technology fields.

In the presented work, a new proportional counter model, called Multiple Cell Proportional Counter (MCPC), involved in a newly proposed active method for continuous airborne radon activity concentration measurements is described and its operation principle presented. This gas-flow proportional counter, consisting in a pile-up of 20 separate proportional counters elements, uses an argon-propane (1%) as a binary gas mixture to which is admixed an appropriate fraction of ambient air, in which radon activity concentration has to be continuously measured through a periodic counting of the α particles emitted by ^{222}Rn and its short-lived decay products produced within its well defined sensitive volume. By adopting this multiple cell pile-up design, it is thus likely possible to compensate for the electron attachment effect loss, inherent to the presence of oxygen contained in the air sample, balancing the losses by integrating in the counting the alpha particles emitted back into the effective sensitive volume of the MCPC by radon isotopes and its progenies located within the discarded end cell volumes. A Monte Carlo simulation program, called RADON-MCPC, which takes into account the major physical processes involved and that determine directly the detector performances, has been written and used for design optimization purposes. It is the aim of the simulation to calculate the pulse height spectra of radon and its decay products for the MCPC configuration and related operation conditions. The radon sensitivity, the alpha counting efficiency as well as the suitable pulse height discriminator threshold as a function of the air

sample fraction in the gas mixture flowing through the MCPC and the set high voltage value are therefore determined. Qualitative and quantitative analyses of the wall effect, the grid opacity effect, the electron attachment effect, the gas gain mechanism were also carried out in the simulation. According to preliminary design parameters calculation, the new device should achieve an absolute α counting efficiency greater than 90 %. The simulation results also show that the admixture of 10 % of ambient air seems to be sufficient to continuously assess radon concentration levels ranging from about 15 Bq/m³ up to 1.5 10⁵ kBq/m³ for as short as possible integral counting period. The expected radon sensitivity should be about 11 cpm /100 Bq·m⁻³, achieving thus a measurement accuracy of ± 10 Bq/m³ at a mean radon concentration level of 100 Bq/m³ for 10 min counting time period.

A prototype of the MCPC was designed and constructed. The first experimental measurements were carried out. The simulated alpha pulse height spectra, obtained by the RADON-MCPC Monte Carlo code, are found in a very good agreement with those recorded experimentally when using the MCPC in minimal configuration, incorporating only 5 effective counting cells.

In this thesis, we present in full details the underlying studies, both theoretical and experimental, necessitated by the achievement of the fixed objective.

Consequently, the present thesis manuscript is articulated upon five sections. In the first section we recall concepts of the NORM/TENORM problem and the radon measurements methods. In the second section, we review the reported attempts of the use of gas-filled detectors for radon assessment applications. In the third section, we report about the design, the optimisazion and the construction of the Multiple cell Proportional Counter. Whereas, in the fourth section, we present in full details the Monte carlo simulation Code, specifically written to carry out optimization studies of the multiple cell proportional counter dedicated for continuous radon measurements. In the fifth section, we present the preliminary experimental measurements of alpha pulse height spectra delivred by the constructed MCPC prototype, compared to those obtained by simulation studies. Finally, we recall briefly the most important results achieved through these research and we present some insights for a future work.



References:

- [1] H. Baysson, M. Tirmarche, G. Tymen, F. Ducloy, D. Laurier; “*Risk of lung cancer and Indoor Radon exposure in France*”, Proceedings of the 11th IRPA International Congress, Madrid, Spain, 23-28 May 2004.
- [2] S. Darby *et al.*, Biomed. J. **330** (2005) 223.
- [3] NCRP 1994. “ *Exposure of the Population in the United States and in Canada from natural Background Radiation* ”, NCRP Report N° 94, National Council on Radiation Protection and measurement, Bethesda, Maryland.
- [4] NCRP 1994. “ *Exposure of the Population in the United States and in Canada from natural Background Radiation* ”, NCRP Report N° 94, National Council on Radiation Protection and measurement, Bethesda, Maryland.
- [5] ICRP 1994, “ *Protection against Radon at Home and at Work* ”, ICRP Publication 65, International Commission on Radiation Protection, Oxford, Pergamon Press.
- [6] WCNC 1995, “ *Guidelines for the Handling of Naturally Occurring Radioactive Materials in Western Canada*”, Western Canadian NORM Committee, 1995
- [7] HPS 1998, “ *Guide for Control and Release of Naturally Occurring Radioactive Materials* ”, Work Draft, January 1998, Health Physics Society, McLean, Va.
- [8] NRC 1998, “ *Health Effects of Exposure to Radon* ”, BEIR VI, National Academy of Sciences, National Research Council, Washington, D.C. 1998.
- [9] NRC 1999, “ *Evaluation of Guidelines for Exposures to Technological Enhanced Normally Occurring Radioactive Materials*”, National Research Council, National Academy Press, Washington, January 1999
- [10] EPA Report 402-R-03-003, June 2003 (<http://www.unscear.org>).
- [11] Charles Simmons, “ *NORM in Europe, A Regulation Perspective* ”, The NORM Report Fall 99/Winter 2000. Peter Gray Editor. Fort Smith, AK.
- [12] Recommendations dated on 2/02/1990, **90/143/Euratom**, and in 29/6/1996, **29/96 Euratom**.
- [13] Decreto Legislativo n.241 del 26 maggio 2000, di attuazione della direttiva **29/96 Euratom**
- [14] F. Bochicchio *et al.*, “*The Italian survey as the basis of the national radon policy*”, Radiation Protection Dosimetry, vol. 56, Nos 1-4 (1994)1-4.
- [15] G. Torri, M. Petruzzi, “*Misure passive di radon con LR-115 : problemi e riposte*”, ANPA, pp.673-681.

Section I

The NORM/TENORM problem and radon assessment

1. Introduction

Background radiation varies over a range of concentrations and exposure rates from a variety of causes. The magnitude of variation can be significant over a short distance and also can vary in the same place from time to time. The background variance can be from natural as well as human activities. Understanding the characteristics of background, and the wide range of background values encountered in the field is beneficial when designing nuclear detectors and/or conducting environmental surveys is especially important because some of the current regulatory exclusion limits are set at a concentration or exposure rate above background. Proposed clean-up guidance is essentially indistinguishable from background. Variation due to geology, chemical and physical mobility and deposition, temporal, and human affects should all be considered.

There are three generic origins for background radiation. These major components constitute therefore "background sources" of radiation which are terrestrial sources (NORM), man-made (TENORM) and cosmic sources.

1. **NORM:** Naturally Occurring Radioactive Materials. These are naturally occurring concentrations of radionuclide isotopes that represent ambient conditions present in the environment and that are in no way influenced by human activity,

2. **TENORM:** Technologically Enhanced Naturally Occurring Radioactive Materials: These arise in concentrations of radionuclides generated from anthropogenic (man-made) sources originating from a dispersion of non-site sources or during and after some technological processes of ore material of a given elemental composition.

3. **COSMIC:** constituted by the incident extraterrestrial radiation and energetic particles fluxes coming beyond the terrestrial atmosphere and/or those created by the interaction of the incident radiation when encounters the particles (atoms, molecules, aerosols) constituting the atmosphere surrounding the earth.

2. About the NORM-TENORM problem

The earth's crust contains radionuclides which constitute the major source of naturally occurring radioactive material (NORM) in the environment. Most of these radionuclides are members of the radioactive decay chains beginning with ^{238}U , ^{235}U and ^{232}Th . TENORM (Technological Enhanced - NORM) arise in various industrial processes in which raw materials containing radionuclides from the natural decay chains of uranium and thorium are being used. Therefore, NORM and TENORM appear as radioactive scaling in process equipment and as process residues with markedly enhanced radionuclide concentrations. Indeed, mineral wool for instance, which has been used on a large scale as high temperature resistant insulation often contains NORM. Diffuse sources of TENORM, which are generally very large-volume, low-activity waste streams produced by industries such as in electronic application of thorium (welding, ..) and in ore beneficiation and treatment (U-Th based ores), in metal treatment and processing waste, in mineral mining, in production of phosphate fertilizers in the agriculture sector, in water treatment and purification, in waste treatment Sludge, in paper and pulp industries, and in oil and gas production, in geothermal energy production, in scrap metal release. During the last years, many reports published throughout the industrialised countries had extensively focused on the NORM-TENORM problem [1-6]. As a consequence, this is a worthy task to investigate the assessment of the relevant problem of NORM/TENORM involved within both of classical industries and emerging technologies. Indeed, according to numerous mentioned reports, the current trends in radiation protection policies lead us to expect that NORM/TENORM would likely be as the central subject to be regulated and disciplined through explicit recommendations at the level of governments and the international organizations [7-9] and research institutions: IAEA, Euratom, ICRP, IRPA, APAT, NCRP, ICRP etc.

3. Activities that lead to the technological enhancement of NORM

There are many human activities that lead to the production of NORM. These include activities which can enhance NORM levels directly, such as the mining, milling and processing of uranium ores and mineral sands [10] (UNSCEAR, 1988), fertiliser manufacture and use [10-12], phosphate manufacture [13], burning of fossil fuels [10,14,15], metal refining [10, 15], and general underground mining and open-cut mining activities. The use of buildings as dwellings and workplaces can also lead

to exposure to NORM [15]. In addition, the use and disposal of waste materials (e.g. mine tailings, phosphogypsum, and fly ash) associated with activities which produce NORM can pose significant radiological problems.

The radiological impact of technologically enhanced naturally occurring radionuclides, processes such as nuclear power generation, nuclear weapons testing, the manufacture and use of radioactive sources (e.g. ^{60}Co), radiopharmaceutical production and use, and medical uses of radiation can be ignored as the radionuclides involved in these processes do not occur in the natural environment. Each of the processes or activities which produce NORM has associated with it a series, or several series, of pathways by which the radioactive material can reach humans. These pathways depend on the process, but fall into several broad categories (on-site, off-site, airborne, waterborne, etc.). The radiological impact on humans (and plants and animals) can depend strongly on the process which produces the NORM and the pathways by which it is transferred from the source to humans. The production of TENORM and the use of and disposal of wastes containing NORM are discussed by UNSCEAR [10].

4. Analysis of Pathways Associated with NORM

NORM can reach humans via several pathways, including the food chain, inhalation or ingestion of airborne radioactive dust and the inhalation of radon isotopes and their progeny which reach the atmosphere as a result of the exhalation of radon isotopes from the ground surface or from the surface of building materials. These pathways can be extremely complex, so a systematic approach to establishing which pathways are important is essential. This process of building up the complexity of each part of a general pathway diagram is an important aid to pathway analysis. The environmental cycles for other naturally occurring radionuclides are similar in principle, but different in detail because of differences in the radioactive decay times and chemical behaviour of the different radionuclides. The pathways by which NORM can move through the environment and impact on humans, animals and biota can be divided into several broad categories.

Therefore, the exposure to ionising natural radiations has been extensively addressed during the early seventies, because it was identified and recognised as the potential threat to population health. Since that, systematic measurements and widest surveys were carried out throughout the world in order to assess not only the

ranges of gamma exposure but also those of radon concentration, which is considered as the largest source of natural radioactivity. Indeed, it was reported that the contribution of radon and its decay products into the average effective dose equivalent exposure of ionising radiation from all sources amounts to about 67 %. This makes then our particular focusing on the best assessment of radon above all, as the potential radioactive source, not only comprehensive but also quiet consistent and seems well justified. Though, this doesn't mean any way that we shall cancel or even neglect the interest in the survey of the other concomitant ionising radiation sources.

5. Regulatory requirements and normative policies in radiation protection :

Today, there seems exist urgent requirements to challenge and very abroad deadlines are scheduled by the entering in vigour of the European Community recommendations [8-9]. Concerning specifically the Italian policies, it has been reported [17] that one of the most important objectives of the 1989 Italian survey was to promote ad hoc policies to reduce radon exposure of the population, and the annual mean value that was recorded that time (1989) was 81.5 Bq/m³, which was found somewhat higher than the reported for other industrialised countries. Thus, concerning such requirements, it is stated [18] that the required (operative) levels, on which the so-called "Action levels" are defined consist in the annual average levels. But, taking into account of the fact of the extreme variability of radon concentration in air, along days and seasons, the relevant need recommends long-termed measurements of average radon concentration levels or otherwise, by continuous radon monitoring along the whole effective period. We shall emphasis however, that if the required kind of measurements have though many advantages (more likely to indicate accurate average radiation level and exposure), they are in contrary too penalized by many other practical limitations (the results are delayed by up to 1 year and cannot inform us adequately about the time variation of the radon concentration). Although there is too many radon monitor devices commonly available in the market, there remains however a huge matter of further development that has to be carried out in order to improve the performances of those existing devices, letting them to operate within special conditions to fulfil more and more constraining requirements.

6. Radon Concentration Measurement

6.1. A short history of Radon :

The naturally radioactive noble gas radon (^{222}Rn) is present in the air and accumulates in all buildings, including workplaces. It is thus an inescapable source of radiation exposure both at home and at work. High radon levels in air can occur in buildings, including workplaces, in some geographical locations and particularly in workplaces such as underground mines, natural caves, tunnels, medical treatment areas in spas, and water supply facilities where ground water with a high radon concentration is treated and stored.

The existence of a high mortality among miners in central Europe was recognised before 1600, and the cause was identified as lung cancer in the late nineteenth century. The cancers were attributed to radon exposure in 1924. Early environmental measurements were largely confined to outdoor air for the study of diverse phenomena such as atmospheric electricity, atmospheric transport, and exhalation gases from soil. The first indoor measures were made in 1950s.

In recent years, there has been an upsurge in the interest in radon in dwellings and workplaces. A more comprehensive review of the story of radon is given in some issues of the Annals of the ICRP [19].

6.2. Radon and its progeny :

The two significant isotopes of Radon are radon-222, the immediate daughter of radium-226, deriving from the uranium series of natural radionuclides, and radon-220, the immediate daughter of radium-224, deriving from the thorium series. Because of their origins, the two isotopes are commonly known as radon and thoron. The element is a noble gas and both isotopes decay to isotopes of solid elements, the atoms of which attach themselves to the condensation nuclei and dust particles present in air. We are concerning here with the isotope radon-222 of which decay properties are shown in Radon Progeny Table (Table 1).

6.3. Special quantities and units :

The special quantities and units used to characterise the concentration of the short lived-lived decay products in air, and the resulting inhalation exposure are : [19]

6.3.1. Potential alpha energy

The potential alpha energy, ϵ_p , of an atom in the decay chain of radon or thoron is the total alpha energy emitted during the decay of this atom to ^{210}Pb or ^{208}Pb , respectively. And the potential alpha energy per unit of activity (Bq) of the considered radionuclide is

$$\frac{\varepsilon_p}{\lambda_r} = \frac{\varepsilon_p t_r}{\ln 2},$$

where, λ_r , is the decay constant and t_r the radioactive half-life of the radionuclide. Values of the constants are listed in Table 1.

TABLE 1 : Potential alpha energy per atom and per unit of activity of radon

Radionuclide	Half-life	Potential alpha energy			
		Per atom		Per unit of activity	
		MeV	10^{-12} J	MeV Bq ⁻¹	10^{-10} J Bq ⁻¹
Radon (²²²Rn) progeny :					
²¹⁸ Po	3.05 min	13.7	2.19	3 620	5.79
²¹⁴ Pb	26.8 min	7.69	1.23	17 800	28.6
²¹⁴ Bi	19.7 min	7.69	1.23	13 100	21.0
²¹⁴ Po	164 μ s	7.69	1.23	$2 \cdot 10^{-3}$	$3 \cdot 10^{-6}$
Total (at equilibrium), per Bq of radon				34 520	55.4

6.3.2. Concentration in air

The potential alpha energy concentration c_p , of any mixture of short-lived radon or thoron decay products in air is the sum of the potential alpha energy of these atoms present per unit volume of air. Thus, if c_i is the activity concentration of a daughter nuclide i , the potential alpha energy concentration of the daughter mixture is

$$c_p = \sum_i c_i \left(\frac{\varepsilon_p}{\lambda_r} \right)_i$$

This quantity is expressed in the SI unit $J m^{-3}$ ($1 J m^{-3} = 6.24 \cdot 10^{12} MeV/m^3$).

6.3.3 The equilibrium equivalent concentration in air

The potential alpha energy concentration of any mixture of radon (or thoron) progeny in air can be also expressed in terms of the so-called equilibrium equivalent concentration, c_{eq} , of their parent nuclide, radon. The equilibrium equivalent concentration, corresponding to a non-equilibrium mixture of radon progeny in air, is that activity concentration of radon in radioactive equilibrium with its short-lived progeny which has the same potential alpha energy concentration, c_p , as the actual non-equilibrium mixture. The equilibrium equivalent concentration is given in Bq m^{-3} .

6.3.4 The equilibrium factor F

The equilibrium factor, F, is defined as the ratio of the equilibrium equivalent concentration to the activity concentration of the parent nuclide, radon, in air. This

factor characterises the disequilibrium between the mixture of the short-lived decay products and their parent nuclide in air in terms of potential alpha energy.

$$F = 0.105 \frac{C_2}{C_1} + 0.515 \frac{C_3}{C_1} + 0.380 \frac{C_4}{C_1}$$

6.3.5 Inhalation exposure of individuals (The Working level month)

The quantity “**Exposure**”, P , of an individual to radon progeny is defined as the time integral of the potential alpha energy concentration in air, c_p , or the corresponding equilibrium equivalent concentration, c_{eq} , of radon to which the individual is exposed over a given time period T , e.g. one year.

Potential α energy exposure : $P_p(T) = \int_0^T c_p(t) dt$

Equilibrium equivalent exposure : $P_{eq}(T) = \int_0^T c_{eq}(t) dt$

The unit of the exposure quantity P_p is $J h m^{-3}$; for the exposure quantity P_{eq} the unit is $Bq h m^{-3}$. The potential alpha energy exposure, P_p , of workers is expressed in the historical unit working level month (WLM), with 1 month = 170 hours.

$$1 \text{ WLM} = 3.51 \text{ mJ h m}^{-3} \quad 1 \text{ mJ h m}^{-3} = 0.285 \text{ WLM}$$

The conversion coefficients between the two exposure quantities, potential alpha energy exposure, P_p , and equilibrium equivalent exposure, P_{eq} , are given in Table 2.

TABLE 2 : Conversion coefficients for different concentration quantities and corresponding exposure quantities

Quotient	Unit	Radon Progeny (^{222}Rn)
c_p / c_{eq}	$J m^{-3}$ per $Bq m^{-3}$	$5.54 \cdot 10^{-9}$
c_{eq} / c_p	$Bq m^{-3}$ per $J m^{-3}$	$1.81 \cdot 10^8$
	$J h m^{-3}$ per $bq h m^{-3}$	$5.54 \cdot 10^{-9}$
P_p / P_{eq}	WLM per $Bq h m^{-3}$	$1.58 \cdot 10^{-6}$
	$Bq h m^{-3}$ per $J h m^{-3}$	$1.81 \cdot 10^8$
P_{eq} / P_p	$Bq h m^{-3}$ per WLM	$6.33 \cdot 10^5$

Quantities :

c_p : concentration of potential alpha energy

c_{eq} : equilibrium equivalent concentration of radon isotope

P_p : time-integrated exposure to potential alpha energy concentration

P_{eq} : time-integrated exposure to equilibrium equivalent concentration of radon

The relationship between the annual exposure and the radon concentration at home or at work can be obtained from the Table 3. For equilibrium factor of 0.4 and an occupancy of 2000 hours per year at work and 7 000 hours indoors while not at work, a continued exposure to a radon concentration of 1 Bq m^{-3} results in an annual exposure of $1.55 \cdot 10^{-2} \text{ mJ h m}^{-3}$ ($4.42 \cdot 10^{-3} \text{ WLM}$) at home or $4.44 \cdot 10^{-3} \text{ mJ h m}^{-3}$ ($1.27 \cdot 10^{-3} \text{ WLM}$) at work.

7. Radon gas measurement methods

7.1. Activated Charcoal Adsorption

For this method, an airtight container with activated charcoal is opened in the area to be sampled and radon in the air adsorbs onto the charcoal granules. At the end of the sampling period, the container is sealed and may be sent to a laboratory for analysis.

The gamma decay from the radon adsorbed to the charcoal is counted on a scintillation detector and a calculation based on calibration information is used to calculate the radon concentration at the sample site. Charcoal adsorption detectors, depending on design, are deployed from 2 to 7 days. Because charcoal allows continual adsorption and desorption of radon, the method does not give a true integrated measurement over the exposure time. Use of a diffusion barrier over the charcoal reduces the effects of drafts and high humidity.

7.2. Alpha Track Detection (filtered)

For this method, the detector is a small piece of special plastic or film inside a small container. Air being tested diffuses through a filter covering a hole in the container. When alpha particles from radon and its decay products strike the detector, they cause damage tracks. At the end of the test the container is sealed and returned to a laboratory for reading.

The plastic or film detector is treated to enhance the damage tracks and then the tracks over a predetermined area are counted using a microscope or optical reader. The number of tracks per area counted is used to calculate the radon concentration of the site tested. Exposure of alpha track detectors is usually 3 to 12 months, but because they are true integrating devices, alpha track detectors may be exposed for shorter lengths of time when they are measuring higher radon concentrations.

7.3. Unfiltered Track Detection

The unfiltered alpha track detector operates on the same principle as the alpha track detector, except that there is no filter present to remove radon decay products and other alpha particle emitters. Without a filter, the concentration of radon decay products decaying within the "striking range" of the detector depends on the equilibrium ratio of radon decay products to radon present in the area being tested, not simply the concentration of radon. Unfiltered detectors that use cellulose nitrate film exhibit an energy dependency that causes radon decay products that plate out on the detector not to be recorded.

This phenomenon lessens, but does not totally compensate for the dependency of the calibration factor on equilibrium ratio. For this reason, EPA currently recommends that these devices not be used when the equilibrium fraction is less than 0.35 or greater than 0.60 without adjusting the calibration factor. EPA is currently evaluating this device further to determine more precisely the effects of equilibrium fraction and other factors on performance. These evaluations will lead to a determination as to whether to finalize the current protocol or remove the method from the list of Program method categories.

7.4. Charcoal Liquid Scintillation

This method employs a small vial containing activated charcoal for sampling the radon. After an exposure period of 2 to 7 days (depending on design) the vial is sealed and returned to a laboratory for analysis. While the adsorption of radon onto the charcoal is the same as for the AC method, analysis is accomplished by treating the charcoal with a scintillation fluid, then analyzing the fluid using a scintillation counter. The radon concentration of the sample site is determined by converting from counts per minute.

7.5. Continuous Radon Monitoring

This method category includes those devices that record real-time continuous measurements of radon gas. Air is either pumped or diffuses into a counting chamber. The counting chamber is typically a scintillation cell or ionization chamber. Scintillation counts are processed by electronics, and radon concentrations for predetermined intervals are stored in the instrument's memory or transmitted directly to a printer.

7.6 Electret Ion Chamber: Long-Term

For this method, an electrostatically charged disk detector (electret) is situated within a small container (ion chamber). During the measurement period, radon diffuses through a filter-covered opening in the chamber, where the ionization resulting from the decay of radon and its progeny reduces the voltage on the electret. A calibration factor relates the measured drop in voltage to the radon concentration. Variations in electret design determine whether detectors are appropriate for making long-term or short-term measurements. EL detectors may be deployed for 1 to 12 months. Since the electret-ion chambers are true integrating detectors, the EL type can be exposed at shorter intervals if radon levels are sufficiently high.

7.7. Electret Ion Chamber: Short-Term

For this method, an electrostatically charged disk detector (electret) is situated within a small container (ion chamber). During the measurement period, radon diffuses through a filter-covered opening in the chamber, where the ionization resulting from the decay of radon and its progeny reduces the voltage on the electret. A calibration factor relates the measured drop in voltage to the radon concentration. Variations in electret design determine whether detectors are appropriate for making long-term or short-term measurements. ES detectors may be deployed for 2 to 7 days. Since electret-ion chambers are true integrating detectors, the ES type can be exposed at longer intervals if radon levels are sufficiently low.

7.8. Grab Radon/Activated Charcoal

This method requires a skilled technician to sample radon by using a pump or a fan to draw air through a cartridge filled with activated charcoal. Depending on the cartridge design and airflow, sampling takes from 15 minutes to 1 hour. After sampling, the cartridge is placed in a sealed container and taken to a laboratory where analysis is approximately the same as for the AC or LS methods.

7.9. Grab Radon/Pump-Collapsible Bag

This method uses a sample bag made of material impervious to radon. At the sample site, a skilled technician using a portable pump fills the bag with air, then transports it to the laboratory for analysis. Usually, the analysis method is to transfer air from the bag to a scintillation cell and perform analysis in the manner described for the grab radon/scintillation cell (GS) method below.

7.10. Grab Radon/Scintillation Cell

For this method, a skilled operator draws air through a filter to remove radon decay products into a scintillation cell either by opening a valve on a scintillation cell that has previously been evacuated using a vacuum pump or by drawing air through the cell until air inside the cell is in equilibrium with the air being sampled, then sealed. To analyze the air sample, the window end of the cell is placed on a photomultiplier tube to count the scintillations (light pulses) produced when alpha particles from radon decay strike the zinc sulfide coating on the inside of the cell. A calculation is made to convert the counts to radon concentrations.

7.11. Three-Day Integrating Evacuated Scintillation Cell

For this method, a scintillation cell is fitted with a restrictor valve and a negative pressure gauge. Prior to deployment, the scintillation cell is evacuated. At the sample site, a skilled technician notes negative pressure reading and opens the valve. The flow through the valve is slow enough that it takes more than the 3-day sample period to fill the cell. At the end of the sample period, the technician closes the valve, notes the negative pressure gauge reading, and returns with the cell to the laboratory. Analysis procedures are approximately the same as for the GS method described above. A variation of this method involves use of the above valve on a rigid container requiring that the sampled air be transferred to a scintillation cell for analysis.

7.12. Pump-Collapsible Bag (1-day)

For this method, a sample bag impervious to radon is filled over a 24-hour period. This is usually accomplished by a pump Programmed to pump small amounts of air at predetermined intervals during the sampling period. After sampling, analysis procedures are similar to those for the GB method.

8. Radon decay products measurement techniques

8.1 Continuous Working Level Monitoring

This method encompasses those devices that record real-time continuous measurement of radon decay products. Radon decay products are sampled by continuously pumping air through a filter. A detector such as a diffused-junction or surface-barrier detector counts the alpha particles produced by radon decay products as they decay on this filter. The monitor typically contains a microprocessor that stores the number of counts for predetermined time intervals for later recall. Measurement time for the Program measurement test is approximately 24 hours.

8.2 Grab Working Level

For this method, a known volume of air is pulled through a filter, collecting the radon decay products onto the filter. Sampling time usually is 5 minutes. The decay products are counted using an alpha detector. Counting must be done with precise timing after the filter sample is taken. The two counting procedures most commonly used are the Kusnitz and the Tsivoglou methods described in the Indoor Radon and Radon Decay Product Measurement Device Protocols.

8.3 Radon Progeny (Decay Product) Integrating Sampling Unit

For this method, a low-flow air pump pulls air continuously through a filter. Depending on the detector used, the radiation emitted by the decay products trapped on the filter is registered on two thermoluminescent dosimeters (TLDs), an alpha track detector, or an electret. The devices presently available require access to a household electrical supply, but do not require a skilled operator. Deployment simply requires turning the device on at the start of the sampling period and off at the end. The sampling period should be at least 72 hours. After sampling, the detector assembly is shipped to a laboratory where analysis of the alpha track and electret types is performed using procedures described for these devices (AT, EL, and ES) elsewhere in this appendix. The TLD detectors are analyzed by an instrument that heats the TLD detector and measures the light emitted. A calculation converts the light measurement to radon concentrations.

9. Conclusion and the special orientation of our contribution

We shall first recall to this respect that there is only fewer laboratories that have chosen to develop gas-flow proportional counters allowing the continuous monitoring of radon concentration in air [20]. Indeed, the detection of α particles in air is very difficult to achieve with an acceptable accuracy. The reason is that the presence of electronegative gases such as oxygen, water vapour (humidity) and other gas species, though rather in traces, but their great affinity for electron attachment, tends to reduce compromisingly the effectiveness of this alternative, letting thus its achievement very difficult if not impossible. Although some research teams [21-23] have already made consistent contributions and an advanced progress ahead within this direction of investigation, there is, to our knowledge, no reported attempt in which gas-flow proportional counters were directly used to measure the radon concentration variation in air by detecting only the α particles emitted by ^{222}Rn itself

and within the sensitive volume constituted by the monitored air sample. This will constitute the main originality we claim through the present research work.



References :

- [1] NCRP 1994. “ *Exposure of the Population in the United States and in Canada from natural Background Radiation* ”, NCRP Report N° 94, National Council on Radiation Protection and measurement, Bethesda, Maryland.
- [2] ICRP 1994, “ *Protection against Radon at Home and at Work* ”, ICRP Publication 65, International Commission on Radiation Protection, Oxford, Pergamon Press.
- [3] WCNC 1995, “ *Guidelines for the Handling of Naturally Occurring Radioactive Materials in Western Canada*”, Western Canadian NORM Committee, 1995
- [4] HPS 1998, “ *Guide for Control and Release of Naturally Occurring Radioactive Materials* ”, Work Draft, January 1998, Health Physics Society, McLean, Va.
- [5] NRC 1998, “ *Health Effects of Exposure to Radon* ”, BEIR VI, National Academy of Sciences, National Research Council, Washington, D.C. 1998.
- [6] NRC 1999, “ *Evaluation of Guidelines for Exposures to Technological Enhanced Normally Occurring Radioactive Materials*”, National Research Council, National Academy Press, Washington, January 1999
- [7] Charles Simmons, “ *NORM in Europe, A Regulation Perspective* ”, The NORM Report Fall 99/Winter 2000. Peter Gray Editor. Fort Smith, AK.
- [8] Recommendations dated on 2/02/1990, **90/143/Euratom**, and in 29/6/1996, **29/96 Euratom**.
- [9] Decreto Legislativo n.241 del 26 maggio 2000, di attuazione della direttiva **29/96 Euratom**
- [10] UNSCEAR, 1988. Sources, Effects and Risks of Ionising Radiation. In: *United Nations Scientific Committee on the Effects of Atomic Radiation Report to the General Assembly with Annexes*, United Nations, New York.
- [11] Burnett, W.C., Schultz, M.K. and Hull, C.D., “*Radionuclide flow during the conversion of phosphogypsum to ammonium sulphate* ”, Journal of Environmental Radioactivity , **32**(1996) 33–52.
- [12] Ravila, A. and Holm, E., “*Assessment of the radiation field from radioactive elements in a wood-ash-treated coniferous forest in southwest Sweden* ” ,1996

- [13] Keating, G.E., McCartney, M. and Davidson, C.M., “*Investigation of the technological enhancement of natural decay series radionuclides by the manufacture of phosphates on the Cumbrian coast*”, J. of Envir. Radioactivity, **32**(1996) 53–66.
- [14] Hedvall, R. and Erlandsson, B., “*Radioactivity concentrations in non-nuclear industries*”, Journal of Environmental Radioactivity, **32**(1996) 19–32.
- [15] Papastefanou C., “*Radiological impact from atmospheric releases of Ra-226 from coal-fired power plants*”, J. of Environmental Radioactivity, **32**(1996) 105–114.
- [16] Baxter *et al.*, “*Technologically enhanced radioactivity: an overview*”, Journal of Environmental Radioactivity, **32**(1996) 3–18. and also : Baxter, M.S., MacKenzie, A.B., East, B.W. and Scott, E.M., “*Natural decay series radionuclides in and around a large metal refinery*”, J. of Env. Radioactivity, **32**(1996) 115–134.
- [17] F. Bochicchio *et al.*, “*The Italian survey as the basis of the national radon policy*”, Radiation Protection Dosimetry, vol. 56, Nos 1-4 (1994)1-4
- [18] G. Torri, M. Petruzzi, “*Misure passive di radon con LR-115 : problemi e riposte*”, ANPA, pp.673-681.
- [19] ICRP Report # 65, 1993, “*Protection against radon-222 at home and at work*”, International Commission of Radiological protection (ICRP), Annals of ICRP, Publication n°65, Oxford, Pergamon Press.
- [20] Indeed, in the preliminary bibliography research we performed in 2003 (more than 300 papers were quoted), only 16 papers have mentioned the use of proportional counters, even in very special conditions, and not more than 12 papers have reported on the possible use of ionisation chambers.
- [21] I. Busch *et al.*, “*Absolute measurement of the activity of ^{222}Rn using a proportional counter*”, Nucl. Instr. and Meth., **A481**(2002)330
- [22] L. Zikovsky, “*Determination of ^{222}Rn in gases by alpha counting of its decay products deposited on the inside of proportional counters*”, Rad. Meas. Vol. **24**, n°3, (1995)315-317
- [23] P. Baltzer *et al.*, “*A pulse-counting ionisation chamber for measuring the radon concentration in air*”, Nucl. Instr. and Meth., **A317**(1992)357-364



Section II

The use of gas-filled detectors for radon activity concentration measurement

1. Introduction

Radiation cannot be perceived by human senses. There are two basic types of instruments used for its detection: Particle counting instruments and Dose measuring instruments. With proper calibration, particle-counting instruments can be used to measure radiation. Internal dose can be deduced from measurements performed with particle counting instruments. Particle counting instruments are used to determine activity of a sample taken from the environment, to measure activity of body fluids, and can be used as portable survey instruments for contamination monitoring. The detector in a particle counting instruments can either be a gas, a solid or liquid. In all cases, passage of an ionizing particle through the detector results in energy dissipation through a burst of ionization. This burst of ionization is converted into an electrical pulse that actuates a readout device, such as a scaler or an ADC, to register a count in a channel corresponding to the signal amplitude. In the present research we are dealing with gas filled detectors. These devices look; in general purpose type, as a cylindrical condenser as sketched in figure 1. A central anode wire for collecting electrons is stretched along the axis of the cylinder, playing the role of cathode, for collecting positive ions. The ionising particle passes through the gas that fills the condenser, creating positive ions and electrons.

There are various types of particle counting instruments filled with gas:

- Ionisation chamber counters (no secondary ions are produced)
- Proportional counters (secondary ions are produced but the number is proportional with initial energy of the radiation)

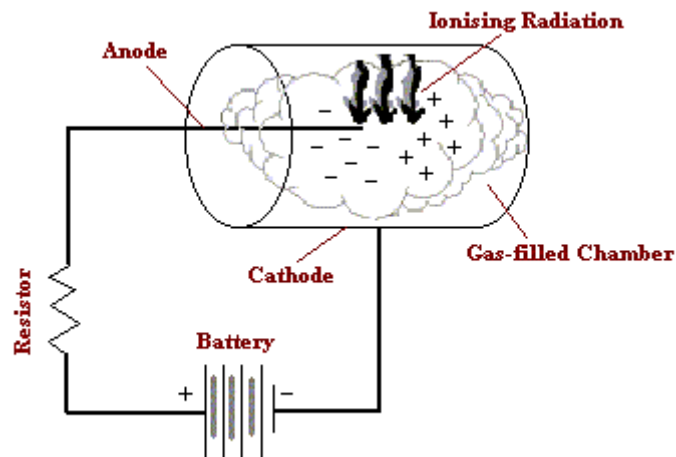


Figure 1 : A very simplified sketch of the gas filled-detector operation

- Geiger-Müller counters (secondary ions are produced in large numbers and the number of ions is no longer proportional with radiation energy)

The main difference between these 3 types of counters simply depends on the voltage used for charging the condenser.

In gas-filled detectors, since the electrical signal is provided by the collection of the primary electrons (and also secondary electrons, in case of gas amplifying devices : proportional counters, Geiger-Muller tubes..) and positive ions, one has obviously to use filling gases that have a very low electron affinity, in order to save the free electrons. Indeed, since the electrons move faster (about 1000 times) than the ions, one has to ensure that the free charge should be born by those fast particles (electrons), in order to get a device provided by a very fast time response and thus, achieving large range of measurable count rates (dynamic range). Therefore, the filling gas has to be free from gases such as air, due to its oxygen content, fluorine radicals, water vapour and so on.

2. Application to airborne radon monitoring

Radon (^{222}Rn) is estimated to be responsible for about 30% of the whole human radiation exposure. This radiation exposure is predominantly caused by the deposition on the respiratory tract and lungs of radon progenies through the aerosols taken in through respiration [1]. Radon also presents very particular properties: it is a radioactive noble gas and diffuses easily out of soils or building materials, spreading out in the environment. Consequently, different concentrations of radon and of its

progenies can be found everywhere around us. For this reason radon is an inescapable radiation exposure source both at home and at work. Since it is an inert gas, ^{222}Rn does not react chemically with other atoms or molecules, making its chemical separation impossible and its physical trapping also difficult. Because of these facts, several detection systems and various measurement methods were developed in the past aiming for an accurate assessment of its activity concentration in air [2]. However, most of those methods present some practical limitations and generally they are not able to measure radon activity concentration on-line and/or are often affected by low detection efficiencies. Therefore, they do not provide the performance required in practice for an on-line measurement of medium radon activity concentrations (1 kBq m^{-3} – 10 kBq m^{-3}). This feature is in fact of fundamental relevance for the study of the time variation of radon airborne activity concentrations and its equilibrium factors, especially when a correlation with environmental parameters is sought.

For this purpose, a design study of a new gas-flow proportional counter suited for such measurements was undertaken in our laboratory. As a first step leading towards the underlined aim and in order to assess the influence of air admixed to standard counting gases within proportional counters, we have investigated the properties of a proportional counter when using three typical air-mixed argon–propane (1%) gas mixtures [3]. It is the scope of this section to present the relevant experimental results obtained through this work.

For the design of a special gas-flow proportional counter intended for a new active measurement method of airborne radon (^{222}Rn) concentration, the amplification properties of four gas compositions were investigated in air-mixed Argon-propane (1%)-based proportional counters [4]. These four gas compositions are: Ar- C_3H_8 (1%); Ar- C_3H_8 (1%) + 2% air; Ar- C_3H_8 (1%) + 6% air and Ar- C_3H_8 (1%) + 10% air. The influence of the electron attachment effect due to oxygen on the saturation and gas amplification characteristics was examined in particular. The semi-microscopic gas gain formula was found to describe accurately the gas gain data obtained in each of the gas mixtures analyzed allowing the determination of the gas constants. The use of air-mixed counting gases in a specially designed gas-flow proportional counter for airborne radon concentration measurements appeared quite viable.

3. The use of gas-filled detectors for radon measurement in ambient air

Few laboratories worldwide are focusing their research activity on the use of gas-flow proportional counters for the continuous monitoring of radon concentration in air. In fact, it is rather difficult to perform α spectroscopy in open air, due to the presence of oxygen, water vapor and other electronegative gas traces. Nevertheless, some research groups have already made significant progress in this direction [5,6,7,8,9,10,11] and some results are briefly reviewed below.

In 1992, Baltzer et al. [5] reported about a wire arrangement pulse-counting ionization chamber for measuring radon concentration in atmospheric air. Their device was based on both positive and negative ion collection (due to electron attachment) and it is severely limited by the excessively long collection times involved. The authors have also noticed the existence of an important microphonic noise, which could be generated by the wire structure vibrations. Klein et al. [6] mentioned the possibility of using proportional counters for in situ radon level characterization, but gave no more details. Zikovsky [7] tried to measure radon concentrations in air by performing alpha counting of the ^{218}Po and ^{214}Po products deposited on the inner walls of the counter. He first filled a proportional counter with an air sample and then evacuated the counter after periods of time between 30 and 216 min, immediately introduced P-10 gas, a standard counting gas (argon–methane (90–10%)), to detect the alphas emitted by the radon decay products. Unfortunately, in addition to the fact that this method cannot provide on-line measurements, it has also a major drawback of fundamental importance: the equilibrium factors are not exactly known [8]. In order to make on-line medium-level measurements of radon activity, Rottger et al. [9] also used a multi-wire pulse ionization chamber, similar to the one described by Baltzer. Their device was designed to permit adequately large volumes (from 5 to 13 l) and presented a special electrode configuration (Archimedean spiral layout). However, the device is still based on ion collection and, since the electrons are captured by electronegative gases, e.g., oxygen, only positive and negative ions are suitable for collection in pulses. This results in very low amplitude and long-current pulses of about 1 fA in 30 ms [10]. Therefore, this multi-wire pulse ionization chamber is naturally subjected to some limitations such as long collection times and residual microphonics noise.

Recently, Busch et al. [11] reported on the first use of a gas-flow proportional counter for performing direct radon activity concentration measurements. However, the gas-flow proportional counter used does not carry out radon measurement in ambient air, but uses the P-10 gas as a suitable counting gas to which radon gas emanating from a radium source is directly mixed.

Therefore, it follows that, to the best of our knowledge, no attempt was reported about the use of gas-flow proportional counters specifically dedicated to measure on-line radon activity concentration in air by counting the alpha particles emitted by ^{222}Rn itself. If the objective is to assess sudden radon concentration variations in time delays as short as possible, especially when a correlation with environmental parameters is sought, it is more convenient to count only the alphas emitted by decaying radon nuclides, avoiding the subsequent time delays necessary for the alpha activity of the radon progenies to become high enough to be significantly measurable. Therefore, this feature would imply that the counter sensitive volume must be filled partly, if not wholly, by a certain fraction of the air sample to be monitored. This prompted us to make a preliminary investigation of the effect of air on some practical properties of air-mixed counting gases in proportional counters, such as the ionization saturation, and particularly by focusing our attention on the gas amplification characteristics.

The gas amplification process has been already extensively studied in air-free counting gas mixtures in several proportional counters [12]. However, we believe that it is quite possible to use air-mixed counting gases as sensitive media in gas-filled counters even when they operate precisely in the proportional region. Thereby, the admixed air component will act primarily as a subsequent quenching gas, through its nitrogen content, providing thus a more stable proportional regime and, at the same time, will constitute the air sample in which radon activity concentration has to be monitored.

In the present paper, we investigate four gas compositions. The first gas mixture examined is air-free argon–propane (1%) to which, thereafter, we successively admixed 2%, 6% and 10% of ambient air, in order to assess the effect of air on the proportional counter regime. We chose the air-free argon–propane (1%) gas mixture as the main counting gas for two reasons: the argon stopping power for alpha particles is

high enough to shorten efficiently the alpha ranges, reducing therefore the wall effect, and argon is available at a low cost. As a quenching gas, we adopted propane with a fraction of 1%. Indeed, this fraction is sufficient to ensure an efficient absorption of the UV photons emitted during the de-excitation of excited argon atoms, and thus allows to achieve a stable proportional regime operation of the counter.

4. The electron attachment effect in air-mixed counting gases

When operated in the ionization regime, air-filled detectors deliver very small electric pulses characterized by strong pulse height fluctuations and very long ion collection times. Because of the presence of electronegative gases, electron collection-based air-filled ionization chambers cannot be used for the purpose in concern. The electron attachment by oxygen contained in air will reduce drastically the number of the primary electrons produced within the sensitive volume of the counter and, consequently, a reliable linear response of the counter versus the actual alpha activity becomes difficult to achieve in practice. Indeed, when released in the sensitive volume of gas-filled detectors, primary electrons undergo well known elastic and inelastic processes [13]. Among these processes, one has to consider carefully the electron attachment by electronegative molecules such as oxygen, especially in the case when an important fraction of this gas, contained in atmospheric air, is intentionally admixed to the main counting gas. The electron attachment effect is well known, both fundamentally [13-14] and regarding its practical implications for gas-filled detectors such as ionization chambers, proportional counters, drift chambers [15-16], etc.

When using a proportional counter, a number of those primary electrons not captured by electronegative molecules will reach the anode wire where they are amplified up to 10^3 times by the high voltage applied. In this way, the electron attachment effect can be compensated by the gas amplification mechanism, although only to a limited level [16].

5. The gas amplification compensation

In proportional counters, we can identify two main evolving regions: the drift space region and the gas amplification region; the latter is also called Townsend avalanche region. In the former, the electric field-to-gas pressure ratio, $S(r)=E(r)/P$, is characterized by rather low values, typically not higher than $35\text{--}45\text{ V cm}^{-1}\text{ Torr}^{-1}$. The primary electron energy is always lower than the first ionization potential of the main

filling gas and there is no electron multiplication. However, the electron attachment, because of the lower values of $S(r)$, has throughout this region such a considerable effect that even the detection process of the counter could be totally compromised. In contrast, within the Townsend avalanche region, $S(r)$ has generally sufficiently high values, such that a large fraction of the avalanche electrons can ionize the gas and create further electrons along their last transit step, just before reaching the anode wire. Therefore, in this region the influence of electron attachment should be considerably less, due to the shorter distances traveled by the avalanche electrons, typically only 5–10 times the wire radius, and also the higher energies gained by the avalanche electrons. This is illustrated in Figure 2, which shows the electron-energy dependence of the dissociative electron attachment cross section of the oxygen molecule: the electron attachment cross section is quite negligible for electrons of energy higher than 9 eV, which are predominant in the avalanche region. Consequently, one can expect that the electron attachment process will introduce only a negligible effect on the gas amplification characteristics of the proportional counter, even in the presence of an important fraction of electronegative gas molecules as in our present case (up to 10% of air, corresponding approximately to an oxygen concentration of about 21000 ppm).

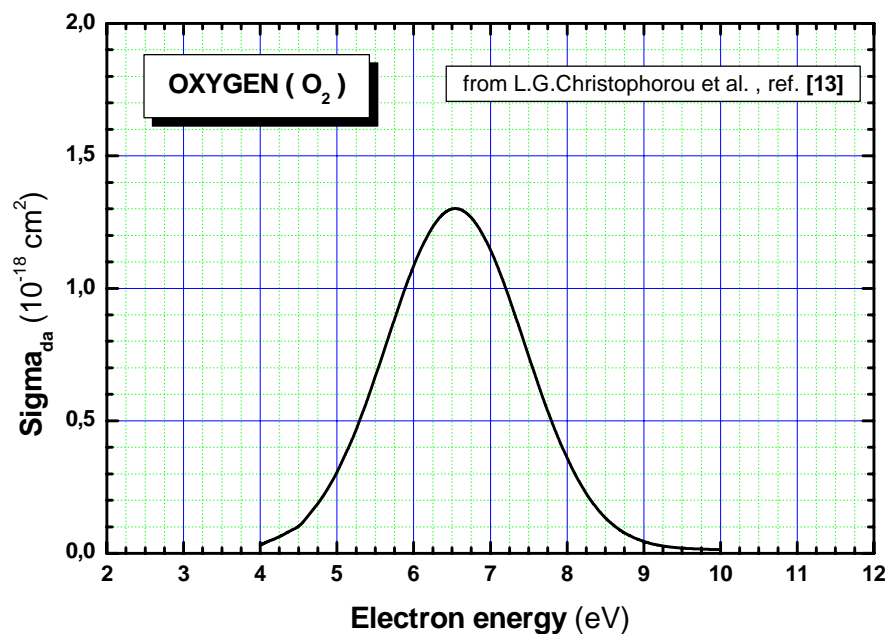


Figure 2: The electron energy dependence of the dissociative electron attachment cross section of oxygen (experimental data taken from [13]).

Since it was pointed out that the yet existing gas amplification models were not well founded theoretically, in order to assess accurately the gas amplification of the electrons released within the sensitive medium of proportional counters, we were lead to develop a semi-microscopic model.

In cylindrical single wire proportional counters, the electron avalanche development in the vicinity of the anode wire can be described only by the first Townsend coefficient α , if the accompanying effects can be neglected such as:

- the charge recombination and the space charge effects,
- the photoionization process and the photoelectric effect,
- the electron extraction through ionic impacts,
- the Penning effect and other three bodies processes.

The gas gain, A , is then simply expressed by

$$A = \exp\left(\int_c^a \alpha dr\right) \quad (1)$$

where a is the anode radius and c the starting point of the gas amplification process.

Since α/P is assumed to be a function of S only, it is more convenient to express the gas gain by the relation, known as the gas gain equation, given by [17]

$$\frac{\ln A}{P a S_a} = \int_{S_c}^{S_a} \frac{\alpha}{P S^2} dS \quad (2)$$

where S_a and S_c are, respectively, the electric field strength to pressure ratio at the anode wire surface and at the avalanche starting point r_c , given by

$$S_a = \frac{V}{P a \ln(b/a)} \quad \text{and} \quad S_c = \frac{V}{P r_c \ln(b/a)}$$

where V is the applied voltage, P the total gas pressure in the counter and a and b are, respectively, the anode and cathode radii.

Using the derived semi-microscopic α/P form given by [18] :

$$\frac{\alpha}{P} = \frac{S}{\Delta V_{\max}} \exp\left[-\left(\frac{S_0}{S}\right)^{1+m}\right] \quad (3)$$

where ΔV_{\max} , S_0 , and m are constants related uniquely to the gas properties, we deduce the semi-microscopic gas gain formula, developed up to its 3rd order approximation. It is expressed as follows :

$$\frac{Ln A}{P a S_a} = K \left[(1+m) Ln \left(\frac{S_a}{S_0} \right) + \frac{1}{1 \cdot 1!} \left(\frac{S_0}{S_a} \right)^{(1+m)} - \frac{1}{2 \cdot 2!} \left(\frac{S_0}{S_a} \right)^{2(1+m)} + \frac{1}{3 \cdot 3!} \left(\frac{S_0}{S_a} \right)^{3(1+m)} \right] - L \quad (4),$$

The constants S_0 , m , K and L characterize the physical nature of the gas mixture inside the counter and are determined on the basis of a suitable fitting analysis of the experimental set of gas-gain data at hand. The expression in brackets of Eq. (4), which depends on external, physical and electrical parameters and on the gas mixture nature, is called here the control variable and is denoted by X . When the left-hand side term of Eq. (4) is plotted versus the control variable X , a straight line should be obtained. Then, by least squares fitting method, the constants K and L are easily determined. The physical significance of the gas constants and also the whole method used for the determination of the primary gas constants m and S_0 , are sufficiently discussed in our previous contributions [18-19], where a practical form of the gas-gain semi-microscopic formula was suggested. One recalls that m is identified as the moderation parameter, and its value is closely related to the shape of the cross-sections of the major inelastic processes involved; S_0 is interpreted as the critical value of the electric field to pressure ratio for which the gas amplification process starts up and its value is also connected to the moderation parameter m . We can also deduce another more explicit gas constant, ΔV_{\max} , given by:

$$\Delta V_{\max} = \frac{1}{(1+m)K} \quad (5).$$

This can be interpreted as the maximum potential difference travelled by an avalanche electron between two successive ionizing collisions. By studying the gas constants values of the air-mixed argon-propane (1%) mixtures, one can assess better the net effect of the air on the amplification properties, in order to choose the most suitable composition for the above-mentioned purpose.

6. Experimental set-up and procedure

The proportional counter used for the gas-gain measurements is a sensitive 16 cm length stainless-steel-made gas-flow proportional counter with a 0.001 in. diameter (25.4 μ m) tungsten wire and a 32 mm diameter cathode tube. The counter was

operated at atmospheric pressure and room temperature (296 K). The gas-flow rate was set at 1 l/min and kept constant during the whole measurements (its fluctuations do not overpass 1% of the indicated values). The counter and the gas mixture manifold are shown in Figure 3. A *silica gel* cell is inserted in the air circuit in order to remove the water vapor excess evenly present in the atmospheric air and then prevents high humidity contents air samples. The radiation source was placed directly inside the counter, on the cathode surface at the midpoint of the tube, limiting thus the so-called “end effects”, i.e., the perturbation of the $1/r$ electric field, resulting in a local reduction of the gas-gain value. Two radiation sources were used: a multi- α source formed by a mixture of ^{239}Pu , ^{241}Am and ^{244}Cm radioisotopes, for low- and medium- gas-gain levels; we used ^{55}Fe radioisotope emitting 5.9 keV X-rays for higher gas-gain values, avoiding excessive space charge accumulation around the anode wire.

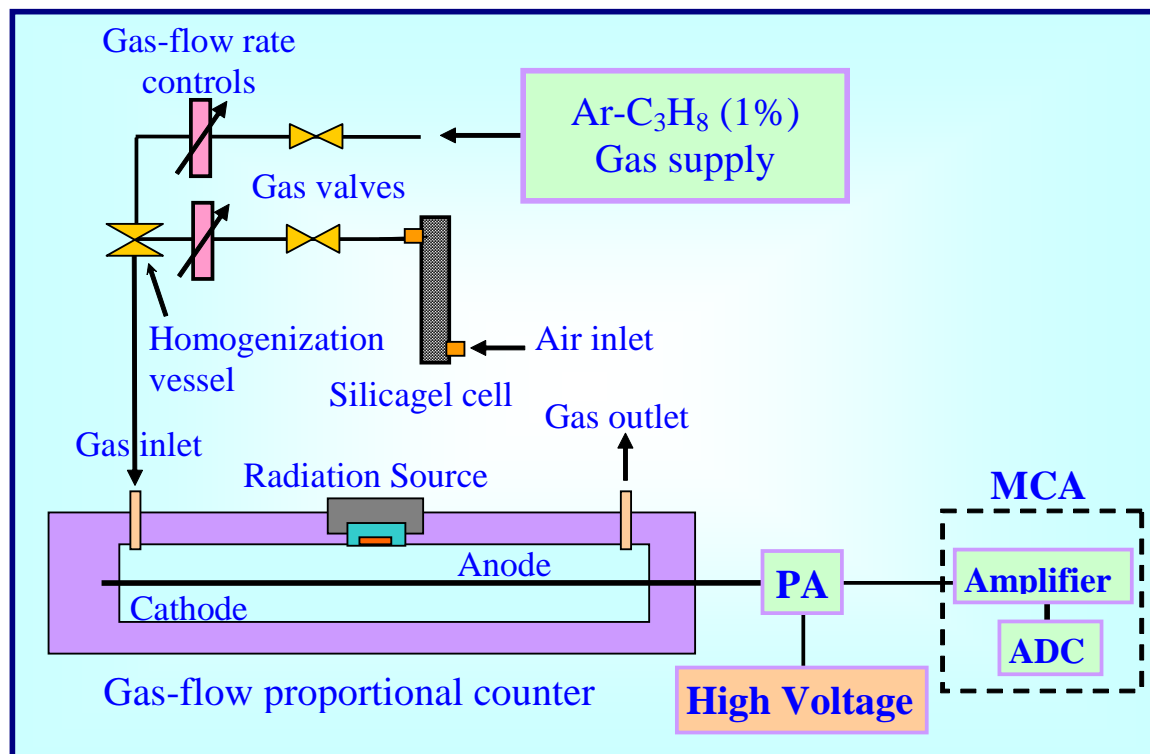


Figure 3 : The proportional counter used and the gas mixtures preparation manifold

First of all, we examined the amplification characteristics in the argon–propane (1%) counting gas mixture free from air, then we added 2%, 6% and 10% of atmospheric air. For each of these gas mixtures the amplification characteristics were measured. The electron collection pulse signals delivered by the proportional counter were fed into a low-noise charge-sensitive preamplifier (ORTEC 142 PC). The

preamplifier output is in turn fed into the built-in amplifier of the MCA (Silena, SNIP 204G). The pulse shaping time was fixed at 2 ns and the amplifier gain was varied according to the pulse height delivered by the preamplifier. Typically, two amplifier gain settings were used: 200 and 10. A gain of 200 was chosen when very low amplitude signals from the preamplifier were processed, i.e., when the counter operates in the ionization chamber regime and also when it operates at low gas-gain values in the proportional regime. A down-shift to gain 10 was adopted for a higher gas-gain operation. The experimental gas-gain measurement method we used is based on the pulse technique that was fully described previously [20]. It consists in the measurement of the channel number corresponding to the main peak in the spectrum as a function of the high voltage value. At low gas-gain values, when using the multi-alpha source, the gas gain $A(V)$ at the set voltage V is simply computed by

$$A(V) = \frac{N^\alpha(V) G_S^\alpha}{N_S^\alpha G_V^\alpha} \quad (6),$$

where, N_S^α is the channel number of the alpha reference peak when the counter operates at the saturated ionization chamber regime and $N^\alpha(V)$ is the channel number of the same peak at the set value V of the high voltage, whereas, G_S^α and G_V^α are the amplifier gain respectively in the saturated ionization chamber regime and when the counter is operated at the high voltage V , using the multialpha radiation source. At higher voltage values, we replaced the multialpha source by the 5.9 keV X-ray ^{55}Fe source, the gas gain $A(V)$ was computed by:

$$A(V) = \frac{N^X(V) G_S^\alpha}{N_S^\alpha} \frac{E_\alpha}{E_X} \frac{W_X}{W_\alpha} \quad (7),$$

where, $N^X(V)$ is channel number corresponding to the 5,9 keV peak recorded for the high voltage V , G_V^X is the adopted amplifier gain when the counter was polarized at voltage V , whereas, E_X and E_α are the energy expended by the ionizing radiation (X and α , respectively) in the sensitive gas. W_X and W_α are the energies necessary for one electron-ion pair production in the sensitive gas mixtures respectively by X-ray photons and by α particles. However, we neglected the small differences that exit between the two values, and set the ratio (W_X/W_α) equal to unity. Indeed, according to Franzen and Cochran [21], in the case of noble gases this ratio is probably equal to

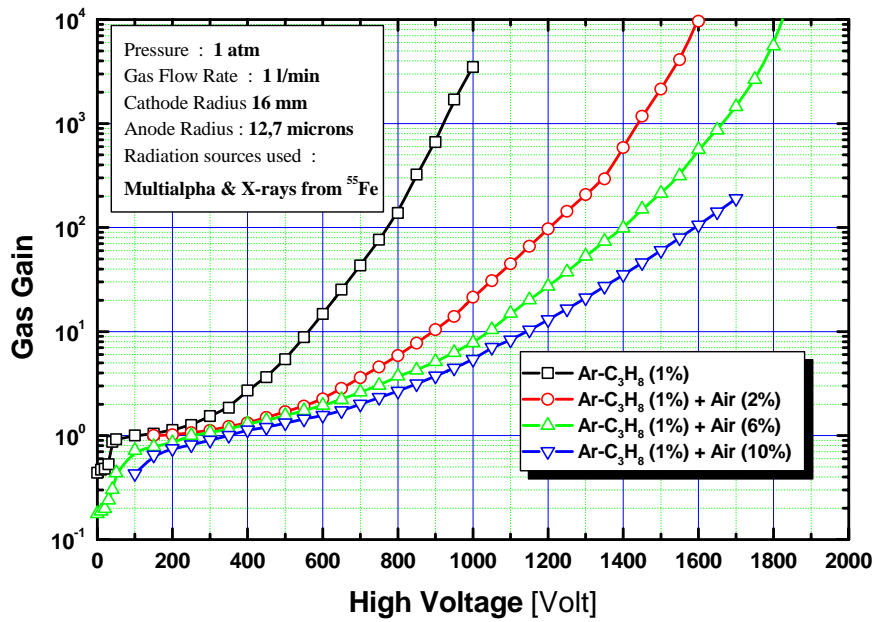


Figure 4: Measured (symbols) and calculated (solid lines) of gas amplification characteristics in air-mixed argon-propane (1%) based gas-mixtures.

unity whereas, in the case of air-filled detectors the difference that arises between W_X and W_0 is not greater than 5%. Therefore, this leads us to conclude that in our present case the maximal error we introduce when setting the W ratio equal to unity should likely not exceed 1% in the extreme case (10% air).

On the other hand, since the uncertainty in the peak channel number determination is about 1%, an error propagation analysis, based on Eqs. (4) and (5), ascertains that the experimental gas-gain data are evaluated with a precision better than about 3%. Consequently, this allows us to conclude that the cumulated error made in the fitting analysis and gas constants determination should not be greater than 5%, which is considered sufficient for our present purpose.

7. Experimental results and discussion

For each gas mixture examined, plotting the gas amplification characteristic $A(V)$ (see figure 4), we can notice the important effect of air admixture. Using the Ar-C₃H₈ (1%) free from air and setting the high voltage to about 800 V, it is possible to achieve

a gas gain of about 100. But, the addition of just 2% air requires to increase the high voltage up to 1200 V to recover the same level of gas gain. For 6% air admixture, a gas gain of 100 is achieved at a voltage of about 1400 V, and when 10% of air is admixed, the high-voltage value must be set at 1600 V, twice the value used in air-free Ar–C₃H₈ (1%). This is expected, since the electrons need much more energy to compensate the losses suffered through inelastic collisions, which they increasingly undergo during their avalanche process in the presence of air. In other words, increasing the voltage value has the effect of preserving the total number of avalanche electrons able to produce subsequent secondary electrons, at nearly the same fraction as in the case of air-free Ar–C₃H₈ (1%) gas mixture.

The effect of the electron attachment, particularly predominant in the drift space, can be noticed in Figure 5, which enlarges the recombination region and the saturated ionization chamber regime. We can notice that the electron attachment effect results in an increased catastrophic degradation of the ionization saturation characteristics. This translates into a progressive increase of the saturation plateau slope as the air fraction in the mixture is increased from 0% to 10%. For a given high-voltage value, this effect can be foreseen since the greater the oxygen fraction in the gas mixture, lower the number of primary electrons that cross the drift space without being attached to an oxygen molecule. Table 1 summarizes the degradation of the ionization saturation plateau as a function of the air fraction in the gas mixture.

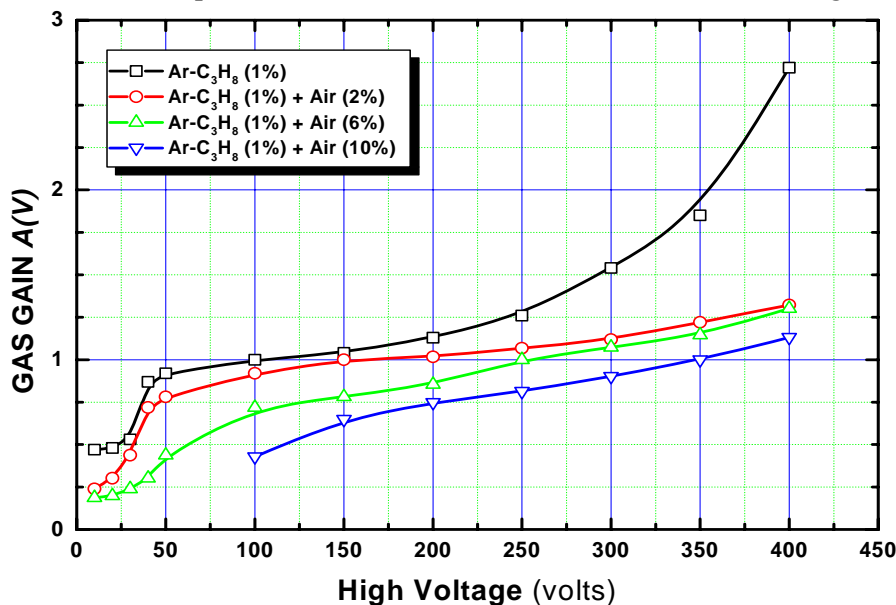


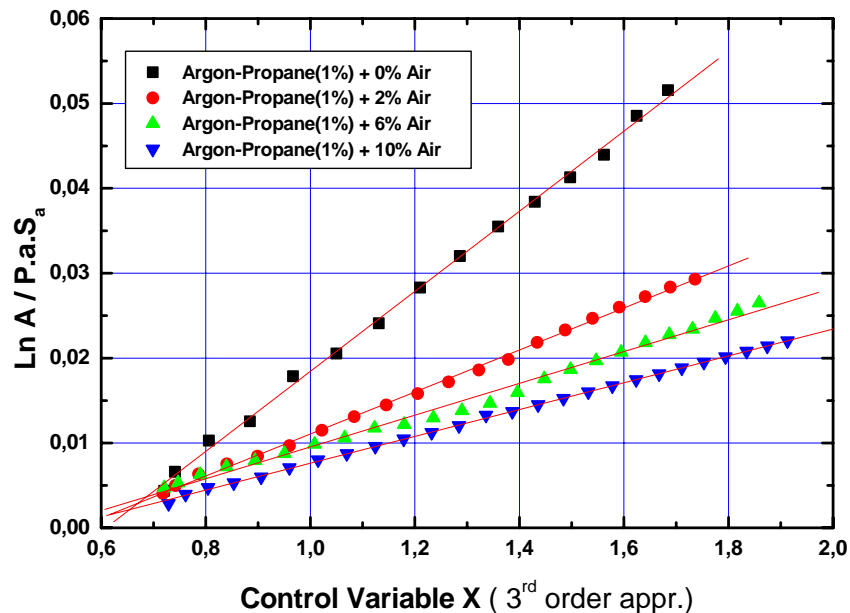
Figure 5: Evolution of the saturation plateau slope in air-mixed argon-propane (1%) based gas-mixtures. The air fraction is varied from 1% up to 10%.

TABLE I: The gas gain constants obtained from the fitting analysis of the measured gas gain data in Ar-C₃H₈ (1%) and air-mixed Ar-C₃H₈ (1%)-based proportional counters.

Air fraction admixed	0 %	2%	6%	10%
Saturation Plateau Slope (% / 100 V)	8	10	14	19

TABLE II: The gas gain constants obtained from the fitting analysis of the measured gas gain data in Ar-C₃H₈ (1%) and air-mixed Ar-C₃H₈ (1%)-based proportional counters.

Air fraction admixed	0 %	2%	6%	10%
m	0.333	0.500	0.530	0.550
S ₀ (V/cm torr)	43.5	65	75	80
Correlation coefficient	0.9991	0.9992	0.9958	0.9997
K (10 ⁻³ V ⁻¹)	47.1	24.8	18.7	15.8
L (10 ⁻³ V ⁻¹)	28.7	13.7	9.2	8.2
ΔV _{max} (V)	15.9	26.9	35.0	40.8

**Figure 6:** The fitting curves of the 3rd order approximation of the semi-microscopic formula to the gain data in the examined air-mixed Ar-C₃H₈ (1%)-based gas mixtures.

By increasing slightly the high-voltage value (hence the electric field to pressure ratio applied on the anode wire surface), the electron energy distribution function in the drift space is shifted a little more to the higher energy side, thus resulting in a reduction of the electron attachment rate within the drift space, since this effect is chiefly predominant at lower electron energies. Therefore, the fraction of collected electrons tends to be restored again, even with negligible gas gain compensation.

The gas amplification characteristics are studied using the semi-microscopic formula given by Eq. (1). Linear fitting curves from this formula for measured gas-gain data are shown in Fig. 6. As expected, the third-order approximation of this equation describes well the obtained gas-gain data, despite the important electron attachment effect due to the high oxygen fraction in the gas mixtures. The computed correlation coefficient of the fittings is greater than 0.99 in all cases and a value of 0.9997 is even achieved in case of Ar–C₃H₁₀ (1%)+10% air. The obtained gas constants are summarized in Table 2. The value taken by the moderation parameter m increases from 0.33 to 0.55 when raising the air fraction in the gas mixture. This trend is nearly the same for S_0 , the critical value for the gas amplification onset. These data can be interpreted considering that the raise in air fraction contributes to an increase in the mean fraction of the total energy that the electrons lose through inelastic non-ionizing collisions. As a result, the electron temperature in the avalanches decreases (cooling effect or moderation effect). This determines a slight increase of the parameter m . The energy losses through inelastic collisions are mainly expended to excite the vibration and optical states of nitrogen and oxygen molecules of the air mixed in the main gas with an increasing fraction. On the other hand, the increase of S_0 , shown in Fig. 7-a, means that the volume of the avalanche space narrows and collapses around the central wire. Therefore, this results in a reduction of the gas gain for a fixed value of the high voltage. This effect appears also in Fig. 7-b, showing the evolution of the maximum potential difference ΔV_{\max} traveled by an avalanche electron between two successive ionizing collisions. Indeed, in order to maintain almost the same gas-gain operation level, when we admix up to 10% of air to the counting gas mixture, the avalanche electrons have to travel a potential distance about 2.5 times greater than they do if the argon–propane (1%) gas mixture is free from air.

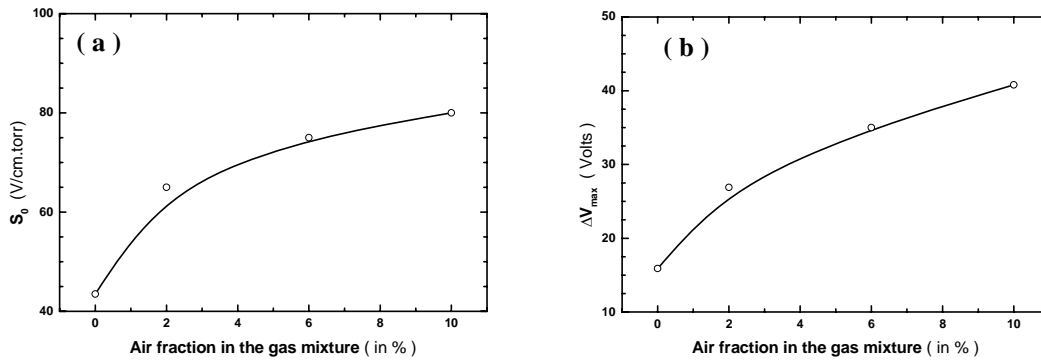


Figure 7: Evolution of the gas constants S_0 (a) and ΔV_{max} (b) in air-mixed Ar-propane(1%)-based gas mixtures as a function of the admixed air fraction.

What concerns us now is the electron attachment effect in argon–propane (1%)+10% air. We remark that even with the presence of an oxygen concentration of about 21,000 ppm in the mixture the proportional counter continues to operate rather well, and the gas amplification mechanism plays a decisive compensation role, remedying the electron attachment effect.

This is consistent with the experimental results reported by Zikovskiy [7]. Indeed, while studying the effect of an occasional air contamination, he admixed an air fraction of about 10.5% with P-10 gas used in his proportional counter and he was still able to count alpha particles although with an efficiency of about 2%, even though his counter had a cathode radius (7.6 cm) about 4.8 times larger than ours. This means that the electron attachment rate in his counter should be correspondingly larger than ours, due to the fact that the drifting electrons have to travel larger distances to reach the gas amplification region. Therefore, in order to reduce the influence of the electron attachment effect, one has to design the proportional counter in such a way that the primary electrons have to cross-minimal drift distances. In this way, as was clearly shown by Andronic et al. [22], the O_2 content of the gas will affect the collected charge only to a small extent. In the light of these primary results, and especially from the gas amplification point of view, we can conclude that the possibility of use of air-mixed counting gases in a suitably designed gas-flow proportional counter for performing on-line measurement of airborne radon activity concentration appears quite viable.

8. Applicability for radon measurements and achievable sensitivity

Following this purpose, a special air-mixed gas-flow proportional counter is designed and constructed. The designed counter, called Multiple Cell Proportional Counter (MCPC), is characterized by a relatively good flexibility and a sufficiently large sensitive volume of about 10 liters. It is composed by an assembly of 20 cylindrical cell elements, each of them having a height 3 cm and a diameter 16 cm. Every single cell consists of a cathode mesh plane and an anode wire plane separated by an electrode distance of 1.5 cm. The anode plane is constituted by a parallel array of interconnected thin wires. The design, operation, and Monte Carlo simulation of the MCPC is detailed forward ahead in this thesis. In order to carry out a number of design optimization studies and to make an estimate of the applicability of this technique for radon measurements, a Monte Carlo simulation code was written and further details were presented [23,24].

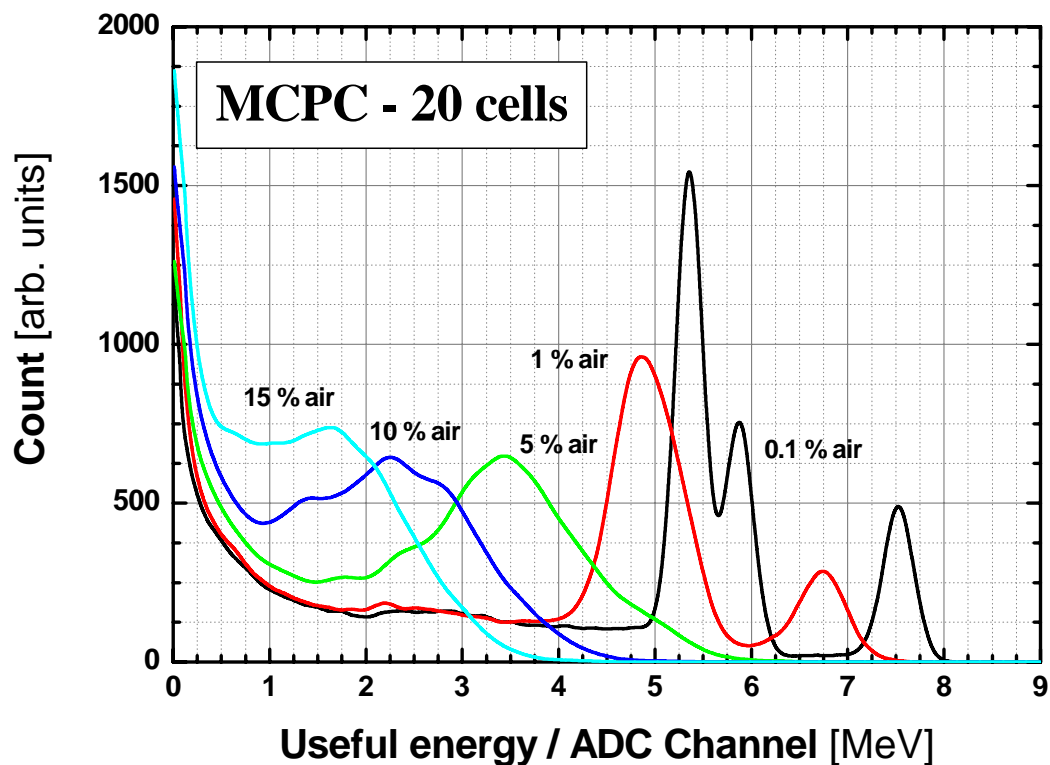


Figure 8: Monte Carlo simulation of the expected alpha pulse height spectra (area-normalized) as the air fraction is increased in argon-propane (1%) counting gas used in the designed MCPC. The integral $1/E$ -type background count rate is assumed to be 5 counts/min.

As should be seen in next sections, according to these results, the admixture of 10% to the main argon–propane (1%) counting gas is found sufficient to assess stepwise airborne radon activity concentration as low as 15 Bq/m^3 for a counting time period of 10 min, with an energy-equivalent discrimination threshold of 0.250 MeV, resulting in an expected radon activity concentration sensitivity of about $1.16 \text{ cpm/10Bq/m}^3$. As an illustration, in Figure 8 is depicted the Monte Carlo calculation of the expected alpha pulse height spectra (area-normalized) as the air fraction is increased from 0.1% to 10% in argon–propane (1%) gas mixture used in the designed MCPC. The ^{222}Rn activity concentration in air is assumed stepwise: it jumps from zero to a constant value at $t = 0$, and remains at this value for at least 10 min. The alpha pulse height spectra collection is started at $t = 0$ for a time duration of 10 min. The simulated α spectra for air fractions of 0.1%, 1%, 5% and 10%, are then area normalized in order to show the net effect of air on the alpha pulse height distributions. It can be seen from Fig. 8 that with admixture of 10% of air, although the designed MCPC can no longer discern between the alpha particles originating from ^{222}Rn (5.489 MeV) and from ^{218}Po (6.002 MeV), it still allows to perform a correct alpha counting if a convenient setting of the energy-equivalent discrimination threshold is adopted. Therefore, this tends to confirm furthermore the consistency of the described active method to measure on-line radon activity concentrations.

9. Conclusions

To achieve more reliable on-line measurements of airborne radon concentration using gas-filled detectors based on α spectrometry technique, it is required to perform the measurement of the radon activity within the sensitive volume by counting directly the alpha particles emitted by decaying radon nuclides. Especially, if the scope is to assess sudden radon concentration variations in time delays as short as possible, it is recommended to count only the alphas emitted by decaying radon nuclides, avoiding subsequent time delays, before the alpha activity of the radon progenies becomes significantly measurable. This implies the need to mix the counting gas with a small fraction of the air sample to be monitored. Hence, the air sample becomes intrinsically a component of the sensitive gas mixture. The presence of oxygen, a highly electronegative gas, introduces serious problems related, in particular, to the attachment effect causing an excessive electron charge loss within

the drift space. However, the electron attachment effect can be counterbalanced by subsequent gas amplification when using suitably designed proportional counters.

In this section, the gas amplification characteristics of three air-mixed argon–propane (1%)-based gas mixtures were studied. Our results show that by mixing the counting gas with a fraction of air up to 10%, the attachment effect does not introduce a critical perturbation within the gas amplification region, but only affects the charge collection process within the drift space of the proportional counter. Hence, it seems quite possible to reduce the electron losses by designing special proportional counters which minimize the drift space dimensions. The presence of a fraction of air as high as 10% does not seem to penalize excessively the detection process if an appropriately designed gas-flow proportional counter is used, and this is confirmed by the preliminary results obtained from a Monte Carlo simulation study.



References

- [1] J. Porstendorfer, T.T. Mercer, “Adsorption probability of atoms and ions on particle surfaces in submicrometer size range”, *J. of Aerosol Science*, Vol. 9 (1978) 469-474.
- [2] A.C. George, “An overview of instrumentation for measuring environmental Radon and Radon progeny”, *IEEE Trans. on Nucl. Sci.*, Vol.37, n°2, (1990) 892-901. and also : A. George, *State-of-the-art instruments for measuring radon/thoron and their progeny in dwellings—a review*, *Health Phys.* **70** (1996) (4), pp. 451–463.
- [3] G. Curzio, D. Mazed, R. Ciolini, A. Del Gratta, A Gentili, “Effect of air on gas amplification characteristics in argon-propane (1 %)-based proportional counters for airborne radon monitoring”, *Nucl. Instr. and Meth.*, **A 537** (2005)672-682.
- [4] D. Mazed, R. Ciolini, “Gas gain in air-mixed argon propane (1%) based proportional counters”, Communication presented at the 11th International Congress of the International Radiation Protection Association, IRPA’11, May 23-28, 2004, Madrid, Spain.
- [5] P. Baltzer, K.G. Gorsten, A. Backlin, “A pulse counting ionization chamber for measuring the radon concentration in air”, *Nucl. Instr. & Meth.*, **A317**(1992)357-64.

-
- [6] D. Klein, R. Barillon, S. Demongeot, E. Tomasella, A. Chambaudet, “*Investigative techniques for Radon Level characterization*”, Rad. Meas., Vol. **25**, n°1-4 (1995)553.
- [7] L. Zikovsky, “*Determination of Radon-222 in gases by alpha counting of its decay products deposited on the inside walls of a proportional counter*”, Rad. Meas., Vol. **24**, n° 3 (1995) 315-317.
- [8] A. Honig, A. Paul, S. Rottger, U. Keyser, “*Environmental control of the German radon reference chamber*”, Nucl. Instr. and Meth., **A416** (1998) 525-530.
- [9] S. Rottger, A. Paul, A. Honig, U. Keyser, “*On-line low-and medium-level measurements of the radon activity concentration*”, Nucl. Instr. and Meth., **A466** (2001) 475-481.
- [10] A. Paul, A. Honig, D. Forkel-Wirth, A. Mueller, A. Marcos, “*Traceable measurements of the activity concentration in air*”, Nucl. Phys. A, **701** (2002) 334c
- [11] I. Busch, H. Greupner, U. Keyser, “*Absolute measurement of the activity of ^{222}Rn using a proportional counter*”, Nucl. Instr. and Meth., **A481** (2002) 330-338.
- [12] D. Mazed, Magister Thesis, n° 13/2002/MPH, University of Sciences and Technology Houari-Boumediène, Algiers, February 2002 (unpublished).
- [13] L.G. Christophorou, J.K. Olthoff, “*Electron interactions with plasma processing gases present status and future needs*”, Appl. Surf. Sci., vol.**192** (2002) 309-326.
- [14] J.D. Skalny, S. Matejcek, T. Mikoviny, J. Vencko, G. Senn, A. Stamatovic, T.D. Mark “*Absolute calibration of relative electron attachment cross section by crossed beams experiments*”, Int. J. of Mas. Spect. vol.**205** (2001) 77-84.
- [15] V. Golovatyuk, F. Grancagnolo, R. Perrino, “*Influence of oxygen and moisture content on electron life time in helium-isobutane gas mixtures*”, Nucl. Instr. & Meth., **A461** (2001)77.
- [16] H. Kuroiwa et al., “*The influence of oxygen contamination on the performance of a mini-jet-cell-type drift chamber for the JLC-CDC*”, Nucl. Instr. & Meth., **A516** (2004) 377.
- [17] A. Zastawny, “*Gas amplification in a proportional counter with carbone dioxide*”. *J. Sci. Instr.* **43** (1966), p. 179.
- [18] D. Mazed, M. Baaliouamer, “*A semi-microscopic derivation of gas gain formula for proportional counters*”, Nucl. Instr. and Meth., **A437** (1999) 381-392.

-
- [19] D. Mazed, A. Amokrane, “*Nouvelle formulation du facteur de Multiplication des électrons dans les compteurs proportionnels*”, Communication presented at the JSGX’2002 international meeting, Saclay-CEA, France, 12-15 October 2002.
- [20] M. Baaliouamer, C. Belaragueb, D. Mazed, “*La technique impulsionnelle pour la caractérisation des détecteurs à gaz*”, CEA Report: CEA-N-2756,(May 1994)p47
- [21] W. Franzen and L.W. Cochran, “*Pulse Ionization Chambers and Proportional Counter*”, in A.H. Snell (Ed.), “*Nuclear instruments and their uses*”, vol.1, J. Wiley & Sons, 1962, p.11.
- [22] A. Andronic et al., “*Pulse height measurements and electron attachment in drift chambers operated with Xe-CO₂*”, Nucl. Instr. and Meth., **A498** (2003) 143-154.
- [23] D. Mazed, G. Curzio, R. Ciolini, “*Monte Carlo simulation of a new air-mixed gas-flow proportional counter for on-line airborne radon activity measurements*”, Communication presented at the 4th European Conference on Protection Against Radon at Home and at Work, June 28-July 2, 2004, Prague, Czech Republic.
- [24] D. Mazed, R. Ciolini, G. Curzio, “*Monte Carlo Simulation and Modelling of a Radon Multiple Cell Proportional Counter (MCPC)*”, submitted for publication to *Radiation Measurements* (Review process in course).



Section III

Design and construction of the Multiple Cell Proportional Counter (MCPC)

1. Introduction

Several detection systems and various measurement methods aiming for an accurate assessment of radon activity concentration in ambient air were developed in the past [1-2]. A large review of those was already presented in the first section of this thesis. In particular, continuous measurements methods were revealed of a fundamental importance for studies of sudden variations of radon activity concentration, especially when correlations with environmental parameters are dealt.

In this framework, we have shown in the previous section the feasibility of a new continuous measurement method, based on the use of a specially designed gas-flow proportional counter operating with an air fraction admixed to the counting gas [3]. Contributions reporting about the use of a proportional counter-based monitor for such an application are rather few in the literature [4-10]. However, in those works, introduction of air, even in small fraction, within the proportional counters being used was never attempted. Instead, those proportional counters were filled only with standard counting gas mixtures, such as P10, free from air. In our case however, as shown experimentally in the previous section, we introduce a given air fraction mixed to the counting which flows through the proportional counter. The radon measurement principle consists thus in counting, during a suitably fixed time preset, all alpha particles emitted within the counter sensitive volume by ^{222}Rn (5.489 MeV) contained in the air fraction admixed and its short-lived progenies: ^{218}Po (6.002 MeV) and ^{214}Po (7.687 MeV), produced within the sensitive volume of the counter. The α count rate is therefore directly proportional to the radon activity concentration prevailing in the ambient air.

However, it is rather difficult to perform α spectroscopy in air, due to the presence of oxygen, water vapour and other electronegative gas traces which cause so excessive electron capture in the detector sensitive volume that even its counting operation becomes impossible in practice. Therefore, in the previous works, the authors adopted the ion collection mode rather than the electron collection mode. To our present knowledge, so far it is reported in no contribution about the use of gas-flow proportional counters specifically dedicated to such a kind of application. If the objective is to resolve sudden radon activity concentration variations, induced by the change of environmental parameters, in shortest time delays, one cannot use ion collection-based gaseous detectors (such as pulse ionization chambers, radon monitor based on solid state silicon detectors and electrostatic collection of radon decay products) where the time delays are so excessive due to the low drift velocities of ions in gases (~ 1 cm/ms), compared to those of electrons (~ 1 cm/ μ s), and the radon measurement range of the detector is subsequently limited. It is better to use electron collection-based detectors (such as proportional counters) and also to count all of the α particles emitted inside the sensitive volume, improving thus greatly the radon detection efficiency (at radioactive equilibrium condition, each radon decay event is detected through the simultaneous emission of three alpha particles) extending thus the radon measurement range to lower values side. This would imply that the proportional counter sensitive volume should be filled partly, if not wholly, by a given fraction of the air sample to be monitored. Thereby, the admixed air component will act primarily as a subsequent quenching gas, especially through its nitrogen content, providing thus a more stable proportional regime and, at the same time, it constitutes the air sample in which radon activity concentration has to be measured.

In the present section, the design criteria, the construction and the operation principle of a new proportional counter, called Multiple Cell Proportional Counter (MCPC), are described. The device uses argon-propane (1%) gas mixture, to which an appropriate fraction of ambient air is admixed. In order to perform a consistent optimization of the measuring device performances, a Monte Carlo simulation code, called RADON-MCPC, has been written [11-12]. This program is presented in full details in the next section. It was used to compute the main design parameters of the MCPC prototype in order to achieve a lower detection limit of about 15 Bq/m³ within a shortest time response.

2. Design criteria and description of the MCPC

2.1. General Features

In order to measure airborne radon activity concentration using the multiple cell proportional counter (MCPC) prototype concept, it is necessary to mix a considerable fraction of air with the counting gas which is generally some binary gas mixture. And the presence of oxygen, a highly electronegative gas, in the gas mixture composition, even in traces, has long been rather a constraining factor. Indeed, the resulting electron attachment effect, chiefly inherent to oxygen component, should likely tend to induce dramatic degradation of the detector performances and even to compromise entirely the detection process in any gas-filled detector. However, in a recent work, it is proved that oxygen, present up to 4% in the mixture, even induces significant charge losses, plays rather a certain benefic role, through complicated microscopic three-body processes involved, and contributes to stabilize the gain operation of proportional counters providing a suitable long counting plateau [3,13]. However to reduce the influence of the induced charge loss effect due to electron attachment, one has obviously to use a proportional counter, where the gas amplification process can play a compensation role for those electrons attached when drifting towards the anode wire. In ionization chambers indeed, there is no other way to compensate for the electrons lost. But, one has to insure that the released primary electrons have to cross as short drift paths as possible, as was concluded in the previous section.

Taking into account these preliminary requirement features, a first prototype of the Multiple Cell Proportional Counter (MCPC) is designed and its structure layout is sketched in figure 1. The proposed gas-flow proportional counter prototype model is characterized by a sufficient configuration flexibility and it consists of a pile-up of a number (20) of polyethylene-made cylindrical ring shaped cell elements, held tight hermetically, side by side as in a “sandwich”, between two end-caps. Thus, this allows to make readily convenient cell configuration changes and further design characteristics adjustments so that to suit consistently any specified application and design requirements.

Hence, the end-cell contribution effect could be suppressed by taking the signal only from inner cells, where the electric field distribution should likely not be perturbed. This configuration permits us to insure a good sensitive volume definition. During the optimization studies, we dealt essentially with two geometry configurations : namely

a Cylindrical Geometry, CG1, and a Planar Geometry PG2, which physical and mechanical characteristics are summarized in table 1. Each cell consists in a polyethylene-made ring body, with internal diameter D_{cell} and H_{cell} height, having a stainless steel perforated cathode grid on the bottom side and an anode plane located at a distance L above the cathode grid, having an hexagonal mesh pattern.

TABLE 1 : *Preliminary mechanical parameters of adopted for simulation study of the cylindrical (CG1) and planar (PG2) configurations.*

Parameter	MCPC-CG1	MCPC-PG2
Internal cell diameter, D_{cell}	16 cm	30 cm
Anode wire pad, p	2 cm	1 cm
Number of wire segments per anode plane	7	29
Cell height, h_{cell}	3 cm	1.5 cm
Anode–Cathode distance, L	2 cm	1 cm
Geometric transparency of Cathode grid, T_g	81.25 %	> 98 %
Total number of cells , N_{cell}	20	20
Total volume, V_{tot}	12 liters	21.2 liters
Total sensitive volume, V_c	10.8 liters	19 liters

In the cylindrical geometry configuration, CG1, the geometric transparency of the cathode grid is about 81 % while as, its electronic transparency depends on the electrode distance and the set value of high voltage. Every anode plane is hold to the same high voltage value and constituted by a parallel array of interconnected 100 μ diameter tungsten wires (refer to figure 1) is connected to its own low noise charge sensitive preamplifier.

As explained in the previous contribution, in order to measure airborne radon activity concentration using a gas-flow proportional counter, it is necessary to mix a given fraction of air with the counting gas. However, to reduce the influence of the induced electron capture due to electron attachment effect, it is necessary to insure that the released primary electrons have to cross as short drift paths as possible to reach the avalanche region in the vicinity of the anode wire [3].

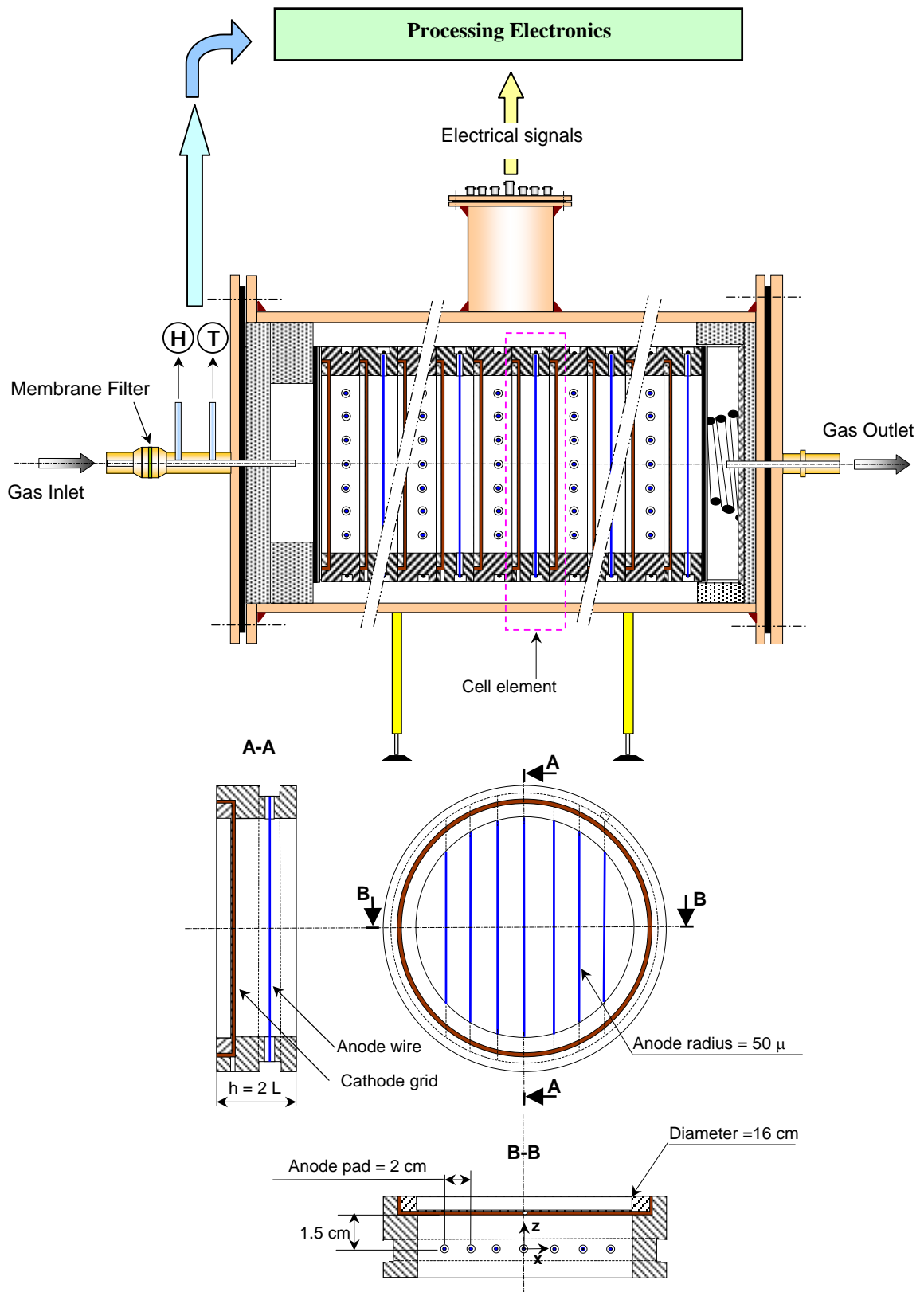


Figure 1: General layout of the CG1 prototype of the Multiple Cell Element Proportional Counter (MCPC). The structure of a single element cell (0.6 litres) is also sketched in the bottom part of the figure. The effective sensitive volume (18 counting cells) is 10.8 litres.



Figure 2: Some photos of the MCPC under construction : (a) the copper container and 20 assembled elements; (b) top view of the assembled cells and the upper end-cap; (c) single cell structure; (d) the MCPC during laboratory tests.

2.2. The designed MCPC

To achieve higher detection efficiencies, it is necessary to design the MCPC with a sufficiently large sensitive volume, reducing thus the so-called wall effect and providing higher alpha counting rates within the given value of the preset time. After several combinations of the geometrical and physical parameters, the most practical configuration of the MCPC prototype was chosen to be CG1, general features of which are presented in Table 1. Hence, the constructed counter prototype is composed by 20 separate cell elements of the same geometry, in such a way that the main performance requirements, especially, the radon sensitivity, and the detection efficiency, can be adjusted by modifying only the total number of effective counting cells. Taking into account this practical feature, a first prototype of the MCPC was constructed adopting CG1 configuration: a schematic layout of it is shown in figure 1 and some photos are depicted in figure 2. Using RADON-MCPC code, the mean electron drift path is estimated to be about 0.95 cm for a total volume of 12 litre.

This gas-flow proportional counter prototype is characterized by great configuration flexibility and consists in a pile-up of 20 cells, each one constituted by a ring-shaped multiwire proportional counter, held tight hermetically side by side between two end-caps. Every cell consists in a polyethylene-made ring body, having a stainless steel perforated cathode grid on the bottom side and an anode plane above the cathode grid located at a distance of 1.5 cm. Each anode plane is constituted by a parallel array of 7 interconnected 100 μ diameter tungsten wires: every parallel array of anodes is connected to its own low noise charge sensitive preamplifier. All the cathode grids, having an hexagonal mesh pattern shown in figure 3, are held to the same negative high voltage value. The preamplifier outputs, from all the effective counting cells, are then fed to the same pulse amplifier through a fast signal adder module. Designed in this way, the end-cell contribution effect can be suppressed readily by taking the radon signal only from the inner cells, i.e., through cell n°2 up to n°19, where the electric field distribution is less perturbed. The MCPC prototype has a total volume of 12 litres and is designed to use a common binary gas mixture constituted by argon (99%) and propane (1%) as a quenching gas. This gas mixture provides good stopping power values for alpha particles and is commercially available at low cost. The most important design parameter of the counter determined by RADON-MCPC code is the

maximum air fraction (10%) we could add to the binary gas mixture in order to achieve best counter performances, for the chosen geometry configuration.

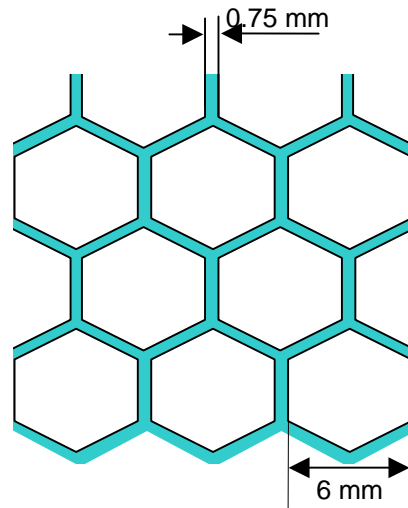


Figure 3: *The pattern of the stainless steel perforated cathode grid of a cell.*

The other mechanical parameters and the estimated physical characteristics of the MCPC, with 10 % fraction of air, are synthesized in Table 2, where some corresponding parameters of a volume-equivalent cylindrical proportional counter that would have approximately the same performances are also included. One can justify thus the choice of the present condensed multiple cell pile-up structure of the designed MCPC: imagine how could be technologically difficult to build a 17 meters long cylindrical proportional counter!

2.3. The operation principle of the MCPC

The operation principle consists to pump-in through the counter the argon-propane (1%) gas mixture, mixed continuously with a sampling fraction of ambient air which has to be analyzed, assuming a constant gas-flow rate value of 10 l/min at a pressure of 760 torr. During the air pumping, only the radon gas contained in the air enters the counter volume through a suitably chosen membrane filter, and all the other solid-state aerosols, especially radon products, are not allowed to enter the sensitive volume, whilst the too low effect of thoron gas (^{220}Rn) is neglected. The activity concentration of ^{222}Rn in air can be deduced from the periodical integral counting of the emitted α -particles, originating both from ^{222}Rn and its short lived progenies (^{218}Po and ^{214}Po), within the effective counting cells of the counter, and then subtracting the contribution of the background counts in the same sampling period.

TABLE 2 : *Mechanical parameters and estimated physical performances of the MCPC configuration using 10 % air fraction and the corresponding volume-equivalent cylindrical proportional counter.*

Parameter	MCPC (10 % Air)
Internal cell diameter	16 cm
Anode wire pad	2 cm
Number of wire segments in each anode plane	7
Anode sensitive length in each cell	95.86 cm
Cell height	3 cm
Anode–cathode distance	1.5 cm
Air fraction in the mixture	10 %
Average electron drift distance	0.9 cm
Geometric transparency of cathode grid	81 %
Total number of cells	20
Number of effective counting cells	18
End Cells Contribution, ECC	3.52 – 3.15 %
Operating high voltage value	3 kV- 3.5 kV
Corresponding gas gain	25 – 100
Mean electron attachment coefficient	$0.62 \text{ cm}^{-1} - 0.65 \text{ cm}^{-1}$
Attachment Effect Loss, AEL	1.91 – 2.27 %
Grid Opacity Effect Loss, GOEL	1.61 – 2.23 %
Ratio of Wall Effect Loss, WEL	9 – 12 %
Total anode sensitive length	17.25 m
Total counter volume	12 liters
Effective sensitive volume	10.8 liters
Estimated Radon sensitivity	1.16 cpm /10 Bq m ⁻³
Radius of volume-equivalent cylindrical proportional counter	1.41 cm
Sensitive length of volume-equivalent proportional counter	17.25 m
Corresponding wall effect loss ratio	> 45 %
Estimation of the corresponding Radon sensitivity	0.86 cpm /10 Bq m ⁻³

3. The MCPC characteristics and parameters definition

In order to carry out as complete as possible design optimization study, we have to define first the main MCPC characteristics and performance parameters that have to be optimized.

3.1 Alpha counting efficiency

During alpha counting purpose one has unavoidably to discriminate (by setting a pulse height counting threshold) concomitant background radiations from alpha pulses emitted by radon and progenies inside the counter. Unfortunately, due to some counter imperfections (such as electron attachment effect, wall effect etc.) that will be described latter in further details, this introduces also alpha counting losses which results in an effective alpha counting efficiency, ε , lower than unity. The alpha counting efficiency, ε , of the counter is defined as follows

$$\varepsilon = \frac{\text{number of counted } \alpha \text{ particles}}{\text{number of } \alpha \text{ particles entering the counter sensitive volume}} \quad (1)$$

3.2 Radon counting efficiency

When the radioactive equilibrium is achieved inside the counter, i.e., radon activity equals those of its decay products (^{218}Po and ^{214}Po), for each decaying radon atom three alpha particles are successively emitted within the counter, but realistically only two are detectable, since the alpha emitting decay products (^{218}Po and ^{214}Po), bearing a positive charge, deposit on the grid material surface and thus emit within a solid angle of 2π . Therefore, we define the radon counting efficiency as follows :

$$\xi (\%) = 100 \times \frac{\text{number of counted } \alpha \text{ particles}}{\text{number of radon decay events within sensitive volume}} \quad (2)$$

We can notice therefore that the maximum achievable radon efficiency is about 200 %.

3.3. The minimum detectable activity concentration of radon

Since there is no way to discriminate exactly the concomitant background radiation that superposes to the alpha radiations originating from radon and progenies, the designed MCPC unfortunately cannot detect airborne radon activity concentrations laying below than a certain value, called Minimum Detectable Activity (η), expressed in Bq/m^3 , and defined as follows:

$$\eta = \frac{bcr}{\varepsilon S_{Rn}} \quad (3)$$

where, bcr is the background count rate (expressed in cpm) measured within the same electronic settings conditions, when the airborne radon activity concentration can be assumed to be zero, whereas ε is the alpha counting efficiency of the counter, and S_{Rn} stands for the radon sensitivity, expressed in $cpm/Bq/m^3$, as will be defined below

3.4 The radon sensitivity

The most important parameter of the designed counter is obviously the radon activity concentration sensitivity, S_{Rn} , defined as the ratio of the net number of registered alpha pulses, N_α , that have an amplitude greater or equal than the set discrimination threshold, E_D , (often expressed in energy-equivalent unit) within one minute time duration to the airborne radon activity concentration, A_{ext} , prevailing in ambient air outside the counter. It is expressed in $(cpm/Bq/m^3)$, and computed by :

$$S_{Rn} = \frac{N_\alpha - bcr}{t_C A_{ext}} \quad (4)$$

where, t_C is the counting time period (expressed in min) and bcr is the background count rate (in cpm) measured using the same electronic settings.

3.5 The Wall Effect Loss, *WEL* :

The wall effect is known as a default of energy transfer to the counter sensitive medium. It occurs when an alpha particle emitted within the counter sensitive volume, is incidentally stopped by the counter inner walls before transmitting all its kinetic energy to the gas mixture. When the corresponding amplitude height of the delivered pulse voltage is lower than the energy-equivalent occurrence discrimination threshold, E_D , this alpha particle is not counted. The Wall Effect Loss fraction (*WEL*) is then defined as follows :

$$WEL (in \%) = 100 X \frac{\alpha \text{ counts lost due to wall effect occurrences}}{\text{total } \alpha \text{ particles counted}} \quad (5)$$

3.6 The Attachment Effect Loss, *AEL* :

The presence of a given oxygen fraction within the gas mixture induces an electron capture fraction through electron attachment process, resulting thus in a so-called Attachment Effect Loss fraction (*AEL*) in alpha counting. This is defined as follows :

$$AEL (in \%) = 100 X \frac{\alpha \text{ counts lost due to electron attachment effect occurrences}}{\text{total } \alpha \text{ particles counted}} \quad (6)$$

3.7 The Grid Opacity Effect Loss, *GOEL* :

Another wall effect-like process, induced by the grid pattern structure, is due to the opacity of the cathode grid pattern to alpha particles. Indeed, sometimes a certain number of alpha particles are stopped by the grid mesh structure, resulting thus in a corresponding count loss, called Grid Opacity Effect Loss fraction (*GOEL*). It is defined as follows:

$$GOEL (in \%) = 100 X \frac{\alpha \text{ counts lost due to grid effect occurrences}}{\text{total } \alpha \text{ particles counted}} \quad (7)$$

3.8 The End Cell Contribution, *ECC* :

First of all, one has to recall that avoiding counting spurious pulses developed within those sensitive volumes, where the electric field distribution is somewhat perturbed, namely within the end cell of both sides (left and right) of the counter cells pile, we discarded intentionally the corresponding electrical signals. However, in the opposite to the loss effects, some alpha particles, emitted within the end cells volumes penetrate back to the adjacent cell volume, and develop voltage pulses with an amplitude greater than the pulse height discrimination threshold, resulting thus in counting excesses. The corresponding counting excess, introduced through this End Cell Contribution (*ECC*), is then defined as follows:

$$ECC (in \%) = 100 X \frac{\alpha \text{ particles emitted within end cells counted}}{\text{total } \alpha \text{ particles counted}} \quad (8)$$

Finally, one has just to recall that all of these defined parameters depend on :

- The MCPC design configuration : cell structure and related dimensions, number of effective counting cells, air fraction added to Ar-propane (1%) gas mixture.
- The adopted electronic settings conditions : the applied high voltage, the amplifier gain and shaping time, the energy-equivalent discriminator threshold, E_D .

3.9 The spectrometric and counting quality factors :

Let's define the spectrometric and counting quality factors as follow

$$\chi_{spectro} = 100 \frac{\text{Peak energy}}{E_{aver}} \quad \text{and,} \quad \chi_{count} = \frac{\text{peak count} - \text{valley count}}{\text{valley count}} \quad (9)$$

with

$$E_{aver} = \frac{5.489 + 1/2 \cdot 6.002 + 1/2 \cdot 7.687}{2} = 6.167 \text{ MeV}$$

being the average energy of the alpha particles, evaluated assuming radioactive equilibrium condition and taking into account the hypothesis that ^{218}Po and ^{214}Po products are attached to the grids at the moment of their alpha decay, thus only half the total number of the emitted alpha particles are detectable.

Therefore, one can also introduce another more general quality factor, called overall optimization factor ψ , defined as follows :

$$\psi = \rho \chi_{\text{spectro}} \chi_{\text{count}} \quad (10)$$

Where,

$$\rho = \frac{f S \varepsilon}{\alpha_{\text{att}} \eta} \frac{\text{Ln}(A)}{V} \quad (11)$$

We can notice that in defining the overall optimization factor, ψ , we take into account the following parameters that define the counter performances

- the radon sensitivity, S_{Rn} (in $\text{cpm}/10\text{Bq}/\text{m}^3$)
- the air fraction in the mixture, f (in %)
- the alpha counting efficiency, ε (in %)
- the averaged gas gain to high voltage ratio, $\text{Ln}(A)/V$ (in kV^{-1})
- the spectrum quality factor, χ_{spectro} ,
- the counting quality factor, χ_{count} ,
- the mean electron attachment coefficient, α_{att} (in cm^{-1})
- the lower detectable activity, η (in Bq/m^3)

Thus, in order to check which configuration that could achieve a simultaneous optimization of the whole counter performance parameters, one has to maximize the so-called overall optimization factor, ψ , as will be explained in next paragraph.

4. The Monte Carlo simulation code RADON-MCPC

After having defined above the counter performance parameters, RADON-MCPC Monte Carlo simulation code was written to perform the design requirements of the MCPC prototype. The code carries out all the calculations necessary for a good prediction of counter performances and the expected alpha pulse height spectra which should be delivered by the MCPC as a response to an assumed radon activity concentration profile in ambient air [14]. The basic physics and modelling of the involved mechanisms and related calculations will be presented in further details in next section.

5. Design optimization and performance requirements

Using RADON-MCPC simulation code, the main design and operation parameters of the MCPC prototype were determined in order to achieve an absolute alpha counting efficiency greater than 90 %, a radon counting efficiency greater than 150 %, a measurement time period not excessively long (from 6 to 12 minutes) with a standard deviation lesser than 10 % at a mean level of 100 Bq/m³ and a lower detectable activity not higher than 15 Bq/m³ with a radon sensitivity as high as achievable.

This will be achieved by maximizing the overall optimization factor, ψ , defined in previous paragraph.

5.1. Maximum air fraction allowed

In order to assess the effect of the air on the counter characteristics, four typical gas mixtures were fully examined in the simulation tests: 0.1 % , 1 % , 5 % and 10 % air-mixed argon-propane (1%). For each air fraction, several output parameters of the MCPC were evaluated: the alpha pulse height spectra and related discrimination curves, the net alpha counting, the MCPC detection efficiency, the radon activity concentration sensitivity, and the MCPC detection limit, and the yielding value of the overall optimization factor [15-16].

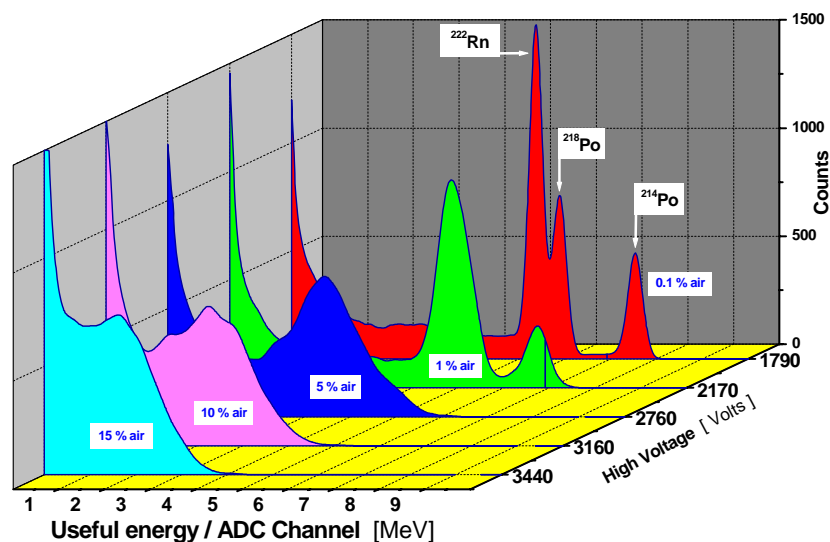


Figure 4 : Evolution of the α pulse height spectra when air fraction in the mixture is increased from 0.1 % to 15 %. The spectra were calculated assuming the high voltage value necessary to reach the same gas amplification level for each gas mixture.

TABLE 3: Some results of the simulation assessment of the air effect. The expected performances of the MCPC (in CG1 configuration) were calculated when increasing the air fraction added to argon-propane (1%) gas mixture from 0.1% up to 15%.

Fraction of air admixed	0.1 %	1 %	5 %	10 %	15 %
Anode High Voltage (Volts)	2265	2750	3500	4000	4350
Averaged Gas Gain	39.40	39.49	38.10	39.12	39.51
Mean attachment coefficient (cm ⁻¹)	0.029	0.167	0.452	0.642	0.764
Airborne ²²² Rn activity concentration (Bq/m ³)	10000	1000	200	100	66.67
Total emitted α part. (10 min count)	194	194	194	194	194
Energy-equivalent Discriminator (keV)	242	242	253	250	250
Net α Counting (time preset : 10 minutes)	139	136	131	126	121
Attachment effect loss ratio, AEL (%)	1.51	1.55	1.75	1.89	2.16
Grid opacity effect loss ratio, GOEL (%)	0.79	0.86	1.30	1.89	2.44
End cells contribution ratio, ECC (%)	4.30	4.18	3.98	3.74	3.47
Wall effect loss ratio, WEL (%)	4.27	5.65	7.12	8.69	10.36
RADON Counting Efficiency (%)	199	194.5	188.3	179	171.3
Mean useful energy (charge-converted) (MeV)	4.43	3.86	2.70	1.87	1.38
Mean peak shift (%)	2.2	12.3	41.0	61.5	71.9
MCPC Alpha Detection Efficiency (%)	97.73	96.12	93.80	91.27	88.50
Radon Sensitivity (cpm / 10 Bq.m ⁻³)	0.013	0.127	0.62	1.17	1.67
MCPC Detection limit (Bq/m ³)	1148.6	120.4	23.1	14.2	10.3

The evolution of the expected alpha pulse height spectra as a function of the admixed air fraction is shown in figure 4, and the obtained numerical results are summarized in Table 3. We can see in figure 4 the rapid degradation of the counter resolution with increasing air fraction in the mixture. One can notice that while it is still possible to resolve all the three alpha peaks due to ²²²Rn, ²¹⁸Po and ²¹⁴Po with a mixing air fraction of 0.1 %, only two alpha peaks are visible when the mixing air fraction is increased up to 1 % and no more than a single broadened peak is seen when the air fraction is increased up to 5 %. Moreover, if the purpose consists only in alpha counting, one can also increase further the mixing air fraction up to about 10 % or 15 %. Therefore, excepting those instruments based on alpha spectrometry, this counter can no longer resolve the emitted alpha energies, and unfortunately, as is also the case in a great number of commercially available radon measuring devices, we can no longer provide an information about the thoron mixing ratio. This consists

therefore a major limit of the herein exposed measurement method. To restore the spectrometric resolution ability, one has to accept a severe compromise on the sensitivity, and reduce the air fraction down to 1 %. In this way, the measuring range of the counter is shifted upward to about 120 Bq/m^3 .

5.2. Cell inner radius selection

Since the Wall Effect Loss fraction decreases with increasing counter dimensions, using RADON-MCPC, we have computed the *WEL* parameter for several counter cell inner radius. The cell inner radius, R_{cell} , is varied from 2 cm up to 18 cm and assuming 3, 7, 12 and 20 incorporated cells. We show in figure 5 the relative behaviour of the wall effect loss, where one can notice that from approximately $R_{\text{cell}} = 8$ and up, the wall effect loss decreases very slowly and tends to saturate close to a given value depending on the number of incorporated cells. Therefore, taking into account practical considerations, the cell dimensions were chosen in order to achieve a *WEL* parameter value lower than 10 %, when incorporating only a limited number of cells, keeping thus the overall dimensions of the prototype device in a reasonable range. The manufactured cells were therefore 3 cm height and 16 cm inner diameter.

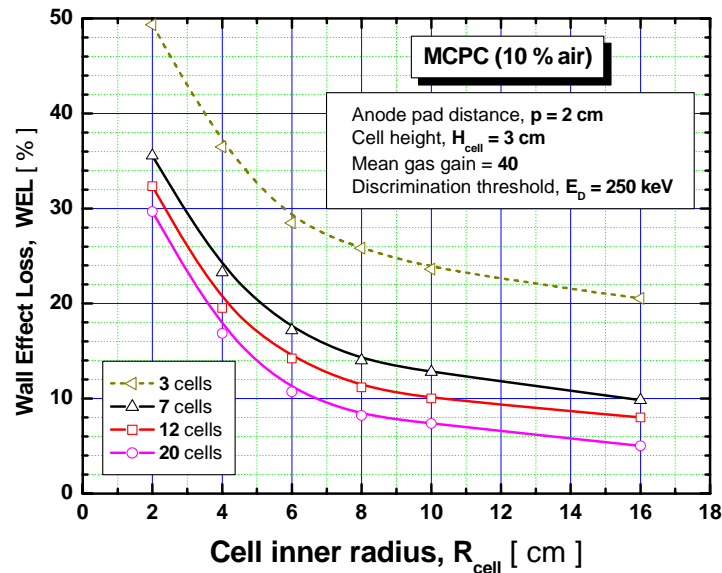


Figure 5 : Evolution of the Wall Effect Loss (*WEL*) against the cell inner radius for 3; 7; 12 and 20 incorporated cells when 10 % of air is added to the binary gas mixture. The applied high voltage value was fixed such that the averaged gas gain is maintained in each case constant and equal 40 and the discrimination threshold (energy-equivalent) E_D was set at 250 keV.

TABLE 4: Computation results (through RADON-MCPC) of the counter main parameters (defined in previous paragraph) when the number of incorporated effective counting cells (NECC) is increased from 1 single cell up to 18 cells. The gas gain and discrimination threshold was kept constants and equal 41 and 254 keV respectively .

NECC	AEL (%)	WEL (%)	GOEL (%)	ECC (%)	S_{Rn} (cpm/10Bq/m ³)	LDA (Bq/m ³)	Efficiency (%)
18	1.89	8.69	1.89	3.74	1.17	14.20	91.27
16	2,12	8.95	1.95	4.11	1.04	16.02	91.09
14	2,41	9.45	1.95	4.60	0.91	18.40	90.79
12	2,68	9.98	1.99	5.18	0.79	21.0	90.53
10	3,1	10.64	2.10	5.74	0.65	25.44	89.90
8	3.72	11.57	2.21	6.86	0.52	32.0	89.36
6	4.46	13.17	2.37	8.24	0.40	40.78	88,24
5	5.01	14.32	2.29	9.04	0.33	49.19	87.42
4	5.81	15.55	2.63	9.87	0.27	60.35	85.88
3	6.80	17.74	2.82	11.04	0.20	81.0	83,68
2	8.45	20.37	3.08	12.45	0.13	124.26	80,55
1	10.52	25.69	3.67	13.04	0.07	224.5	73,16

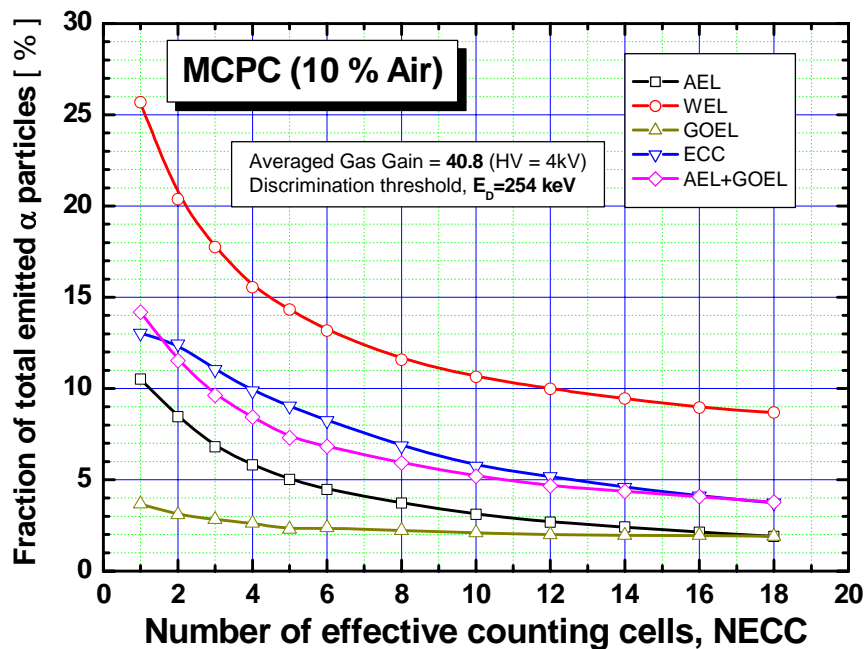


Figure 6: Evolution of some MCPC parameters when increasing NECC from 1 up to 18. The parameters kept constants are indicated in upper frames (see text for comments).

5.3. Selection of the Number of effective counting cells, NECC

Another RADON-MCPC simulation run was carried out with the scope of assessing evolution of the counter main parameters when increasing the number of effective counting cells (*NECC*) from 1 up to 18 cells, keeping in each case two electrically discarded cells. The numerical results are synthesized in Table 4 and relative decrease of the defined counting loss factors are graphically shown in figure 6, where we can notice that saturation limit is approached with the incorporation of only 6 effective counting cells. Evolution of the lower detectable activity and the counter alpha counting efficiency are shown in figures 7.

In order to determine a minimum counter configuration, we studied evolution of the expected alpha pulse height spectra. These are shown in figure 8-a. In figure 8-b, the alpha pulse height spectra were normalized to the main peak count, to be easily compared. A perusal of the spectra relative shapes, indicates that the minimum *NECC* number, should be around 5 and 6, since the main alpha peak begins to appear completely detached from the relative counter background when *NECC* = 5 cells are incorporated. We thus conclude that one has to connect at less 5 effective counting cells to reach normal operation of the counter when designed in the CG1 configuration and using only 10 % of air added to the binary gas mixture (Ar-propane (1%)).

6. Operating high voltage

Concerning the most convenient high voltage value, it should be necessary set to a suitable value, permitting to achieve simultaneously:

- the highest radon sensitivity, S (in cpm/10Bq/m³)
- The highest air fraction in the mixture, f , (in %)-
- The highest alpha detection efficiency, ε (in %)
- The highest averaged gas gain to high voltage ratio, $Ln(A)/V$ (in kV⁻¹)
- The highest spectrum quality factor, α , (in MeV)
- The lowest mean electron attachment coefficient, α_{att} (in cm⁻¹)
- The radon concentration limit, η (in Bq/m³)

Therefore, one has to find the optimal operating high voltage value which maximises the overall optimization factor ψ . We show in figure 9 the evolution of the simulated alpha pulse height spectra when the anode high voltage is varied from 1 kV up to 5 kV and, in figure 10, the corresponding changes in the yet defined MCPC parameters. The numerical results are provided in Table 5 for each assumed high voltage.

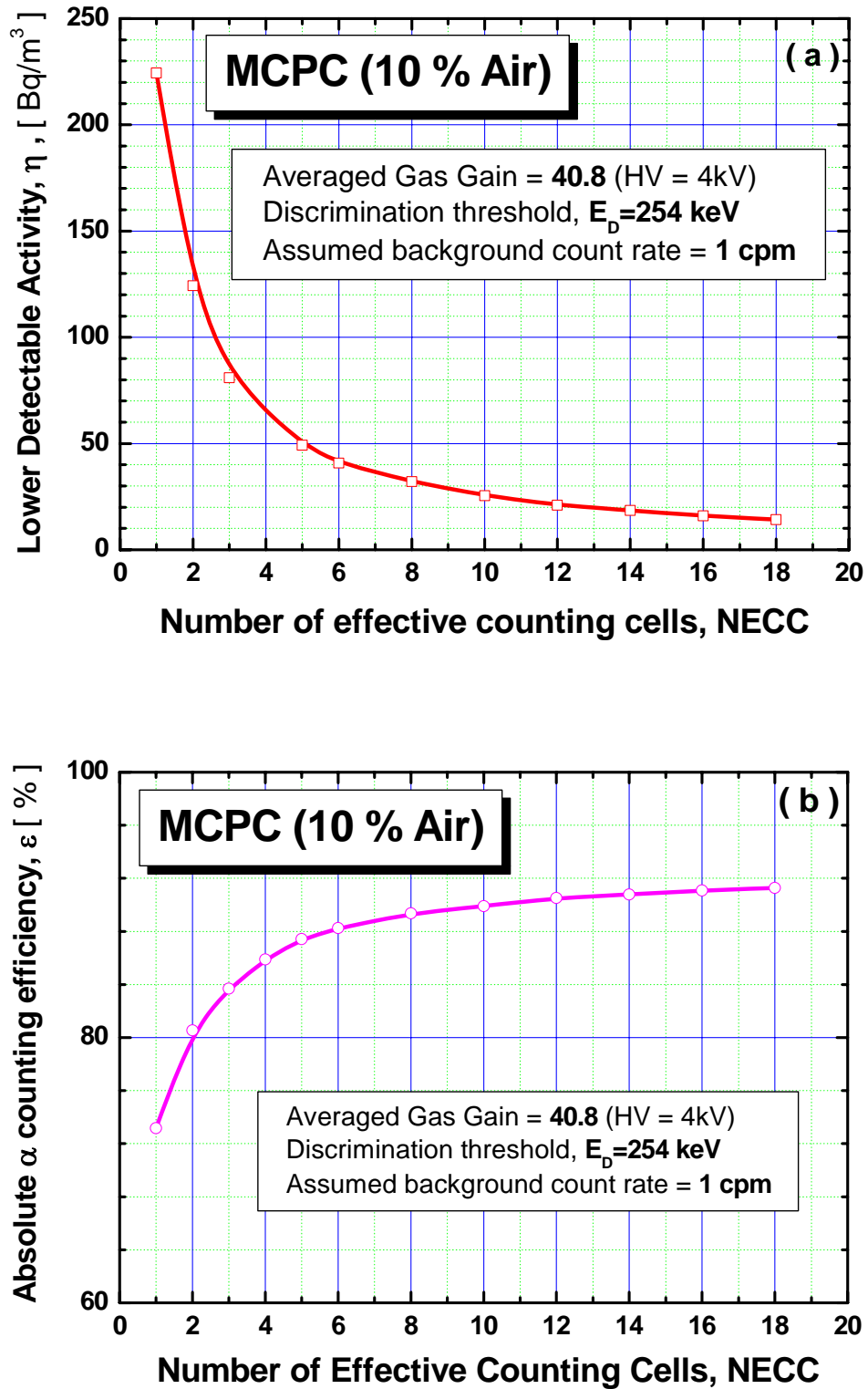


Figure 7: Evolution of the lower detectable activity, η , (a) and absolute alpha counting efficiency, ε , (b) versus the number of incorporated effective counting cells, NECC.

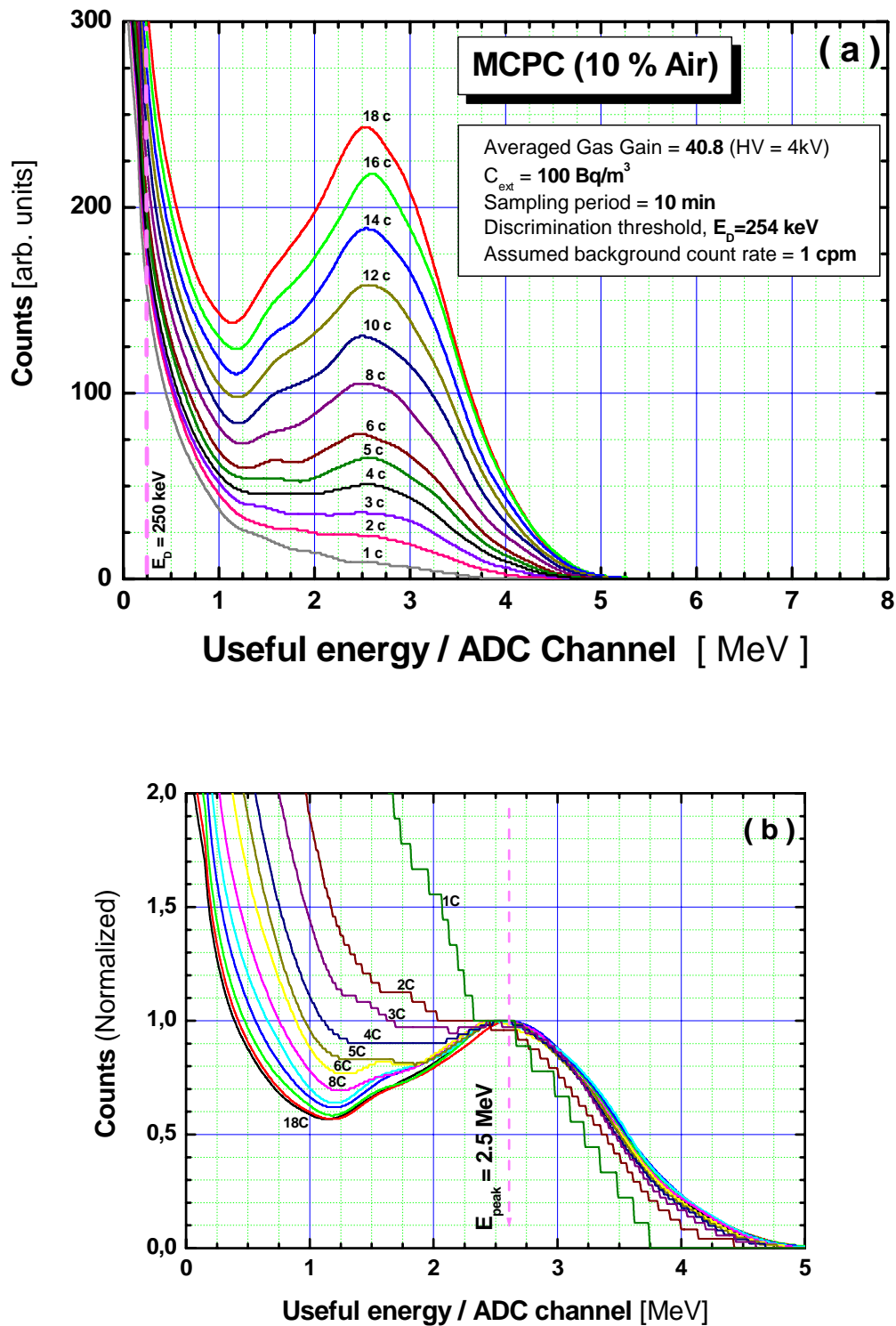


Figure 8: Simulation of the alpha pulse height spectra evolution (a) when the number of incorporated effective counting cells (NECC) is increased from 1 single cell up to 18 cells. In figure8-b the spectra were normalized to number of counts recorded in the main peak location channel ($E_{peak} = 2.5 \text{ MeV}$).

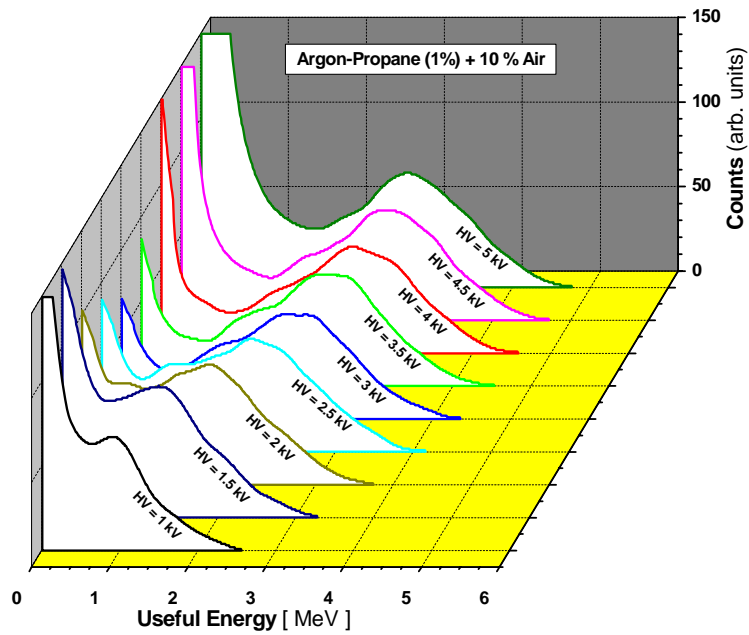


Figure 9 : Evolution of the α pulse height spectra versus anode high voltage. The MCPC constituted by 18 effective counting and 10 % air is added to the binary gas mixture.

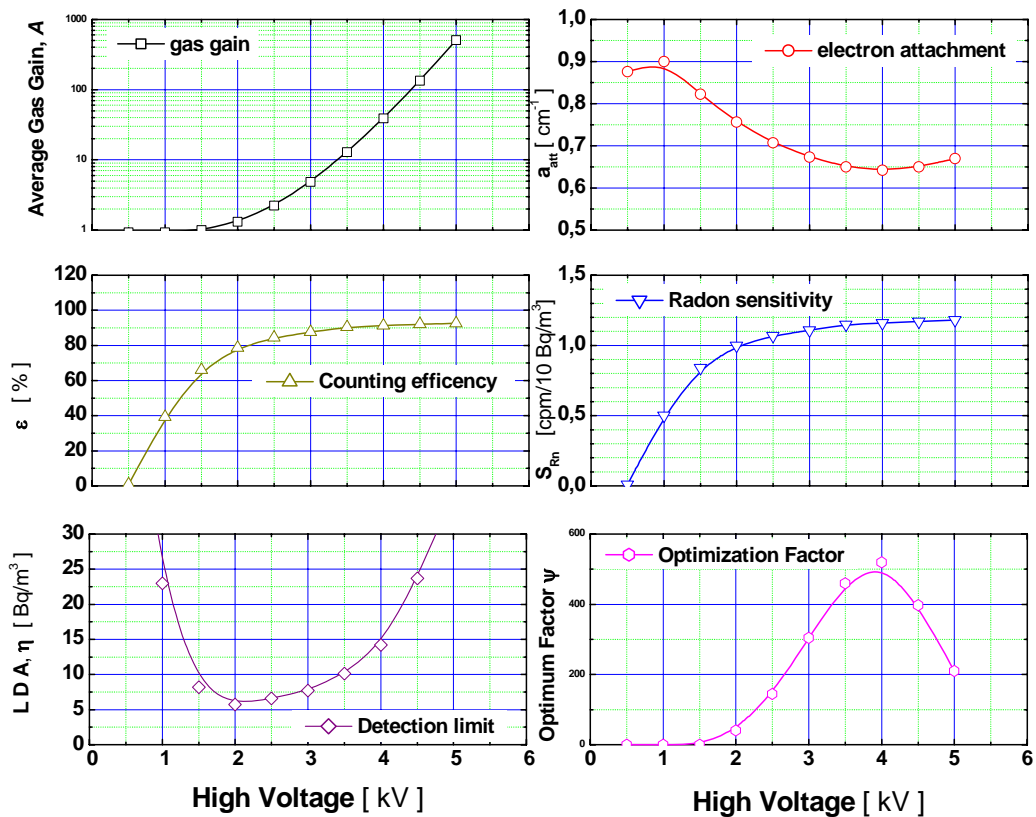


Figure 10 : Evolution of the gas gain, electron attachment, counting efficiency, radon sensitivity, detection limit and the optimization factor with anode voltage for 10% air mixture.

TABLE 5 : Numerical results of the Monte Carlo simulation (obtained using RADON-MCPC code) of the MCPC, constituted by 18 effective counting cells (in CGI configuration) with 10 % of air. The anode high voltage is varied from 0.5 kV up to 5 kV.

High Voltage (kV)	0,5	1	1,5	2	2,5	3	3,5	4	4,5	5
Averaged gas gain	0,93	0,934	1,002	1,316	2,24	4,86	12,78	39,11	134,6	507,5
Mean attachment coefficient (cm ⁻¹)	0,876	0,9	0,822	0,756	0,707	0,673	0,65	0,64	0,65	0,67
Alpha detection efficiency (%)	0,91	39,3	66	78,6	84,5	87,7	90,4	91,3	92,2	92,6
Radon sensitivity (cpm/Bq.m ⁻³)	1E-3	0,05	0,084	0,1	0,107	0,111	0,115	0,116	0,117	0,118
Lower Detectable Activity (Bq/m ³)	43507,2	23	8,2	5,74	6,6	7,7	10,1	14,2	23,7	35,9
Peak energy	0,604	0,757	1,297	1,587	1,897	2,161	2,334	2,513	2,672	2,877
Peak count	945	1563	1568	1422	1281	1217	1205	1256	1169	1051
Valley energy	0,38	0,53	0,49	0,7	1,03	1,21	1,46	1,7	1,77	1,76
Valley count	715	1502	1146	870	730	648	587	572	531	585
Spect. fact. ($\chi_{spectro}$)	9,794	12,275	21,031	25,734	30,76	35,035	37,847	40,742	43,327	46,652
Count. Fact. (χ_{count})	0,322	0,041	0,368	0,634	0,755	0,878	1,053	1,196	1,202	0,797
$\chi_{spectro} \chi_{count}$	3,151	0,499	7,745	16,328	23,218	30,764	39,845	48,747	52,058	37,162
Quality factor ρ	0	0	0,011	2,487	6,251	9,9	11,528	10,649	7,629	5,66
Optimal factor ψ	0	0	0,085	40,605	145,128	304,562	459,325	519,422	397,129	210,331

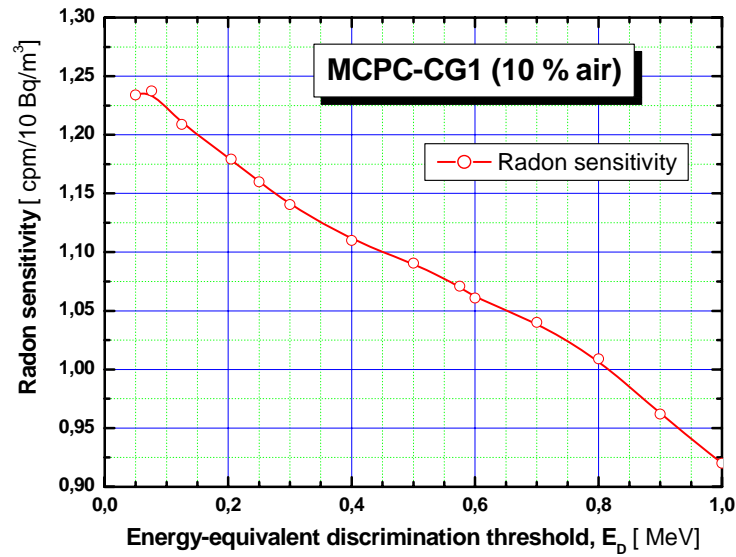


Figure 11 : Evolution of MCPC radon sensitivity against the set discrimination threshold (energy-equivalent) in the CG1 configuration (10 % air).

7. Selection of the optimum discrimination level

In order to check the suitable value of the discrimination level, we have studied the effect of the chosen discrimination threshold (energy-equivalent) on some defined statistical factors : Attachment Effect Loss (AEL), Grid Opacity Effect Loss (GOEL), Wall Effect Loss (WEL), End Cell Contribution (ECC) fraction, using RADON-MCPC code. We show in figure 11 the decrease of the resulting MCPC radon sensitivity when the bias level (energy-equivalent) is increased from 0.1 up to 1 MeV. Since there exists a strong background down to about 150 keV, one has to select the discrimination threshold above 250 keV in order to ensure a good compromise between a counting stability, avoiding the high rate fluctuations of the intrinsic background count rate, and a sufficiently high value of radon sensitivity.

8. Selection of the suitable gas flow rate

To determine the suitable value of the gas flow rate, Q , the behaviour of the activity of alpha emitting isotopes within the counter, as a response to a sudden Gaussian-shaped radon pulse, assuming three typical values of Q : 1 l/min, 5 l/min and 10 l/min are shown on figure 12. Taking as a requirement, a lowest counting gas consuming (thus a longest time autonomy), together with the ability of the counter to follow as closely as possible airborne radon activity variation, we have concluded that adopting the value of $Q = 10$ l/minutes seems a quite reasonable choice.

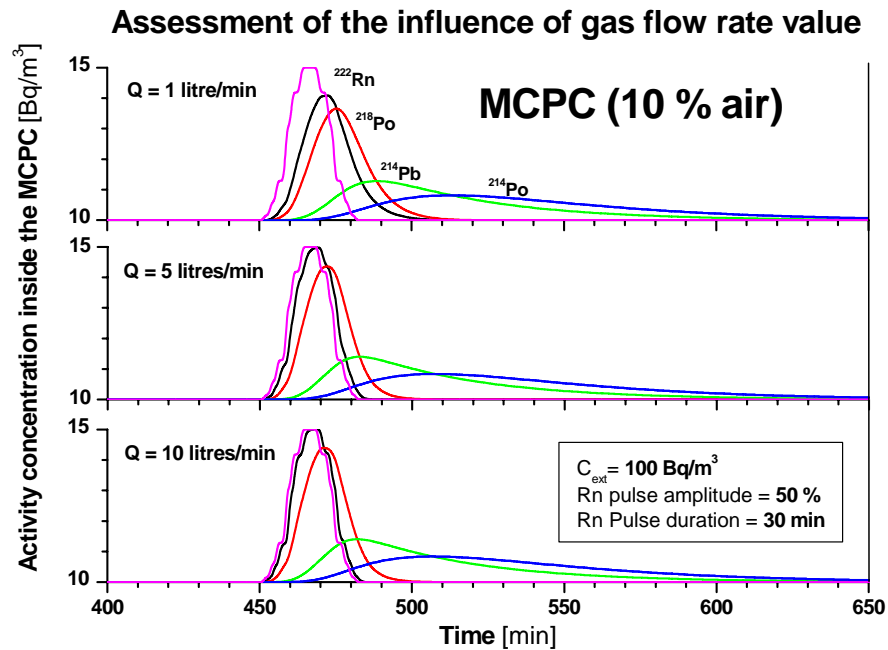


Figure 12 : Evolution of the radon and its progenies activities inside the counter as a response to a Gaussian-shaped pulse of radon activity variation in ambient air assuming three typical gas flow rates in the CG1 configuration (10 % air).

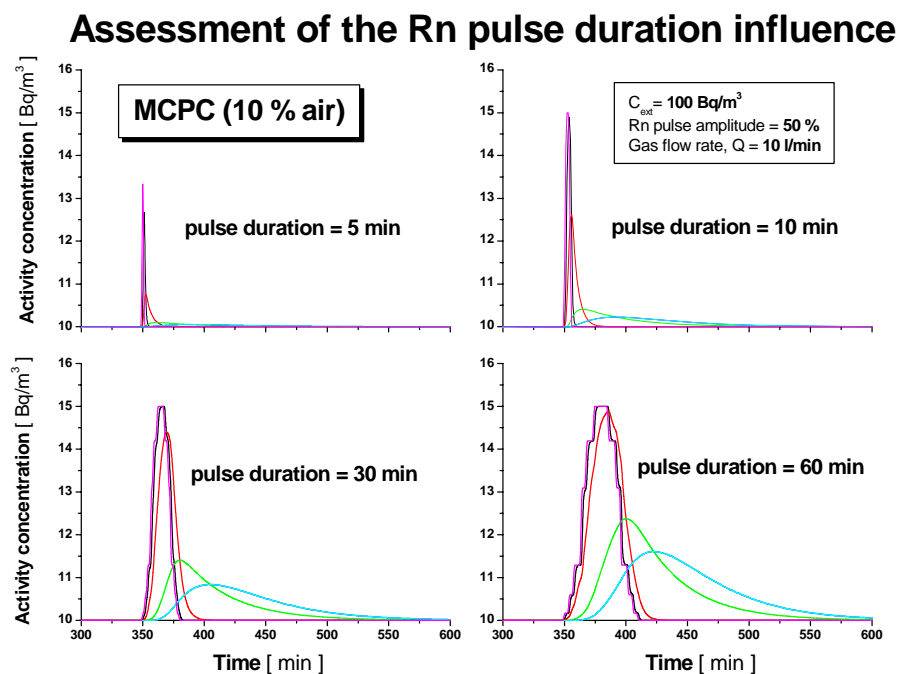


Figure 13 : Evolution of the radon and its progenies activities inside the counter as a response to a Gaussian-shaped pulse of radon activity variation in ambient air assuming three typical gas flow rates in the CG1 configuration (10 % air).

9. Response to a short duration radon pulse : Measurement time period

Since a fast response of the counter and as short as possible time assessment are desired, one has obviously to minimize the measurement time period. But, unfortunately, for low radon levels, which are often encountered in practice, the recorded alpha counting rates are also too low and the unavoidable statistical fluctuations involved give rise to large uncertainties.

In order to assess the suitable counting time period, we studied the MCPC response to sudden radon pulses, keeping as a requirement their temporal resolution. We show in figure 13, the in-MCPC activity behavior as a response to a sudden 50 % relative amplitude radon pulse variations of pulse durations of 5, 10, 30 and 60 minutes, where one can notice that when adopting a gas flow rate of 10 l/min, the counter follows closely the radon transient if its total duration is greater than 30 minutes, which should be considered rather a fast transient, giving the fact radon significant variations are typically of the hour orders. In figure 14, we show the MCPC response to sharp radon pulse variations of 15%, 30% and 50 % relative amplitude above an average airborne radon level of about 100 Bq/m³, for radon pulse durations of 10 min and 30 min respectively. We can see that by adopting a counting time period of 10 min and a measurement sampling frequency of 1 measurement/minute, it is possible to resolve 30 minutes duration radon pulse variations of only 15 % relative amplitude above a mean radon level of 100 Bq/m³. The suitable value of the measurement time period t_0 was fixed therefore to 10 minutes which was found more convenient, taking also into account the following parameters:

- the total sensitive volume V_c ,
- the detection limit,
- the gas flow rate Q ,
- the counter detection efficiency,
- the background level,
- typical α count rates,
- counting statistic's errors,
- alpha spectrum quality,
- quasi continuous measurement operation.

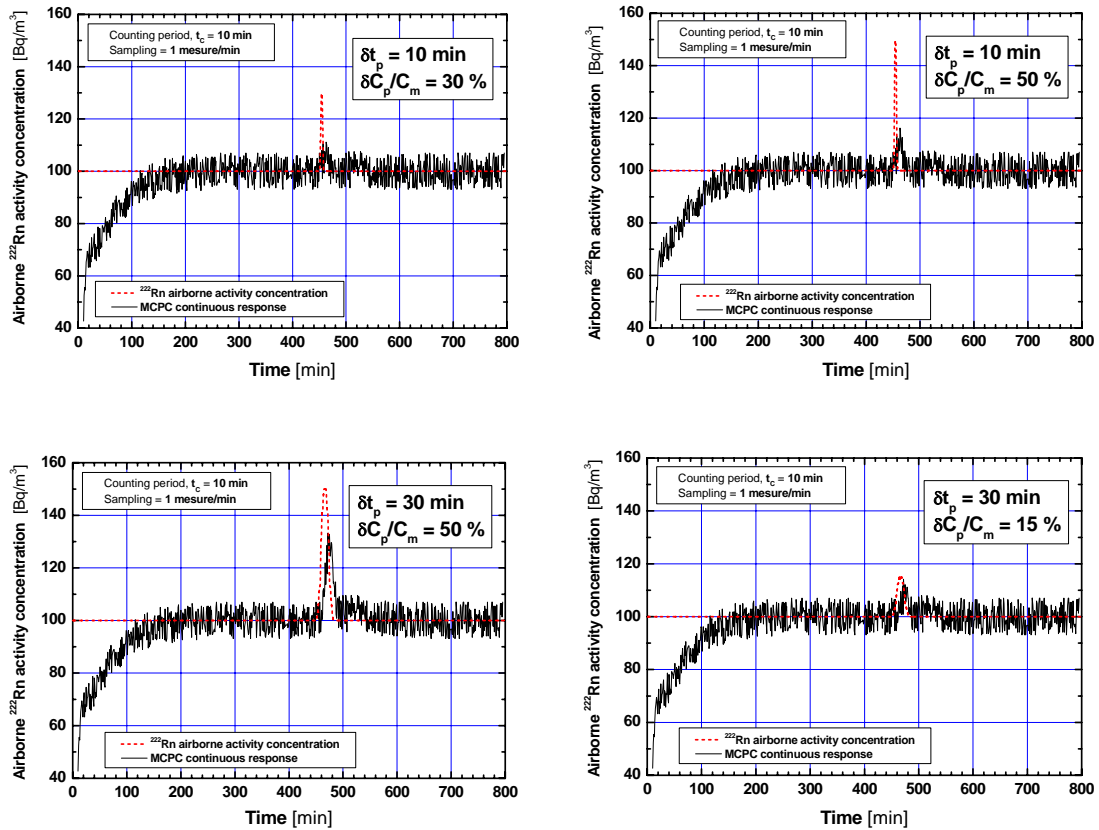


Figure 14 : MCPC response to sharp radon pulse variations of 15%, 30% and 50 % relative amplitude above a 100 Bq/m^3 average radon level, for 10 min and 30 min radon pulse durations. The adopted counting time period is 10.

10. Conclusion

A new proportional counter model, baptized Multiple Cell Proportional Counter (MCPC), intended for continuous airborne radon activity concentration measurements is described and its operation principle presented. This gas-flow proportional counter, consisting in a pile-up of 20 separate proportional counter elements, uses an argon-propane (1%) as a binary gas mixture to which is admixed an appropriate fraction of ambient air, in which radon activity concentration has to be continuously measured through a periodic counting of the α particles emitted by ^{222}Rn and its short-lived decay products within its well defined sensitive volume. A Monte Carlo simulation program, which takes into account the major physical processes involved that determine directly the detector performances, has been written and used for design optimization purposes. According to preliminary design calculations the MCPC model, now under construction, should achieve an α

counting efficiency greater than 100 %. The simulation results also show that the admixture of 10 % of ambient air seems to be sufficient to continuously assess radon concentration levels ranging from about 15 Bq/m³ up to 1.5 10⁵ kBq/m³ for an integral counting period of 10 minutes, when setting the energy discrimination at 250 keV. The expected radon sensitivity is about 1 cpm /10 Bq·m⁻³, achieving thus a measurement accuracy of ± 10 Bq/m³ at a mean radon concentration level of 100 Bq/m³ for 10 min detector time response.



References:

- [1] A.C. George, “An overview of instrumentation for measuring environmental Radon and Radon progeny”, IEEE Trans. on Nucl. Sci., Vol.37, n°2, (1990) 892-901.
- [2] A. George, *State-of-the-art instruments for measuring radon/thoron and their progeny in dwellings—a review*, *Health Phys.* **70** (1996) (4), pp. 451–463.
- [3] G. Curzio, D. Mazed, R. Ciolini, A. Del Gratta, A Gentili, “Effect of air on gas amplification characteristics in argon-propane (1 %)-based proportional counters for airborne radon monitoring”, *Nucl. Instr. and Meth.*, **A 537** (2005)672-682.
- [4] D. Klein, R. Barillon, S. Demongeot, E. Tomasella, A. Chambaudet, “Investigative techniques for Radon Level characterization”, *Rad. Meas.*, Vol. **25**, n°1-4 (1995)553.
- [5] L. Zikovsky, “Determination of radon-222 in gases by alpha counting of its decay products deposited on the inside walls of a proportional counter”, *Rad. Meas.*, **24** (1995) 315-317
- [6] A. Klett, W. Reuter, L. De Mey, “Dynamical calibration of an aerosol monitor with natural and artificial alpha-emitters”, *IEEE Nucl. Symp.*, **2** (1996) 875-876.
- [7] W.R. Russ, D.O. Stuenkel, J.D. Valentine, K.C. Gross, “Improved radioxenon detection techniques for use with fluid-based concentration”, *IEEE Trans. on Nucl. Sci.*, **47** (2000) 908-913.
- [8] G. Heusser, W. Rau, B. Freudiger, M. Laubenstein, M. Balata and T. Kirsten, “²²²Rn detection at the \square Bq/m³ range in nitrogen gas and a new Rn purification technique for liquid nitrogen”, *Appl. Rad. And Isot.*, **52** (2000) 691-695.

- [9] I. Busch, H. Greupner, U. Keyser, “*Absolute measurement of the activity of ^{222}Rn using a proportional counter*”, Nucl. Instr. and Meth. A **481** (2002) 330-338.
- [10] G. Zuzel, *Highly sensitive measurements of ^{222}Rn diffusion and emanation*, in AIP Conference Proceedings, **785** (2005) 142-149
- [11] D. Mazed, G. Curzio, R. Ciolini, “*Monte Carlo simulation of a new air-mixed gas-flow proportional counter for on-line airborne radon activity measurements*”, Communication presented at the 4th European Conference on Protection Against Radon at Home and at Work, June 28-July 2, 2004, Prague, Czech Republic.
- [12] D. Mazed, R. Ciolini, G. Curzio, “*Monte Carlo Simulation and Modelling of a Radon Multiple Cell Proportional Counter (MCPC)*”, submitted for publication to *Radiation Measurements* (Review process in course).
- [13] D. Mazed, R. Ciolini, “*Gas gain in air-mixed argon propane (1%) based proportional counters*”, Communication presented at the 11th International Congress of the International Radiation Protection Association, IRPA’11, May 23-28, 2004, Madrid, Spain.
- [14] Dahmane Mazed, Giorgio Curzio, Riccardo Ciolini, “*Conception optimisée par simulation Monte Carlo d’un Compteur Proportionnel Multiélément destiné à la Mesure du Radon dans l’Air*”, Communication presented at the SFRP National Radiation Protection Congress, Nantes (France) 14-16 June 2005.
- [15] D. Mazed, R. Ciolini, G. Curzio, A. Del Gratta, “*A new active method for continuous radon concentration measurements based in a Multiple Cell Proportional Counter (MCPC)*”, submitted for publication to *Nuclear Instruments and Methods in Physics Research*, (review process in course NIMA-D-06-00783).
- [16] D. Mazed, G. Curzio, R. Ciolini, A. Del Gratta, “*Mise au point d’une nouvelle méthode active pour la mesure en continu du radon dans l’air ambient*”, communication accepted for oral presentation at the SFRP National Congress of Radiation Protection, at Reims (France), 19-21 June 2007.



Section IV

The Monte Carlo Simulation code RADON-MCPC

1. Simulation of gas-filled detectors

In order to achieve a well optimized design of a given gas detector, it would be very helpful to simulate as accurate as possible the major physical processes involved within the operation of such a device.

Detectors based on the registration of ionization produced by charged particles in gases are still widely used in many areas of experimental nuclear physics and especially for radiation protection purposes. Their main role is the detection and counting of incident particles when passing across the gas detector sensitive volume. The amount of ionization deposited therein can thus be measured with a consistent precision and thus gives information about the particle energy. Despite the wide use of gas-filled detectors, their computer modeling still represents a difficult problem. The large variety of phenomena and microscopic processes involved is difficult to simulate realistically or to reproduce reliably in a phenomenological way. The existing models are approximate and based on combining microscopic modeling of some phenomena and well-established experimental features of the others.

When a charged incident particle passes through matter, it transfers part of its energy to atoms through inelastic collisions. This energy is dissipated in matter and results in ionization of atoms of the filling gas. After that, the liberated electrons remain free for some significant time of about 1-2 ns, depending the local strength of the electric field to gas pressure ratio. Together with ions, they constitute the initial ionization. The modeling of the exact number of these primary electrons, their spatial distribution along the particle track, and their energy distribution along their drift process within the gaseous medium for reaching their respective collecting electrodes, are still difficult to achieve with a reliable accuracy. However, many macroscopic features are well known which give a sufficient description (collective behaviour) of their transport properties (macroscopic coefficients) for what concerns us within the subject at hand.

On the other hand, when dealing with charge amplifying detectors, such as proportional counters, the established spatial distribution of the electric field to pressure ratio exhibits two distinguishable spatial regions : in the first, called drift region, defined by low values of the electric field to pressure ratio, the free electrons, characterized by a correspondingly low kinetic energy, move slowly in low-spreaded electron swarm, following the electric field lines. In the second region, called Townsend region and located in the vicinity of the thin anode wires, the gas multiplication of liberated electrons takes place and is developed therefore a gas-amplified measurable electrical pulse output. Many important characteristics of the proportional counters and drift chambers are then deduced from consistent assessment of these two major processes in cascade :

- ◆ the incident charged particle stopping process, the amount and spatial distribution of the initial ionization (primary charges), and some undesired incidental effects that perturb the detection process have to be assessed, such as some sudden encounters of the detector wall or some incorporated material structure delimiting spatially and defining electrically the sensitive volume: detector walls, electrodes, grids, field shaping structures etc.

- ◆ the primary electrons (and positive ions) drift process along the electric field lines towards the anode wire, during which a number of important phenomena have to be also taken into account : the electron removal from the swarm population, inherent to the attachment to electronegative atoms or molecules (electron attachment) which could be present in the gaseous medium, the secondary electron production through diverse ionization processes (direct electron ionizing impacts, dissociative ionization, photoionization and so on, as described by the three Townsend coefficients).

Since we have a significant knowledge of those basic phenomena, and by adopting some simplifying assumptions, it is possible to write computer codes permitting an acceptable prediction of a great number of important electron transport coefficients that describe their macroscopic properties in gases [1-2]. Some existing codes, such as MAGBOLTZ [3], allowing the computation of the electron energy distribution function, can also predict their relative macroscopic transport coefficients which are effectively measurable with great precision.

Therefore, using simulation programs, more detailed characteristics of gas detectors can be drawn from numerical evaluation of the underlying microscopic processes. Complete models, such as GARFIELD [4], include also simulation of the drift of electrons and ions to chamber electrodes with various additional effects such as attachment, recombination, diffusion, fluorescence, avalanche amplification in the vicinity of the wires, space charge, charge induction at electrodes, influence of magnetic field and so on. The complete simulation however still remains a tedious challenging task.

In our case, a Monte Carlo simulation code, called RADON-MCPC, was written in order to complete and to ascertain the optimization of the designed MCPC prototype model dedicated for on-line assessment of airborne radon activity concentration. It is the scope of this section to describe in full details this simulation code.

2. Description of the Monte Carlo simulation code RADON-MCPC

The code is written following a highly flexible modular structure such that it can be readily adapted to simulate any other gas detector of a given geometry (cylindrical proportional counters, ionization chambers etc.). It carries out all the calculations necessary for a good prediction of the expected detector characteristics and performances such as the alpha pulse height spectra which should be delivered by the MCPC as a response to an assumed ^{222}Rn activity concentration, $C_{ext}(t)$, in the ambient air.

The general flow-chart of RADON-MCPC code is shown in figure 1. This code integrates many modular subroutines in order to take into account the major physical processes involved during its operation, such as :

- ◆ the time-varying concentrations of ^{222}Rn and its short lived progenies (^{218}Po , ^{214}Pb , ^{214}Bi and ^{214}Po) inside the counter, during the whole measurement period, for a given ^{222}Rn activity concentration (C_0) in the ambient air, the admixed air fraction f and the assumed gas flow rate Q . Thus, using the simulation program, the equilibrium factors inside the counter can be exactly computed at any time if the radon activity concentration $C_{ext}(t)$ in the ambient air is known. All these calculations are carried out by ACTIVITY subroutine;
- ◆ the electric field distribution throughout the sensitive volume, computed by a set of separated functions;

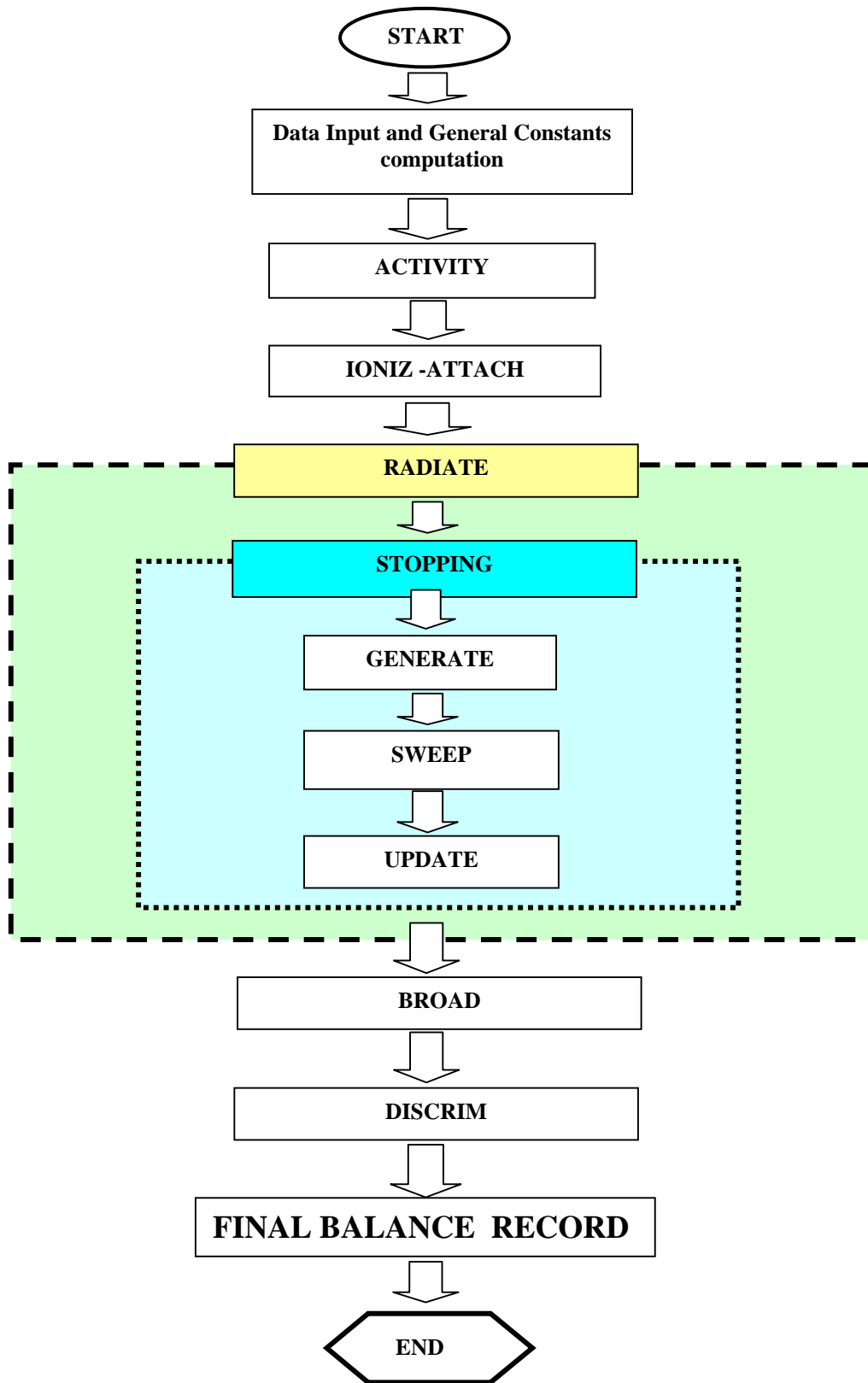


Figure 1 : *RADON-MCPC* flow-chart describing the general structure of the code and showing only the subroutine modules.

- ◆ the energy-expenditure during the alpha stopping process in the air-mixed gas mixture and the wall effect (i.e., when the α particles are incidentally stopped by the detector walls, before depositing all their initial energy within the sensitive volume) are carried out by the STOPPING subroutine;
- ◆ the primary electron-ion pairs production rate along the alpha tracks (the δ -rays taken into account indirectly), is taken into account within the SWEEP subroutine;
- ◆ the electron attachment coefficient and its dependence on the electric field to pressure ratio E/P , computed within the IONIZ-ATTACH subroutine and thereafter is integrated within SWEEP subroutine;
- ◆ the voltage-dependence of the gas amplification process in the vicinity of the anode wires. It is computed within the IONIZ-ATTACH subroutine and therefore it is integrated within the SWEEP subroutine
- ◆ the statistical fluctuations resulting in the Gaussian broadening of the alpha pulse height spectra. It is carried out through the BROAD subroutine.

It is the purpose of this chapter, to present in details how are modeled the above enumerated physical processes.

3. The activity concentration evolution of ^{222}Rn and progenies in the counter

^{222}Rn is produced in the natural decay chain of ^{238}U and it has various decay products which are also radioactive. According to their half-lives, these are divided into short-lived and long-lived progenies as listed in table 1 and figure 2 show a representative decay scheme related to the ^{226}Ra family.

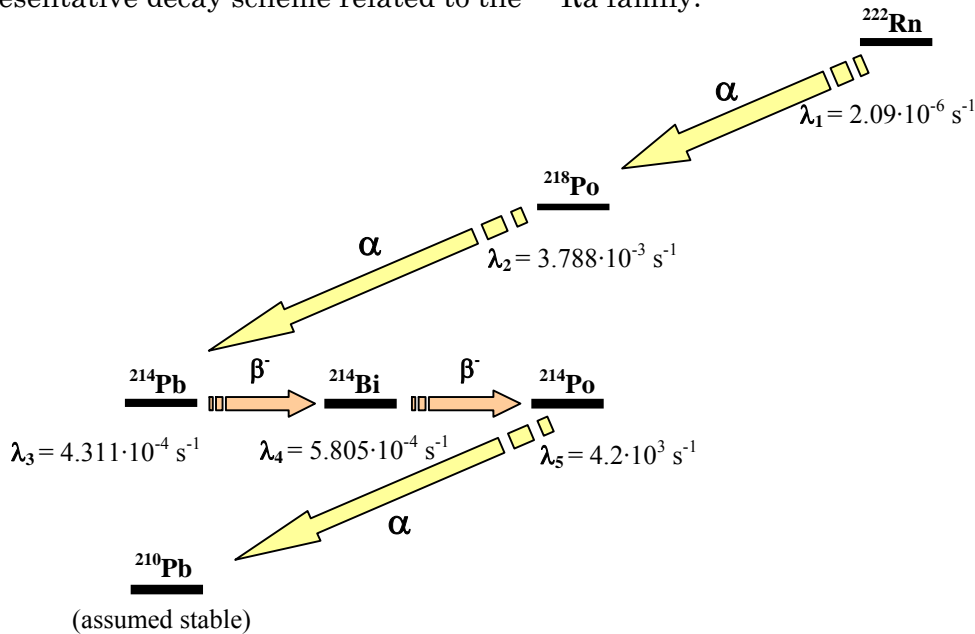


Figure 2 : The radioactive decay scheme of radon (^{222}Rn).

Table 1 : Decay mode, particle energy, decay constant and half life time of radon and its progenies [5]. In the first column are specified the label number for each nuclide adopted throughout the present thesis.

Label	Nuclide	Decay mode	Main energy	Half-life	Decay constant	Type
1	^{222}Rn	α	5.489 MeV	3.82 d	$2.09 \cdot 10^{-6} \text{ s}^{-1}$	short-lived
2	^{218}Po	α	6.002 MeV	3.1 min	$3.788 \cdot 10^{-3} \text{ s}^{-1}$	short-lived
3	^{214}Pb	$\beta - \gamma$	352 keV (γ)	26.8 min	$4.311 \cdot 10^{-4} \text{ s}^{-1}$	short-lived
4	^{214}Bi	$\beta - \gamma$	609 keV (γ)	19.9 min	$5.805 \cdot 10^{-4} \text{ s}^{-1}$	short-lived
5	^{214}Po	α	7.687 MeV	164 μs	$4.234 \cdot 10^3 \text{ s}^{-1}$	short-lived
6	^{210}Pb	$\beta - \gamma$	46.5 keV (γ)	8145 d	$4.234 \cdot 10^3 \text{ s}^{-1}$	long-lived
7	^{210}Bi	$\beta - \gamma$	1.2 MeV (β)	5.013 d	$1.60 \cdot 10^{-6} \text{ s}^{-1}$	long-lived
8	^{210}Po	α	5.304 MeV	138.4 d	$8.36 \cdot 10^{-8} \text{ s}^{-1}$	long-lived
9	^{210}Pb	-	-	-	-	stable

First of all, RADON-MCPC code computes the time evolution of the concentrations of ^{222}Rn and of its short lived progenies (^{218}Po , ^{214}Pb , ^{214}Bi and ^{214}Po) inside the counter sensitive volume V_c for the adopted value f of the air fraction mixed to binary gas mixture, assuming a value Q of the gas-flow rate. During air pumping, only radon gas is allowed to enter the counter through a suitably chosen membrane filter, retaining all the other solid-state aerosols, especially all radon daughters isotopes are not allowed to enter the sensitive volume, whilst the effect of thoron gas (^{220}Rn) and also other airborne α -emitting gas traces are neglected. Therefore, at any time the equilibrium factor inside the counter could be exactly known.

The actual time-dependent concentrations $C_i(t)$ of ^{222}Rn ($i = 1$), ^{218}Po ($i = 2$), ^{214}Pb ($i = 3$), ^{214}Bi ($i = 4$) and ^{214}Po ($i = 5$), inside the counter and also the integrated alpha activity, evaluated with a sampling period t_0 , is computed analytically for each alpha emitter according to the following radioactive equilibrium equations :

$$^{222}\text{Rn} : \quad \frac{dC_1(t)}{dt} + (1 + \beta)\lambda_1 C_1(t) - f\beta\lambda_1 C_o = 0 ; \quad \text{where} \quad \beta = \frac{Q}{V_c} \frac{1}{\lambda_1}$$

$$^{218}\text{Po} : \quad \frac{dC_2(t)}{dt} + \lambda_2 C_2(t) = \lambda_1 C_1(t)$$

$${}^{214}\text{Pb} : \quad \frac{dC_3(t)}{dt} + \lambda_3 C_3(t) = \lambda_2 C_2(t) \quad (1)$$

$${}^{214}\text{Bi} : \quad \frac{dC_4(t)}{dt} + \lambda_4 C_4(t) = \lambda_3 C_3(t)$$

$${}^{214}\text{Po} : \quad \frac{dC_5(t)}{dt} + \lambda_5 C_5(t) = \lambda_4 C_4(t)$$

where, the λ_i ($i = 1,2,3,4,5$) stand for the decay constants of the corresponding isotopes and are listed in table 1. At each time, t , the integrated alpha activity, $n_\alpha(t_0, t)$, in the counting volume, assuming a sampling period t_0 , is analytically computed according the following expression

$$n_\alpha(t_0, t) = V_c \int_{t-t_0}^t (\lambda_1 C_1(t') + \lambda_2 C_2(t') + \lambda_5 C_5(t')) dt' \quad (2)$$

The expected MCPC alpha count rate $N_\alpha(t)$ is thereafter numerically computed using several subroutines that will be described in next sections.

3.1. The radioactive equilibrium inside the counter

The equilibrium factor F and the unattached fraction of the progenies play a central role in the estimation of the lung dose from radon activity concentration $C(^{222}\text{Rn})$ measurements. Since the dose directly caused by radon is small compared to that from the progenies for almost all practical situations in radiation protection, the study of the airborne radon progeny activity concentration is of great importance. The quantity which defines the fraction of short-lived radon progeny activity concentration within the counter in comparison with the radon activity concentration is the equilibrium factor F , given by :

$$C_{eq} = 0.106 C_2 + 0.513 C_3 + 0.381 C_4 + 5.2 \cdot 10^{-8} C_5 \cong 0.106 C_2 + 0.513 C_3 + 0.381 C_4$$

$$F = \frac{C_{eq}}{C_1}, \quad F \in [0, 1] \quad (3)$$

such that at, at radioactive equilibrium condition, one has $F = 1$.

it can be understood as a relative measure (normalized to one and weighted for each progeny according to its potential α -energy [6]) of the fraction of short-lived progenies either in equilibrium or not in equilibrium

Our calculations show that the radioactive equilibrium inside the counter is achieved after a flushing time t_{eq} that depends weakly on the value of the gas flow rate Q and the air fraction f in the mixture. We show in figure 3 the evolution of the

activity concentration of radon and its progenies inside the counter when a fraction $f = 10\%$ of air is added to the argon-propane (1%) gas mixture for two values of the gas flow rate: $Q = 10$ l/min and $Q = 1$ l/min. The radioactive equilibrium is achieved for a time $t_{eq} = 240$ min and $t_{eq} = 260$ min respectively. In equilibrium saturation condition, the activities of all the radioactive species present within the counter should be the same, i.e.,

$$a_1(t_s) \approx a_2(t_s) \approx a_5(t_s) \approx \frac{1}{3} A_t(t_s) \quad (4),$$

where $A_t(t_s)$, is the total alpha activity within the sensitive volume.

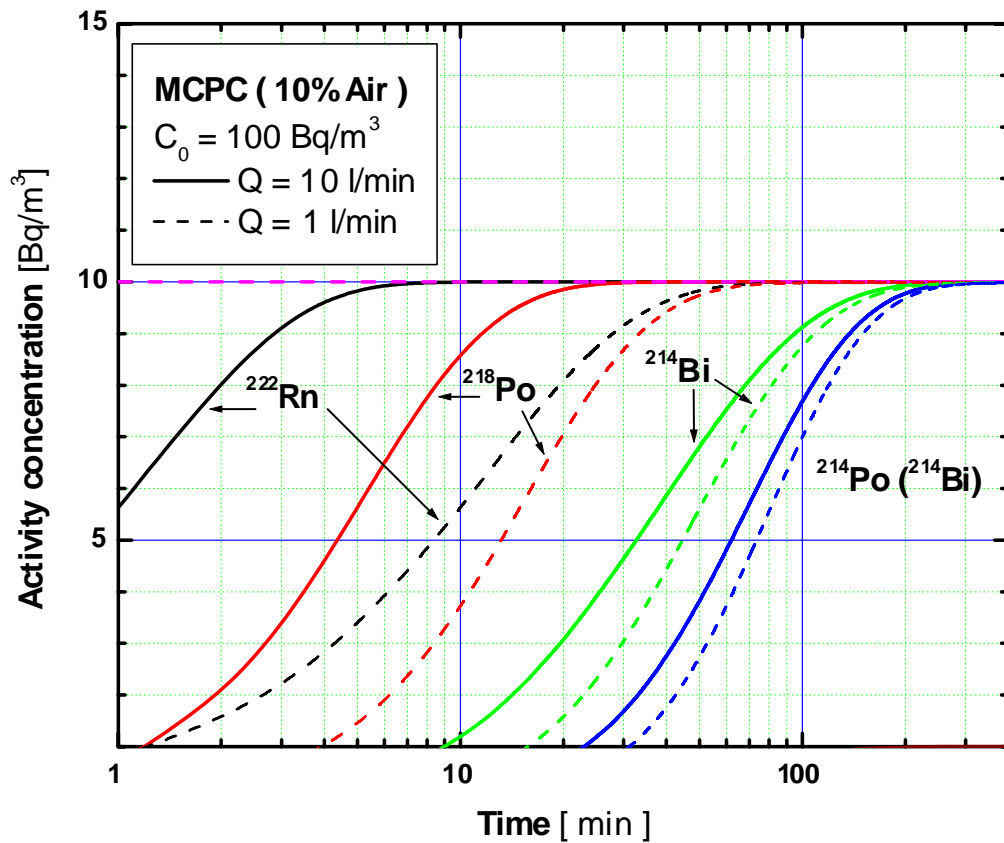


Figure 3 : Evolution of the activity concentration of radon and progenies inside the MCPC when 10 % of air is added to argon-propane (1%) for two values of gas flow rate : $Q = 10$ l/min (solid lines) and $Q = 1$ l/min (dashed lines). The radioactive equilibrium is achieved at $t_s = 240$ min and $t_s = 260$ min respectively.

3.2. Response to a stepwise variation of radon activity concentration

In the simulation, we have also considered a basic case of radon activity concentration behavior in ambient air, such as schematized in figure 4. It is first assumed that the ^{222}Rn activity concentration in air is nearly constant and equals C_0 . Taking as the time origin the beginning of gas circulation through the counter, and after a certain time period t_{pi} greater than the equilibrium time t_e required for reaching the radioactive equilibrium of all the short lived radioactive daughters that are continuously produced inside the counter (cf, table 1), we consider a prompt jump of radon activity concentration in the ambient air to a higher level intensity $(1+\delta)C_0$ and, at a time t_{pf} , the airborne radon concentration falls down to a lower level $(1-\gamma)C_0$.

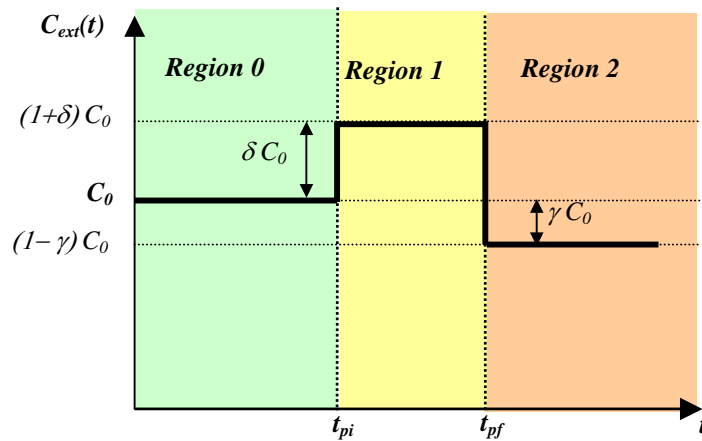


Figure 4: A basic example of the assumed behaviour of the radon activity concentration $C_{ext}(t)$ in ambient air.

Figure 5 shows typical evolutions of the activity concentrations of ^{222}Rn , ^{218}Po , ^{214}Pb , ^{214}Bi and ^{214}Po , obtained when the airborne radon activity concentration in air is assumed to follow the stepwise profile schematized in figure 4. While figure 6 shows the evolution of the integrated alpha activities for 10 minutes period.

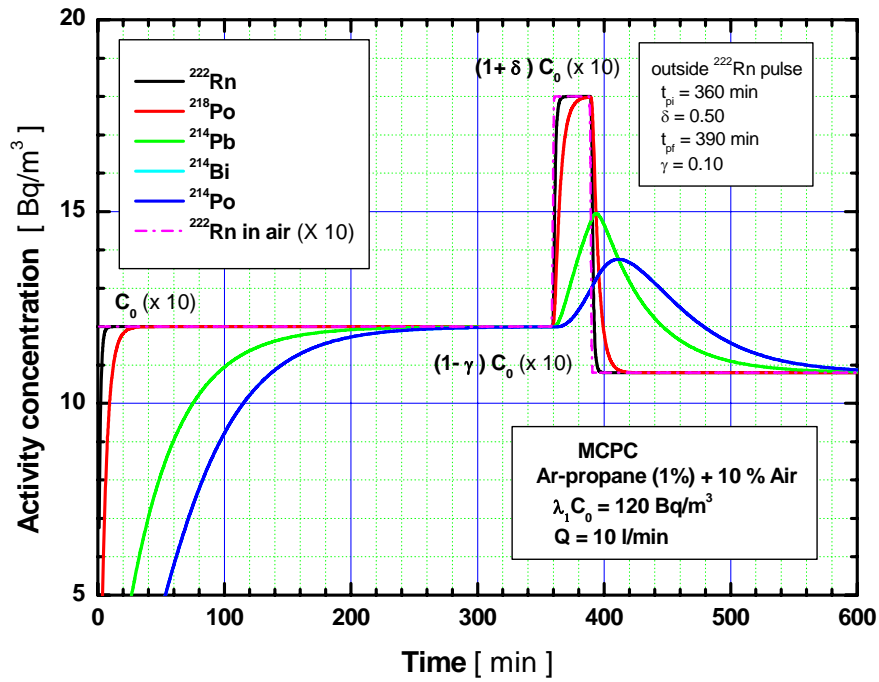


Figure 5: Time evolution of the activity concentration of radon and its decay products inside the counter. The assumed stepwise variation of radon activity concentration in ambient air is shown in figure 4.

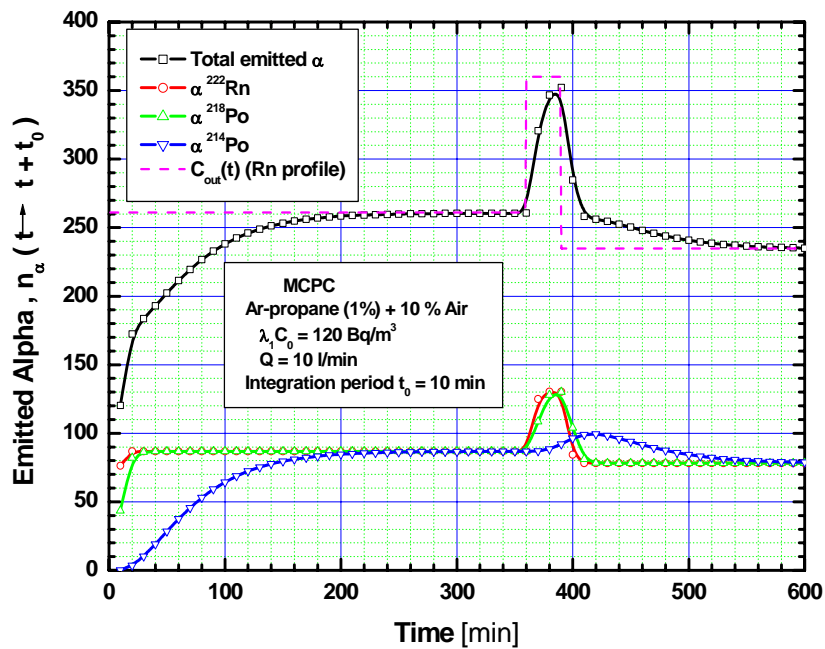


Figure 6: Total alpha activity inside the sensitive volume of the counter corresponding to the stepwise radon variation shown in figure 3. Each measurement point represents the integrated activity for a period of 10 minutes.

3.3. Response to a Gaussian-shaped radon pulse transient

In order to assess the response of the counter to a sudden radon pulse in air, we have simulated the following case. It is first assumed that the ^{222}Rn activity concentration in air, C_0 , is nearly constant, assumed to be $C_0 = 100 \text{ Bq/m}^3$. Also as earlier, taking as the time origin the beginning of gas circulation through the counter, and after a certain time period t_p ($= 462 \text{ min}$) greater than the equilibrium time t_{eq} required for reaching the radioactive equilibrium inside the counter, we consider a sudden radon pulse variation characterized by a Gaussian shape, 50 % relative amplitude (referring to the assumed stationary level C_0) and 30 min total time duration (14 min at half maximum). The simulation results are sketched in figure 7, where are shown the corresponding evolution of activity concentration of radon and progenies inside the counter, when a fraction of 10 % of air is added to the binary gas mixture (Argon-propane (1%)) assuming two values of the gas flow rate: namely, $Q = 10 \text{ l/min}$ and $Q = 1 \text{ l/min}$.

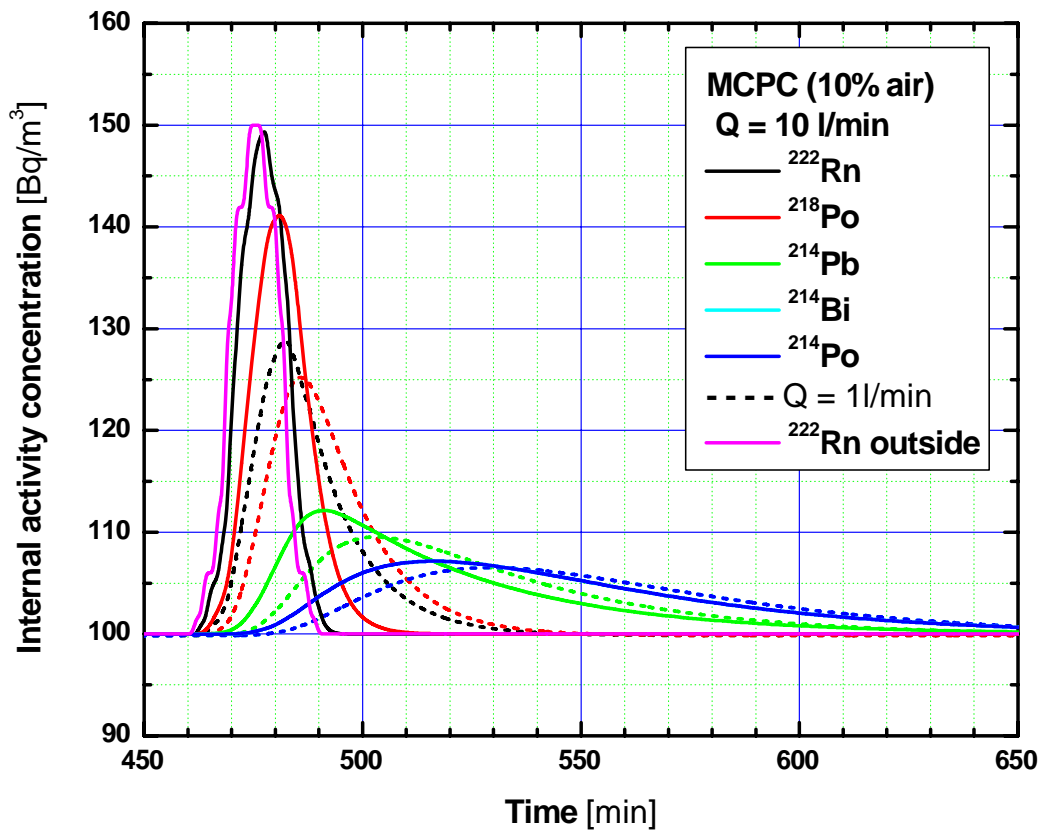


Figure 7: Time evolution of the activity concentration of radon and its decay products inside the counter as a response to a sudden Gaussian shape radon pulse in ambient air.

One can notice that while adopting the higher gas flow rate value ($Q=10$ l/min) the radon concentration inside the counter peaks nearly at 149.63 Bq/m³ almost 3 minutes after the radon pulse in air (outside) has reached its maximum amplitude (150 Bq/m³), while assuming the lower gas flow rate value ($Q=1$ l/min), radon activity concentration inside the counter peaks only at 128.83 Bq/m³ after rather a long delay time of 21 minutes, i.e., only 9 minutes before the total fall-down of the radon transient outside. Though the radioactive equilibrium inside the counter depends weakly on the adopted gas flow rate value, one can conclude that when increasing the gas flow rate, the internal activity concentration of radon and progenies tend to follow closely that prevailing outside, especially that of ²²²Rn and ²¹⁸Po. Thus, the integrated alpha activities are much more increased for a fixed sampling time period, and therefore the counter response is much faster. Since the designed MCPC should be able to resolve also sudden as weak as possible radon variations above a given mean activity concentration level, in shortest delay time, one has therefore to adopt the highest value possible of gas flow rate. But, we have also to make a good compromise, since we have to avoid excessive consuming rates of gas mixture.

4. *The derivation of the electric field distribution*

RADON-MCP code integrates also a set of functions that compute the established unperturbed electric field distribution within each cell. For this purpose, we define in one cell the x and y axis on the anode plane, respectively perpendicular and parallel to the anode wires, having their common origin on the central anode axis, whereas the z axis is taken perpendicular to the same anode plane, always having the same origin (cf. figure 8).

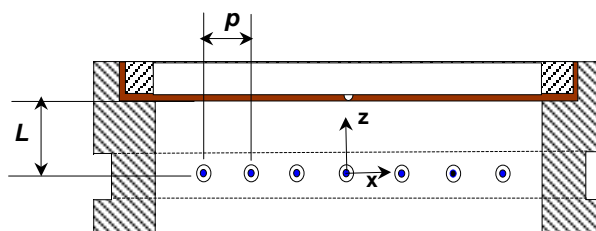


Figure 8: A sketch of a single cell assumed for electric field distribution computation.

Though the apparent complexity of the counter electrodes structure, the spatial distribution of the electrostatic potential and related distribution of the electric field to pressure ratio can be derived analytically, using the electrostatic Maxwell equations:

$$\begin{aligned} \vec{E} &= -\vec{\nabla}V \\ \text{div } \vec{E} &= 0 \quad \Rightarrow \quad \Delta V = \frac{\partial^2 V}{\partial x^2} + \frac{\partial^2 V}{\partial y^2} + \frac{\partial^2 V}{\partial z^2} = 0 \end{aligned} \quad (5)$$

The obtained Laplace equation (5) should be solved for each point (x,y,z) of the restricted space domain delimited by :

$$\begin{aligned} a &\leq x \leq p/2 \\ y^2 &\leq (R^2 - x^2) \\ a &\leq z \leq (L - a) \end{aligned} \quad (5-a)$$

assuming the following boundary conditions

$$\begin{aligned} V(a, y, z) &= V_0 \\ V(x, y, a) &= V_0 \\ V(x, y, L) &= 0 \end{aligned} \quad (5-b)$$

adopting the geometry approximations :

$$\begin{aligned} R &\gg a \quad ; \quad L \gg a \quad ; \quad p \gg a \\ R &\gg p \quad ; \quad R \gg L \end{aligned} \quad (5-c)$$

and making use of the fact that farer from the anode wire plane, i.e.,

$$x \gg a \quad \text{and} \quad z \gg a$$

the electric field distribution is almost uniform, thus the analytic expression of the potential distribution is simply given by

$$\begin{aligned} \frac{\partial V(x, y, z)}{\partial x} &= 0 \\ \frac{\partial V(x, y, z)}{\partial y} &= 0 \end{aligned} \quad \Rightarrow \quad V(x, y, z) \equiv V(z) \approx \frac{(L - z)}{(L - a)} V_0 \quad (5-d)$$

The geometry approximations (5-c and 5-d) are quiet consistent and induce only a negligible error, since the anode wire radius, a , is about 50 μm , and the pad p of the anode wire array is about 2 cm; and the anode-cathode separation distance L is about 1.5 cm, where as the cell radius R , is about 8 cm.

Since the anode wires are assumed parallel to OY axis and taking due account of the fact that the cell radius R is much greater than the anode-electrode distance (see equations (5-c)), the electrostatic potential distribution should not depend on y -coordinate. Thus,

$$V(x, y, z) \equiv V(x, z)$$

The analytical solution of the electrostatic potential distribution $V(x,y,z)$ throughout the defined space domain is therefore derived as follows :

$$V(x,z) = q_l \text{Ln} \left[\sin^2 \left(\frac{\pi x}{p} \right) + \sinh^2 \left(\frac{\pi z}{p} \right) \right] \quad (6-a),$$

where, q_l is the established anode wire linear charge density (assumed uniform), from which is deduced the electrostatic potential distribution within the whole cell sensitive volume, and thereafter, within the entire counter sensitive volume, by making use of the evident geometrical symmetry conditions, such as :

$$\begin{aligned} V(x,z) &= V(-x,z) = V(x,-z) = V(-x,-z) \\ V(x,z) &= V(kp-x,z) \quad (x \geq a; \quad z \geq a; \quad k : \text{integer and } kp-x \leq R) \\ V(x,z) &= V(kp+x,z) \quad (x \geq a; \quad z \geq a; \quad k : \text{integer and } kp+x \leq R) \\ V(x,z) &= V(x,z+kL) \quad (x \geq a; \quad z \geq a; \quad k : \text{integer and } -H/2 \leq (kL+z) \leq H/2) \end{aligned} \quad (6-b)$$

b)

The resulting particular components of the electric field are then derived using the Maxwell formulae and are stated as follows

$$V(0,z) = 2q_l \text{Ln} \left[\text{sh} \left(\frac{\pi z}{p} \right) \right] \Rightarrow E_y = \frac{2\pi q_l}{p} \text{coth} \left(\frac{\pi z}{p} \right) \quad (\text{for } x=0) \quad (7-a),$$

$$V(x,0) = 2q_l \text{Ln} \left[\sin \left(\frac{\pi x}{p} \right) \right] \Rightarrow E_x = \frac{2\pi q_l}{p} \cot g \left(\frac{\pi x}{p} \right) \quad (\text{for } z=0) \quad (7-b),$$

$$V\left(\frac{p}{2}, z\right) = 2q_l \text{Ln} \left[\text{cosh} \left(\frac{\pi z}{p} \right) \right] \Rightarrow E_y = \frac{2\pi q_l}{p} \text{th} \left(\frac{\pi z}{p} \right) \quad (\text{for } x=p/2) \quad (7-c).$$

Assuming V_0 be the potential difference between the cathode and the anode wire surface, the wire linear charge density q_l should thus be

$$q_l = \frac{1}{2} V_0 \left/ \left[\text{Ln} \left(\text{sh} \frac{\pi L}{p} \right) - \text{Ln} \left(\text{sh} \frac{\pi a}{p} \right) \right] \right. \quad (8),$$

where, L is the length of the gap between the anode plane and the cathode grid, whereas, a is the anode wire radius. Therefore, at any point within the sensitive volume of the counter, the electrostatic potential and the electric field strength can be computed for each configuration assumed. The 3-dimension pattern of the equipotentials is shown in figure 9-a and the electric field lines and equipotential surfaces over the whole volume of a single cell looks as depicted in figure 9-b, while we show in figure 9-c the particular structure of the electrostatic pattern around one anode wire and two adjacent cathode grids in a single cell.

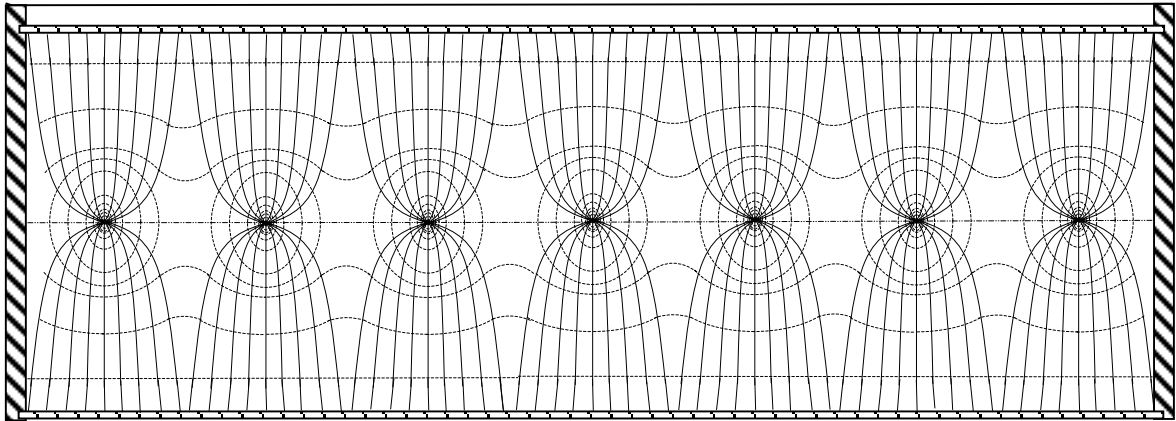


Figure 9-b: The electric field lines pattern (solid lines) and equipotential surfaces (dashed lines) throughout a single cell element sensitive volume: a central anode plane (parallel seven segment array) between two adjacent cathode grids.

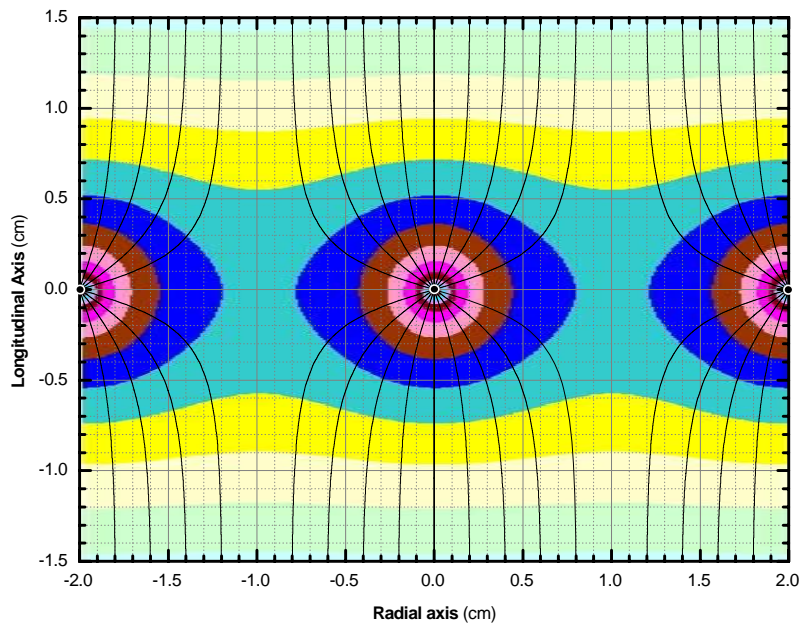


Figure 9-c: Electric field lines and equipotentials pattern between two adjacent grids of a cell

For a given high voltage value V_0 , one can identify two main evolving regions : the drift space region and the gas amplification region (or Townsend region). Within the former, the local values of electric field to pressure ratio, $S(x,y,z) = E(x,y,z)/P$, where P is the gas pressure and $E(x,y,z)$ is the electric field strength, are lower than a critical value S_c . Within this region the energy of the drifting electrons is always lower than the first ionization potential of the main filling gas and there is no ionization of the gas, i.e., no electron multiplication occurs. Thus the primary electrons released at a given point move with low kinetic energy towards the closest anode wire, following the electric field lines. However, in the Townsend region (avalanche region), located in the vicinity of the anode wire, extending throughout the space where $S(x,y,z) > S_c$, some fraction of the swarm electrons reach such higher kinetic energies that they can ionize the gas, producing thus secondary electrons by triggering Townsend avalanches and thus the charge amplification starts-up. For argon-propane (1%) with 10 % air, the critical value S_c of amplification upset is estimated to be about 30 V/cm.torr.

5. Random alpha particles emission and the stopping process

For a selected sampling period t_0 , the code RADON-MCPC (through ACTIVITY subroutine) computes at each time t , multiple of the sampling period t_0 , $n_1(t_0,t)$, $n_2(t_0,t)$, $n_5(t_0,t)$, the emitted α particles respectively from ^{222}Rn , ^{218}Po and ^{214}Po , within the time interval $[t - t_0, t]$ by numerical integration of the activity corresponding concentration prevailing within the sensitive volume of the counter in that time period. Thereafter, a Monte Carlo simulation routine is initiated, allowing the control of the whole process of random emission the α -particles throughout the counter sensitive volume. For each alpha particle emission, the subsequent stopping process within the gaseous volume of the counter is assessed through STOPPING subroutine. For each emitted alpha particle by a given nuclide, the history generator (subroutine GENERATE) provides the cylindrical coordinates of the random emission point $P_0 (r_0, \eta, z_0)$, along with the corresponding emission direction angles (φ, θ) of the alpha ionization track, as sketched in figure 10.

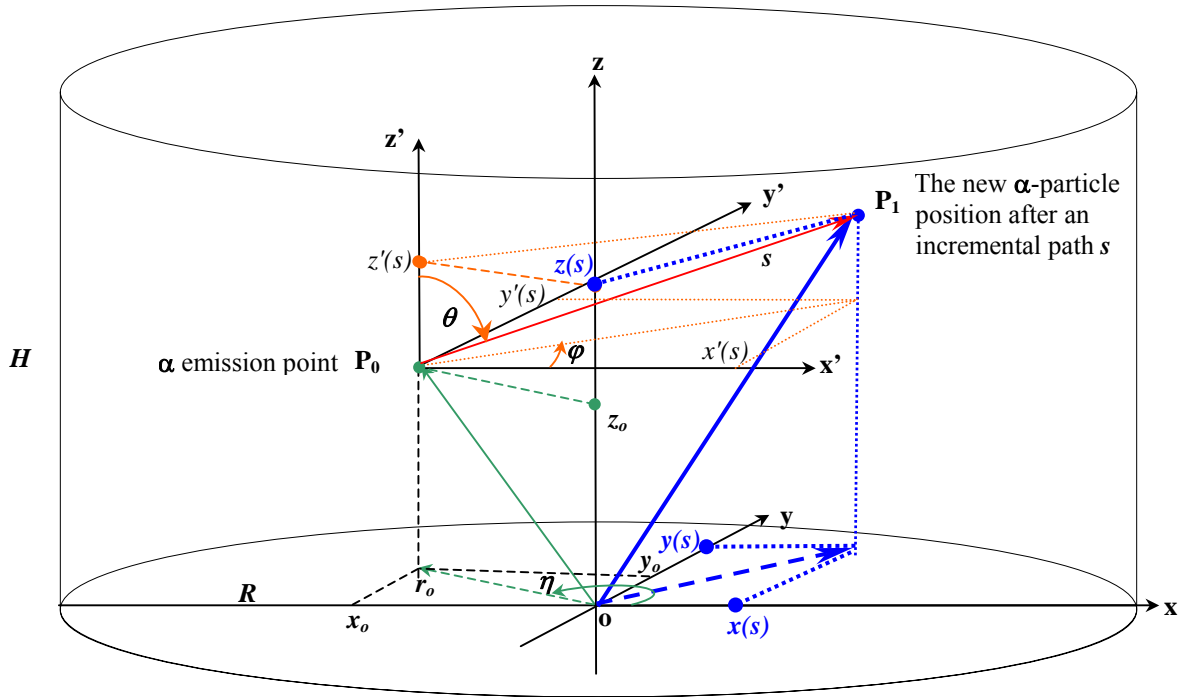


Figure 10 : Schematic diagram showing the random position of the α -particle emission and its new position, after a partial straight path s , during the stopping process, within the limits of the counter sensitive volume.

This random process is simulated by the generation of a set of 5 random numbers (γ_i , $i = 1, \dots, 5$) having uniform distributions between 0 and 1. A uniform spatial distribution for ^{222}Rn nuclides is assumed for the emission points as well as the ionization track orientation throughout the sensitive volume. However, in case of ^{218}Po and ^{214}Po , since bearing a positive charge, the emission points are located only on the cathode grid surfaces, as can be seen in figure 11, showing the distribution of the emission point reduced coordinates $(x_0/R, y_0/R, z_0/H)$, where, R and H are respectively the inner radius and the total length of the counter, and the two alpha track orientation angles (φ, θ).

The randomly generated cylindrical coordinates (r_0, η, z_0) , of the initial α position (P_0) along with its corresponding ionization track orientation angles (φ, θ) were evaluated as follows:

$$\begin{aligned} r_0 &= R \sqrt{\gamma_1} & ; & & \eta &= 2\pi\gamma_2 & ; & & z_0 &= H\gamma_3 & & (9), \\ \varphi &= 2\pi\gamma_4 & ; & & \theta &= \arccos(1-2\gamma_5) \end{aligned}$$

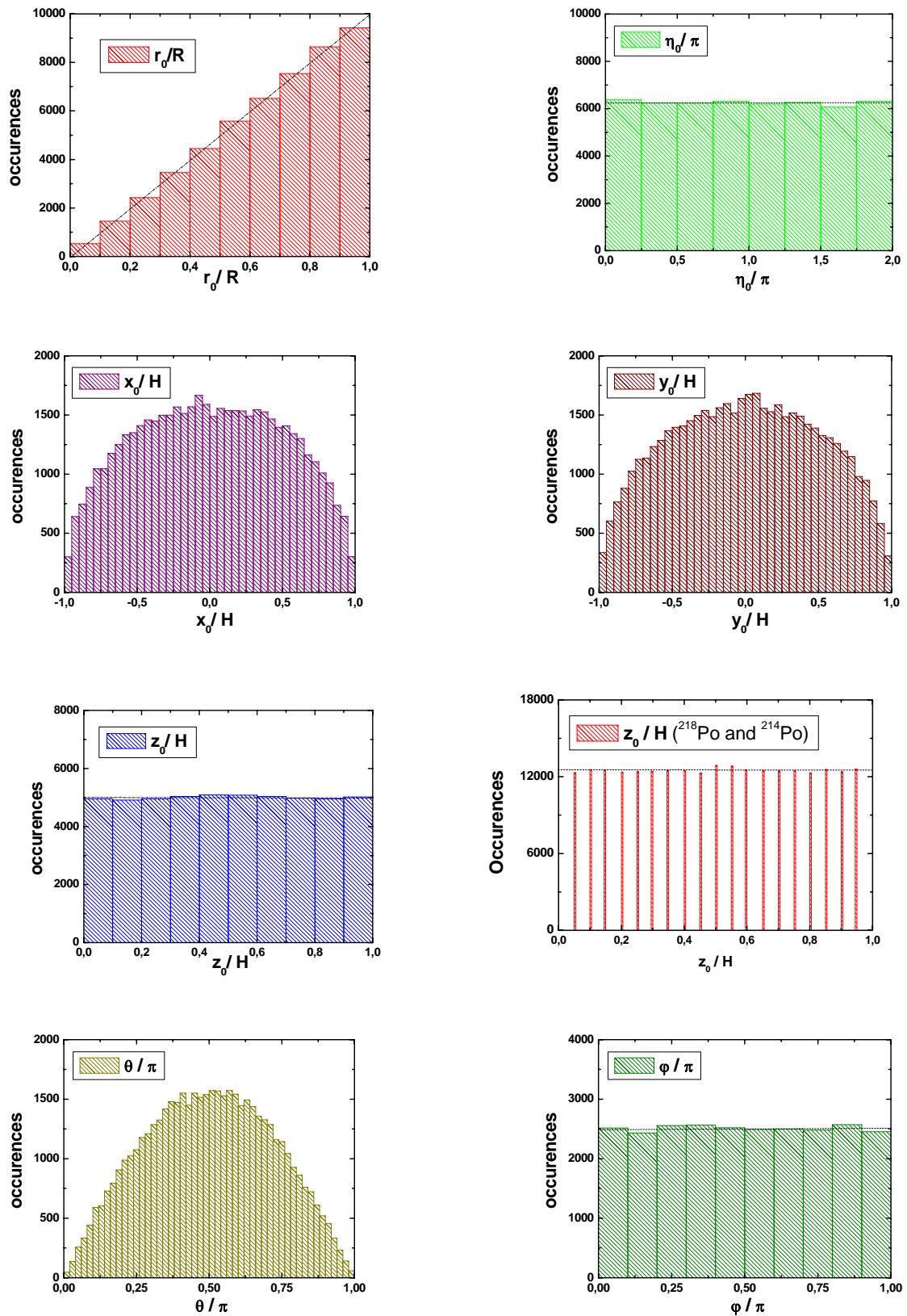


Figure 11: Distributions of the α emission point coordinates and the α track orientation angles

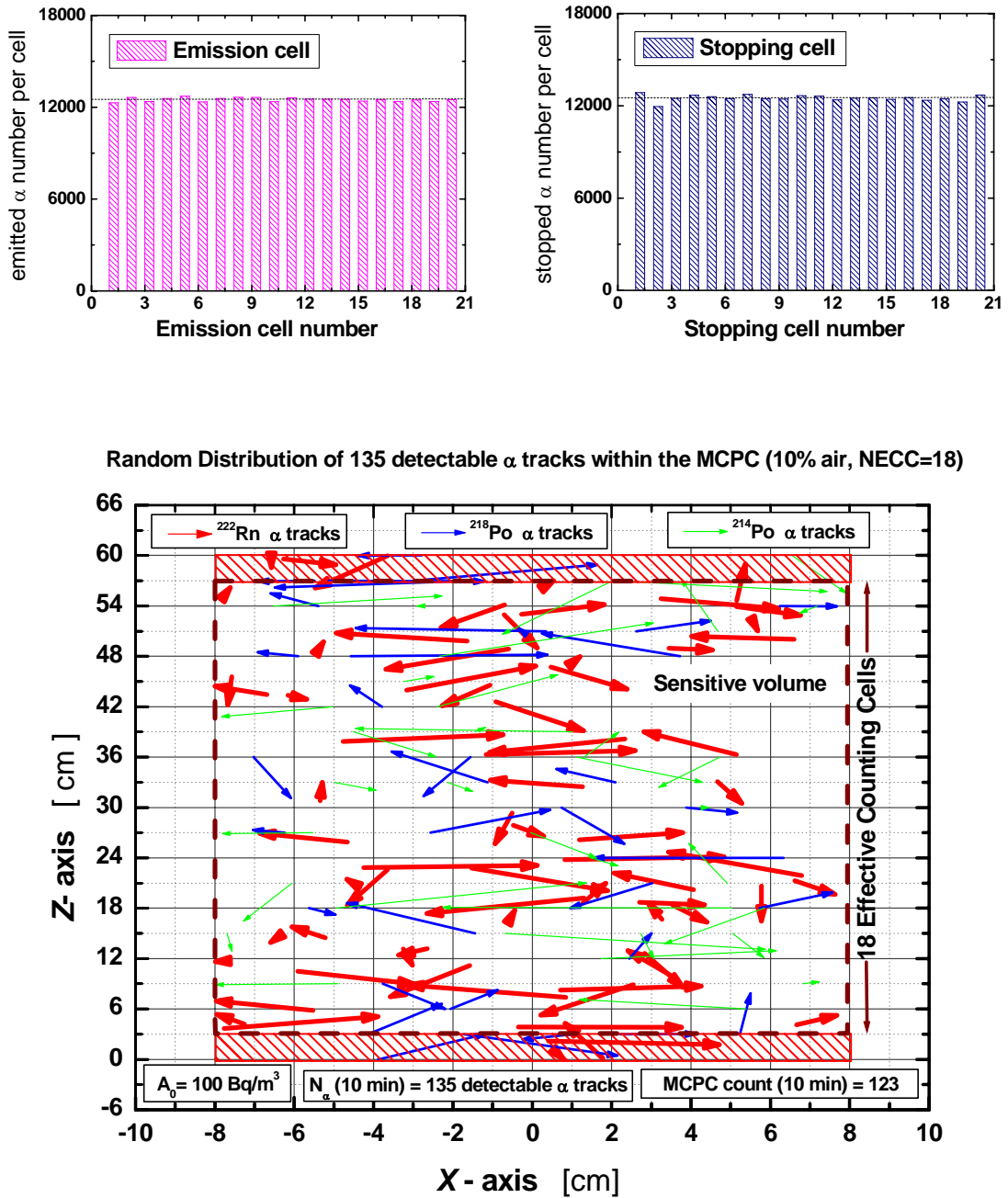


Figure 12: Distributions of the α emission cell number and α stopping cell number

Prior to initiate any simulation run, the minimal stories number was determined by checking that the resulting distributions of the random values $(r_0/R)^2$, $(\eta/2\pi)$, (z_0/H) , $(\varphi/2\pi)$ and $(1-\cos(\theta))/2$ are accurately uniform with a non-uniformity ratio less than 1/1000.

In the simulation, during the α stopping process, it was assumed that the particle trajectories are straight lines, and both the straggling effect and the δ -electrons projection were neglected.

For each α path increment Δs (variable, see next step (b)), RADON-MCPC executes successively the following tasks [from (a) through (f)] :

- a) – The code computes the new position coordinates $(x(s), y(s), z(s))$ of the α particle as a function of s , using the following expressions

$$\begin{aligned} x(s) &= \mathbf{r}_0 \cos \eta + \mathbf{s} \sin \theta \cos \varphi \\ y(s) &= \mathbf{r}_0 \sin \eta + \mathbf{s} \sin \theta \sin \varphi \\ z(s) &= \mathbf{z}_0 + \mathbf{s} \cos \theta \end{aligned} \quad (10)$$

- b) – The code evaluates the quantity of energy transferred ΔE to the gas mixture along the path increment deducing thus the residual energy E_i of the α particle :

$$E_i = E_{i-1} - \Delta E = E_{i-1} - \left(\frac{dE}{ds} \right) (E_{i-1}) \Delta s \quad (11)$$

where, E_{i-1} is the “old” energy value (i.e., the energy of the α particle just before that step), while $(dE/ds)(E_{i-1})$ stands for the α stopping power computed for the counting gas-mixture being used, whereas the value of the variable path increment Δs was varied such that at each stopping step one has to deal with a fixed number of primary electrons. The number of 2000 primary electrons in each swarm was assumed in the simulation, which corresponds approximately to a value of Δs varying between a maximum of 500 μm (as long as the α energy is greater than 500 keV) and a minimum of 100 μm , to take into account for the rapid drop of the stopping power, just before the alpha particle is fully stopped within the gaseous medium.

The energy-dependent α stopping power data in air-mixed argon-propane (1%) were recalculated by Avogadro addition of the values given in the data table for the constituents available from ICRU Report 49 [7]. In figure 13, an example of the deduced Bragg curves of the three α particles is shown for the gas consisting 90 % of binary gas (argon-propane (1%)) and 10 % air.

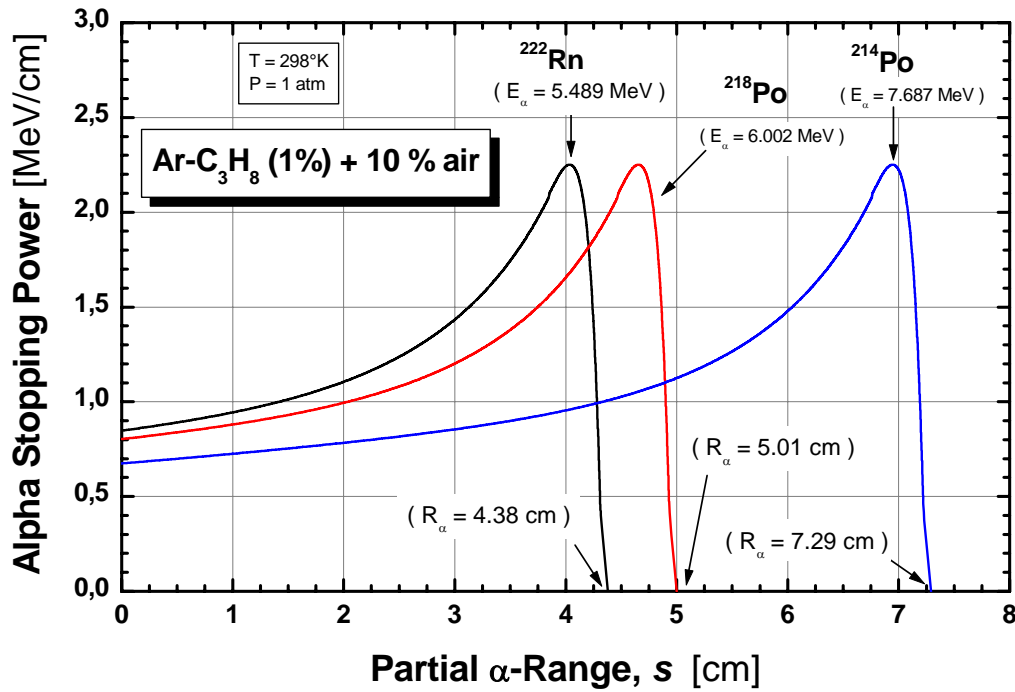


Figure 13 : The Bragg curves of the α particles from ^{222}Rn (5.489 MeV), ^{218}Po (6.002 MeV) and ^{214}Po (7.687 MeV), recalculated for argon-propane (1%) + 10 % air, making use of the alpha stopping power data taken from ref. [7].

The number of primary electrons released in the gas mixture at the current α -position (x, y, z) , along the increment Δs of the trajectory path, is then estimated

$$n_p(x, y, z) = \frac{\Delta E}{W_g} \quad (12),$$

where, W_g is the mean energy necessary to create one electron-ion pair in the gas mixture in concern and is evaluated using the Blanc's law

$$\frac{1}{W_g} = \frac{f}{W_{air}} + \left(\frac{0.99}{W_{Ar}} + \frac{0.01}{W_{C_3H_8}} \right) (1-f) \quad (13),$$

where f is the admixed air fraction, whereas W_{air} ($= 34.2$ eV) [8], W_{Argon} ($= 26$ eV), $W_{propane}$ ($= 23.5$ eV) [9] are the W-values assumed in our calculation for α particles respectively in air, argon and propane. The W-value of an argon-propane (1%) + 10 % air is thus estimated to about 26.7 eV/ion pair.

c) – The code identifies thereafter the cell number where is located the α particle, and thus, where the free electrons are actually released,

d) – The code identifies also the effective collecting anode wire segment : the nearest anode wire to the current position of the alpha particle within the identified cell, following the actual electric field line,

e) – The codes simulates the electron drift process of the primary electrons, released within the current cell, when are drawn along the electric field lines towards their corresponding collecting anode wire segment. During this important process, both electron attachment and gas amplification processes are taken into account, until the saved electrons (unattached) reach the anode wire.

f) – Finally, RADON-MCPC estimates the net charge (in electrons) actually collected as a result of this α -increment path.

The above steps (from (a) through (f)) were then iterated as long as the residual α energy is greater than a critical threshold value E_c (taken equal to 50 keV) and as long as the α -particle is not incidentally stopped by the detector wall or grid array cathode (wall effect or grid opacity effect). Modeling of these incidental events is described in the next paragraph.

6. Modeling of the wall effect and the grid opacity effect

The wall effect is the most predominant perturbing effect due to the inner wall of the cylindrical cells. The grid opacity effect influence is lesser and is inherent to the cathode grid particular structure, as shown in figure 14.

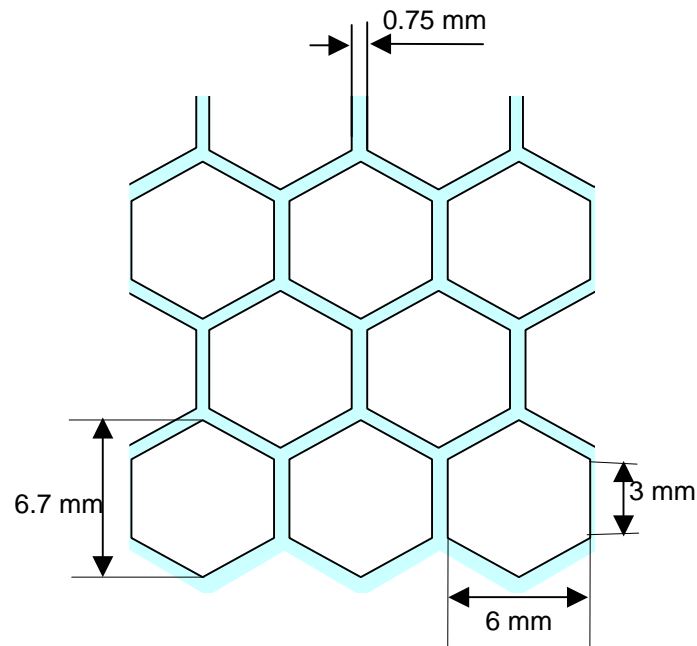


Figure 14 : The cathode grid pattern structure and relative dimensions, characterized by a geometrical opacity coefficient estimated to 19 %.

The wall effect is rather well known in gas counters used to detect charged particles characterized by extended ionization tracks. In our case, it is due to the fact that a number of alpha particles are prematurely stopped by the cell inner wall before transferring entirely their initial energy to sensitive gas mixture, the residual energy is thus considered sterilely lost. Whereas the grid opacity effect effect, is mainly due to the particular structure of the cathode grid pattern. Since the cathode grid material is made from a uniformly hexagonal holes-perforated stainless steel plate, its geometrical transparency, for the alpha particles, is lesser than 100 %. Indeed, the probability that has a randomly emitted alpha particle, when reaching the cathode grid surface, to be stopped by the cathode grid material is almost equal to the grid opacity coefficient (about 0.19 in our case). Therefore, this brings in another contribution for the classical wall effect and thus, introduces another source of sterile energy loss, which has to be taken into account.

During the alpha stopping process, the wall effect is taken into account whenever one of the three test conditions fails :

$$\begin{aligned} x^2(s) + y^2(s) &\leq R^2 \\ z(s) &\leq H \quad \text{and} \quad z(s) \geq 0 \end{aligned} \quad (14),$$

where, $(x(s), y(s), z(s))$ are the position coordinates of the alpha particle, R is the inner cell radius and H the active height of the counter sensitive volume.

Concerning the non-transparent grid effect, it is taken into account in the following way. During its stopping process within the gas mixture, the incident particle α , following an ionization track having an orientation θ with respect to OZ- axis, has a probability P_{pt} to pass through the grid slits given by

$$P_{pt} = T_g \cos\theta$$

where, T_g stands for the geometrical transparency. Then each time an alpha particle has to penetrate through over a cathode grid, when moving towards an adjacent cell element during its stopping process, a random transfer probability number P_t is generated and compared to the pass-through probability. The stopping process is interrupted (and the grid opacity effect occurs), whenever the obtained value of P_t is less than $(1-P_{pt})$. The residual energy of the alpha particle is then considered lost inefficiently, i.e., with no more primary electrons release.

According to the simulation analysis of these two effects, the Wall Effect Loss fraction (WEL) decreases rapidly with increasing cell internal radius (see figure 14),

whereas, the Grid Opacity Effect Loss fraction (GOEL) increases slightly when the cathode-anode distance decreases. For example, while keeping the gas gain constant (about 40), and setting $L = 1.5$ cm, the GOEL fraction is estimated to be 8.5 % and the expected MCPC (10% air) radon sensitivity is about 1.1 cpm/10Bq/m³ and for $L = 1$ cm, one obtains a GOEL fraction of 9.9 % , resulting in a radon sensitivity of about 0.72 cpm/10 Bq/m³

A convenient configuration is thus obtained, when adopting a cell internal radius of 8 cm with a cathode-anode distance $L = 1.5$ cm, taking into account for other parameters requirement, as will be seen in next chapter.

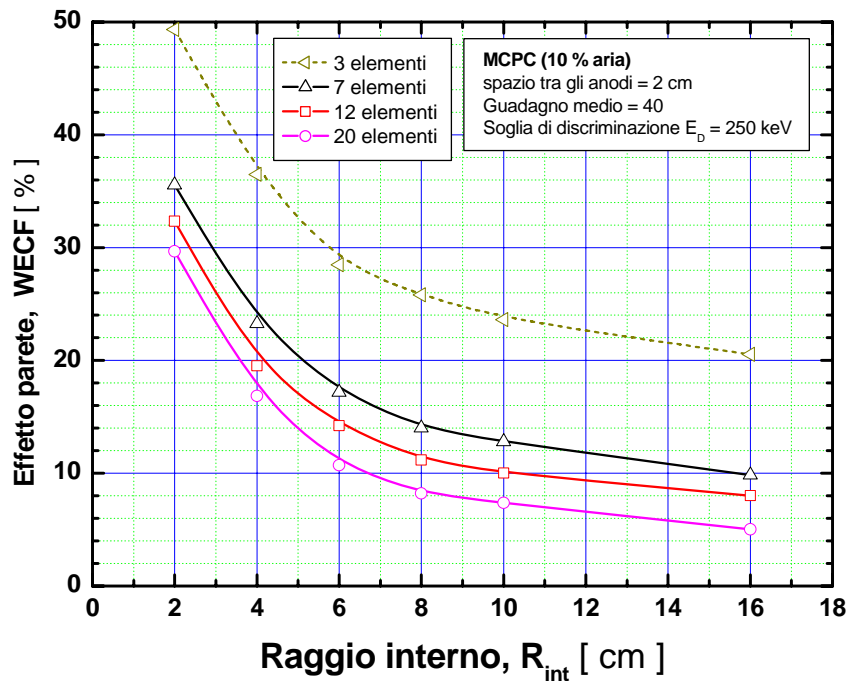


Figure 15 : Evolution of the Wall Effect Loss (WEL) against the cell internal radius and the total incorporated cells when 10 % of air is added to the binary gas mixture. The high voltage value was set such that the averaged gas gain is maintained constant and equal 40.

7. The electron attachment effect and the gas amplification mechanism

During their drift path towards the collecting anode, a number of the primary electrons $n_p(x,y,z)$ are attached by oxygen molecules and thus are considered lost. The remainders produce electron avalanches in the vicinity of the anode wire, contributing thus to compensate for the attached electrons. For each emitted alpha particle, the total number of collected electrons $N_e(S_{max})$ at the anode wire is computed by

$$N_e(S_{\max}) = \sum_0^{s_{\max}} \int_0^{d(s)} n_p [\alpha(E/P) - a_{\text{att}}(E/P)] ds \quad (15)$$

where $d(s)$ is the electron drift path length along the electric field lines towards the collecting anode wire, $\alpha(E/P)$ and $a_{\text{att}}(E/P)$ are respectively the position-dependent first Townsend ionization and electron attachment coefficients in the counting gas mixture and n_p is the number of primary electrons produced by the α particle at the point of coordinates $(x(s), y(s), z(s))$, and, S_{\max} is the effective range of the α particle within the counter sensitive volume.

7.1 The electron attachment coefficient distribution

The functional dependence of the electron attachment coefficient $a_{\text{att}}(E/P)$ on the electric field to pressure ratio E/P is evaluated by taken into account only the main contribution of oxygen component present in the mixture. The values of the electron attachment coefficient $a_{\text{att}}(E/P)$ for air-mixed argon-propane (1%) were recalculated using the experimental data for molecular oxygen of Chanin et al. [10], for E/P values lower than 10 V/cm.torr, and those of J.B. Freely et al. [11], for higher E/P values. The obtained fitted curve used in the RADON-MCPC code is shown in figure 16.

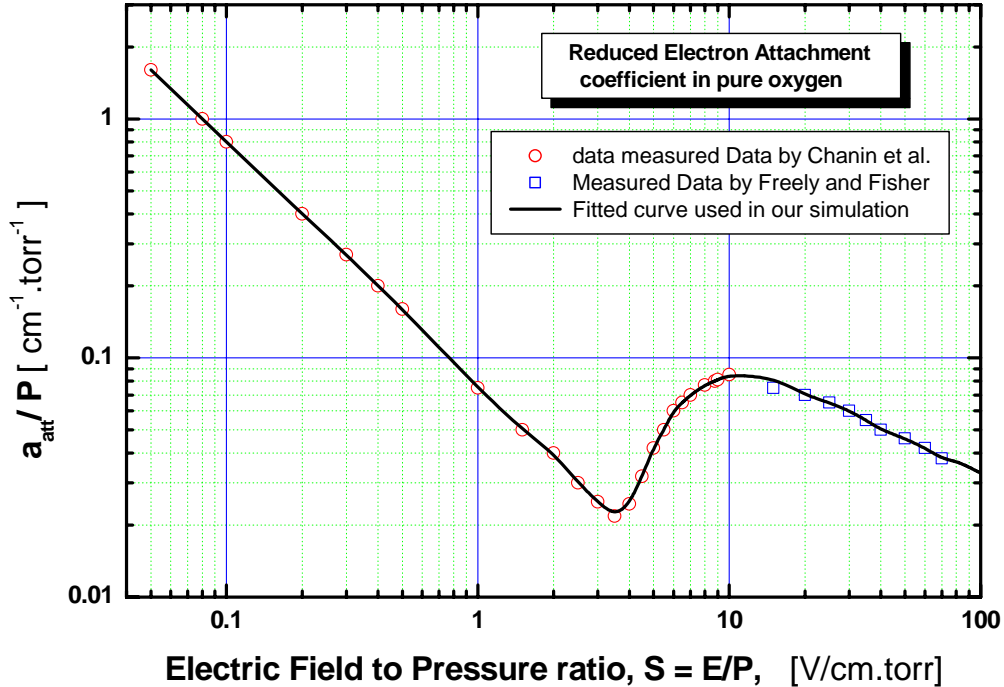


Figure 16 : Fitting curve of the reduced electron attachment coefficient in oxygen, used in the simulation. The experimental data are taken from refs [10-11]

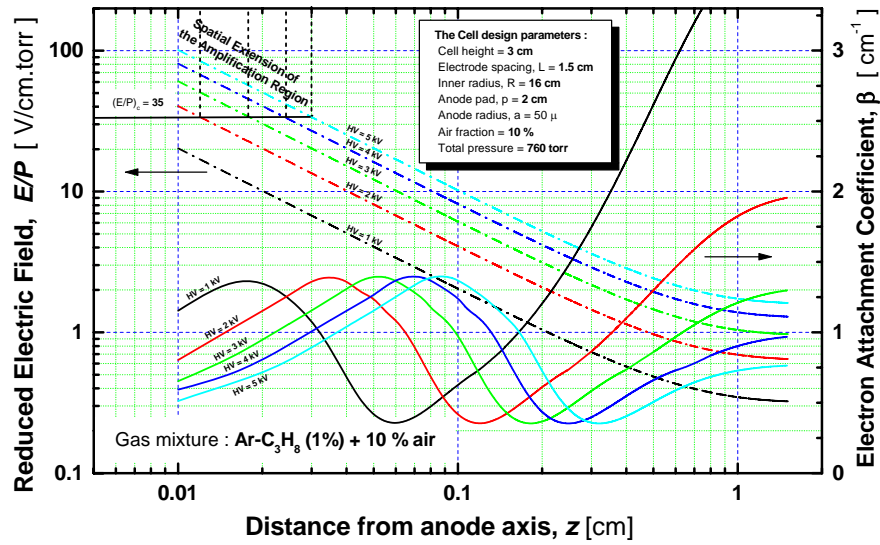


Figure 17 : Evolution the electron attachment coefficient (taking into account only the contribution of oxygen) as a function of the distance from anode axis and also the electric field to pressure ratio, E/P , in the MCPC, using 10 % of air-mixed argon-propane (1%) as the counting gas mixture, as the anode high voltage is increased from 1 kV up to 5 kV. The resulting spatial extension of the amplification region around the anode wire is also shown , indicating the critical value $(E/P)_c$ at which the gas amplification starts up.

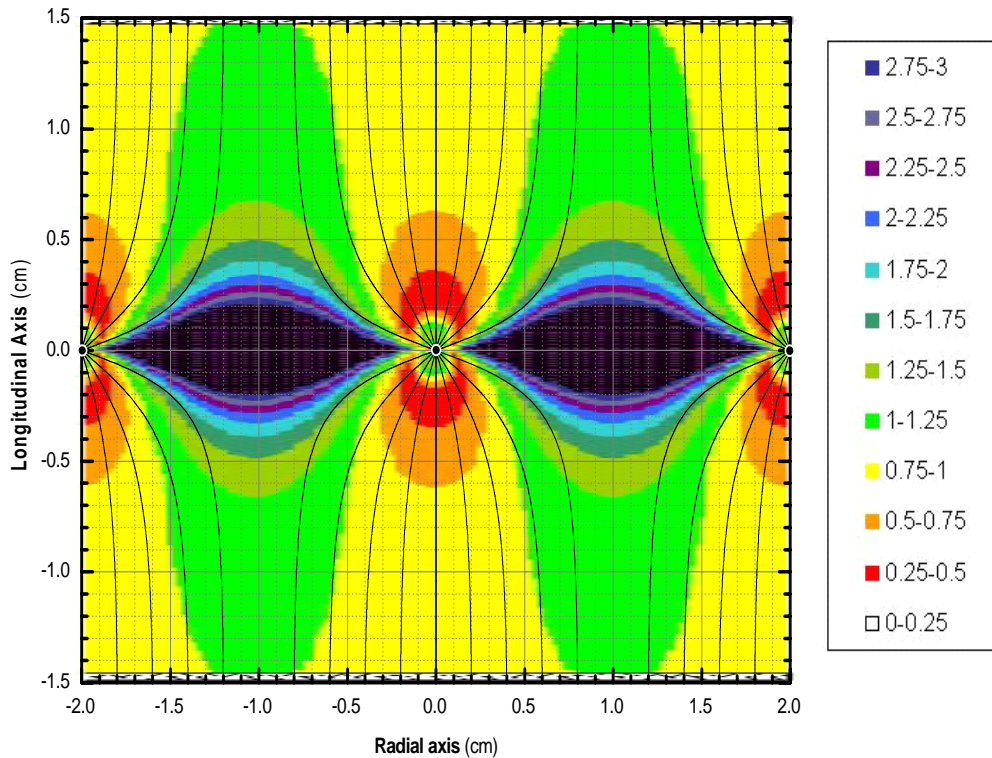


Figure 18 : Spatial distribution of the electron attachment coefficient between anode wires and two adjacent cathode grids, in the MCPC, using 10 % of air-mixed argon-propane (1%) as the counting gas mixture. The anode voltage is set at 4 kV.

In figure 17, we show the calculated behavior of the electron attachment coefficient in a radial direction within the sensitive volume for anode high voltage values varied from 1 kV up to 5 kV, when the MCPC uses an air mixture fraction of 10 %. The corresponding evolution of the electric field to pressure ratio is also included within the same figure in order to illustrate the spatial extension of the gas amplification region around the wires, when the anode voltage is increased. Whereas, in figure 18 we show the calculated spatial distribution of the electron attachment coefficient between two cathode grids, to get a best illustration of the electron attachment mechanism around the anode wires and between two adjacent grids through a single cell sensitive volume. We can see in figure 19 that as the high voltage value is increased the mean value of the electron attachment throughout the drift space decreases, and the “black” regions collapse more and more, except at the middle space between two successive wires, while the gas amplification region, close to anode wires, extends more and more farer from the anode axis as can be seen in figure 17.

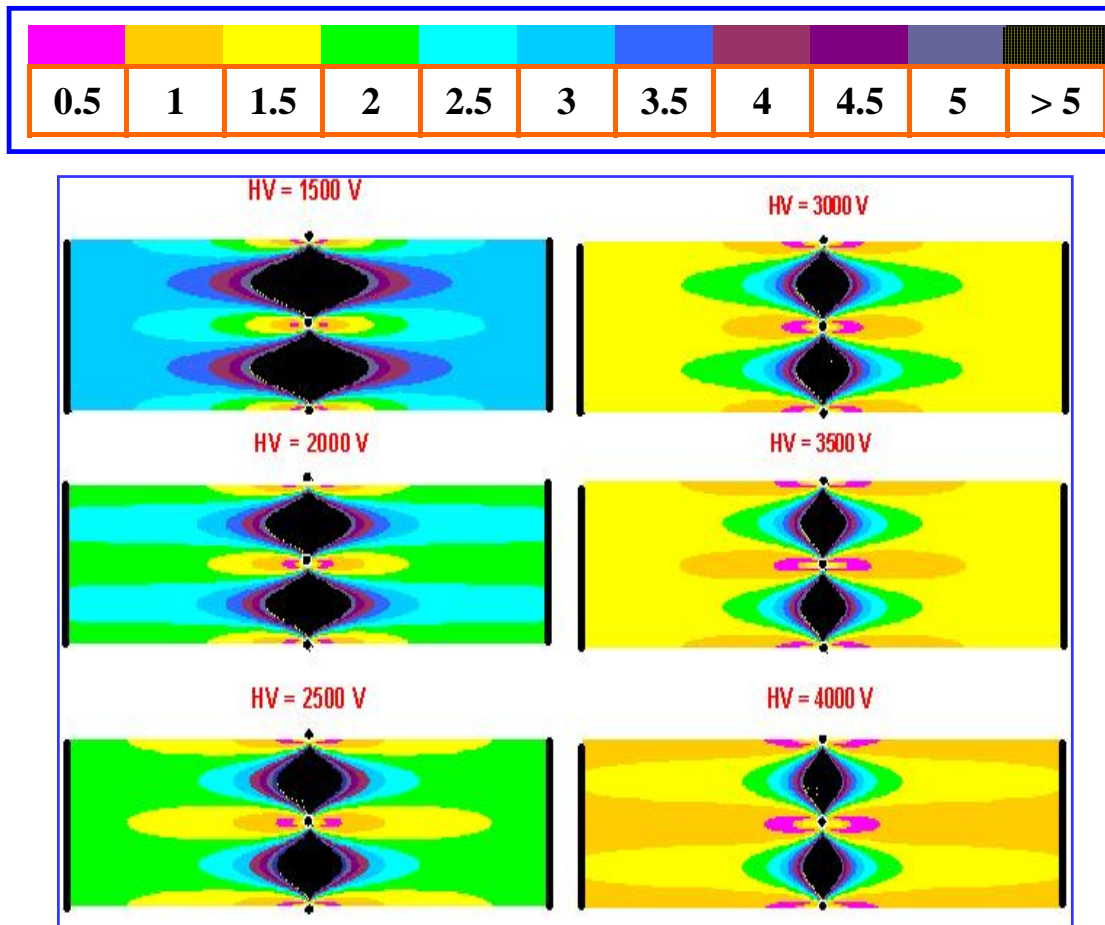


Figure 19 : Evolution of the spatial distribution of the electron attachment coefficient between anode wires and adjacent cathode grids, in the MCPC, using 10 % of air. The anode voltage is varied from 1.5 kV up to 4 kV.

7.2 The gas amplification mechanism

When reaching the Townsend avalanche region, located in the vicinity around each anode wire, each primary electron trigger a Townsend avalanche through secondary ionizations by which the number of the electrons is multiplied by a constant factor, called gas gain or gas amplification factor. In order to assess this charge amplification mechanism within the flowing gas mixture being used, we have studied experimentally the effect of air on gas amplification characteristics in argon–propane (1%)-based proportional counters dedicated for such an application (airborne radon monitoring) which results were presented in chapter two of this thesis.

The dependence of the first Townsend ionization coefficient on the reduced electric field E/P is thus numerically recalculated using the semi-microscopic gas gain formula [12]. The corresponding air-mixed ar-propane (1%) gas gain constants used were measured experimentally [13].

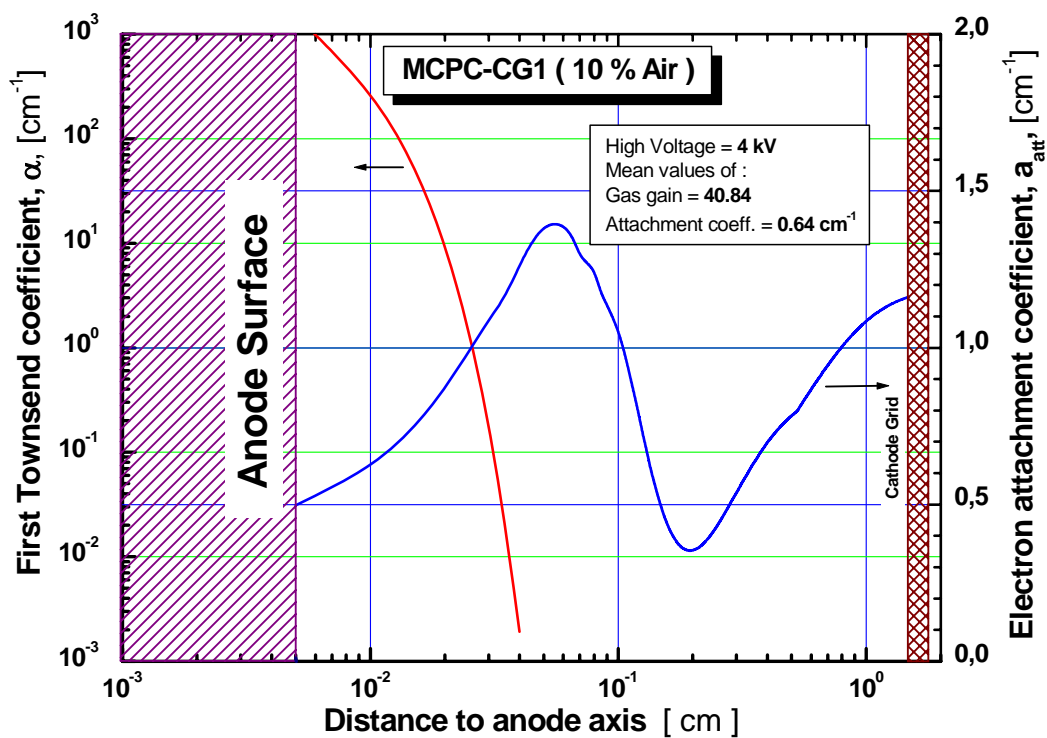


Figure 20 : Spatial dependence of the first Townsend coefficient (ionization coefficient) and electron attachment between the anode plane and the cathode grid along the z-axis in a single cell of the MCPC, using 10 % of air-mixed argon-propane (1%) as the counting gas mixture. The anode voltage is set at 4 kV.

In figure 20, we show the spatial dependence of evolution of the first Townsend ionization coefficient in argon-propane (1%) + 10 % air . One can notice that the gas amplification mechanism starts-up when the electron swarm (initially constituted of 2000 primary electrons in our simulation) is located at a distance of about $350 \mu\text{m}$ ($\approx 7a$, where a is the anode wire radius).

The obtained gas gain characteristics as a function of the applied anode voltage, when a fraction of 0.1 %, 1 %, 5 % and 10 % of air is added to the main argon-propane (1%) counting gas mixture are shown in figure 21.

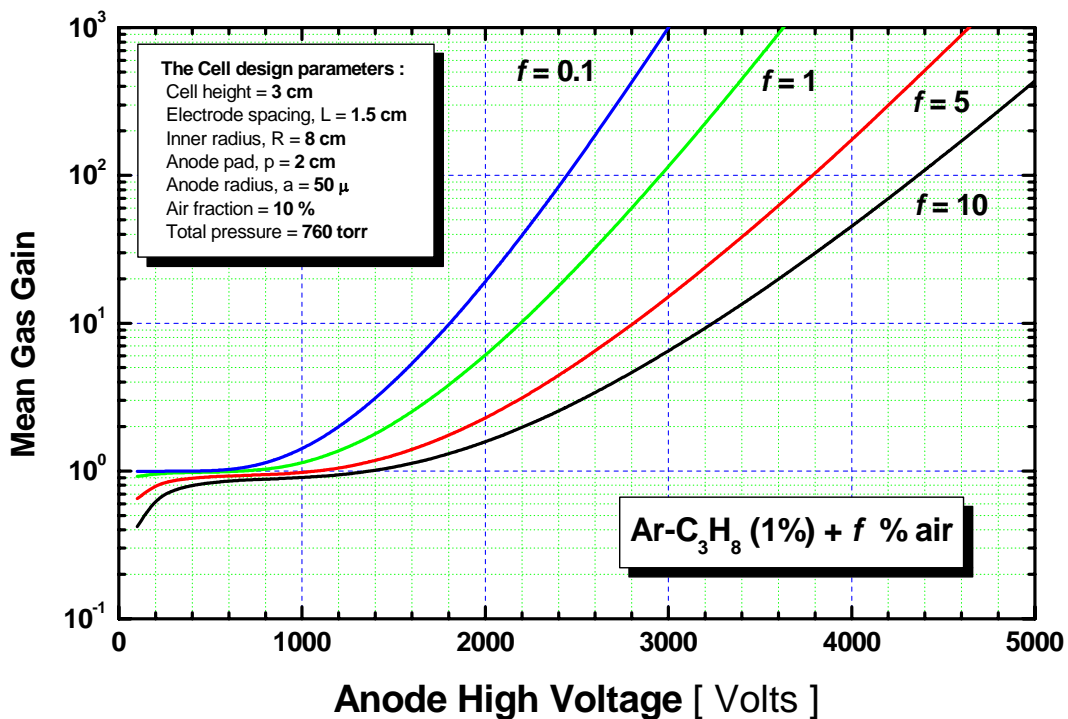


Figure 21 : Evolution of the mean gas gain versus high voltage value for several air fractions in argon-propane (1%) gas mixture. The MCPC design features are indicated.

8. The alpha pulse height spectra

For each α particle emitted inside the counter, the code computes the total number of the electrons collected at each anode wire and throughout all the cells crossed by the α -particles, taking into account for the electron attachment effect and the gas multiplication process as described in the previous section. Then UPDATE subroutine assigns the obtained charge pulse to a channel number N_i proportional to the number of electrons collected, thus, the effective energy deposited by the α particle inside the counter. This routine is iterated N_S times, where N_S is the number of stories assumed in the Monte Carlo simulation. When the acquisition is completed, an alpha pulse height spectrum recorded over 1024 channels is obtained for the total $(N_0(t_0)+N_1(t_0)+N_2(t_0))$ number of emitted α particles during the selected preset time t_0 . Successively, the code superimposes an assumed background spectrum (noise spectrum) due to cosmic rays, radiations emitted by the counter structure materials (especially the polyethylene of which are manufactured the cells) and also the electronic noise. In the present case, it is modeled by an $1/E$ distribution, where E is the energy proportional to the channel number where the corresponding count is recorded. Finally, in order to reduce the fluctuations inherent to the subsequent electronic amplification of the delivered pulses (due to the ballistic effect) [14], the code effects a smoothing (BROAD subroutine) of the three separated alpha energy-deposited distributions corresponding to the emitted alpha particles from ^{222}Rn (5.489 MeV), ^{218}Po (6.002 MeV) and ^{214}Po (7.687 MeV). This routine is done by recalculating the new counts number N_j in each channel j using a Gaussian type weighting function over j_0 adjacent channels :

$$N_j = \frac{\sum_{i=j-j_0}^{j+j_0} N_i \exp\left(-\frac{(E_i - E_j)^2}{2 \sigma_\alpha^2}\right)}{\sum_{i=j-j_0}^{j+j_0} \exp\left(-\frac{(E_i - E_j)^2}{2 \sigma_\alpha^2}\right)} \quad j = 1, \dots, 1024 \quad (16)$$

where,

$$j_0 = \sigma_\alpha / h_E \quad \text{and} \quad \sigma_\alpha^2 = \sigma_n^2 + (F + g) W_g E_\alpha \quad (17)$$

where, h_E is the energy-equivalent width of each channel (MeV/channel), σ_n^2 is the energy-equivalent of the variance of the electronic noise, F is the Fano factor which characterizes the statistical fluctuations in the number of the primary electrons

released in the sensitive gas, whereas, g is a normalizing factor taking into account for the fluctuations of the total number of secondary electrons produced in each electron avalanche [14-15]. In our simulation we take

$$F + g = 1$$

We show in figure 22 an illustration of the resulting spectral broadening induced by the statistical fluctuations and in figure 23, one can see the effect of smoothing routine on the pulse height spectra .

The final pulse height distribution is obtained by summing the three separated alpha spectra obtained, and adding the assumed background. The estimation of the contribution of the counter background takes into account also for the effect of the high voltage value. Indeed, the spurious pulses due to external events are also amplified within the gas mixture, resulting thus in a slight shift of the background to the high channel number side, as can be seen in figure 22.

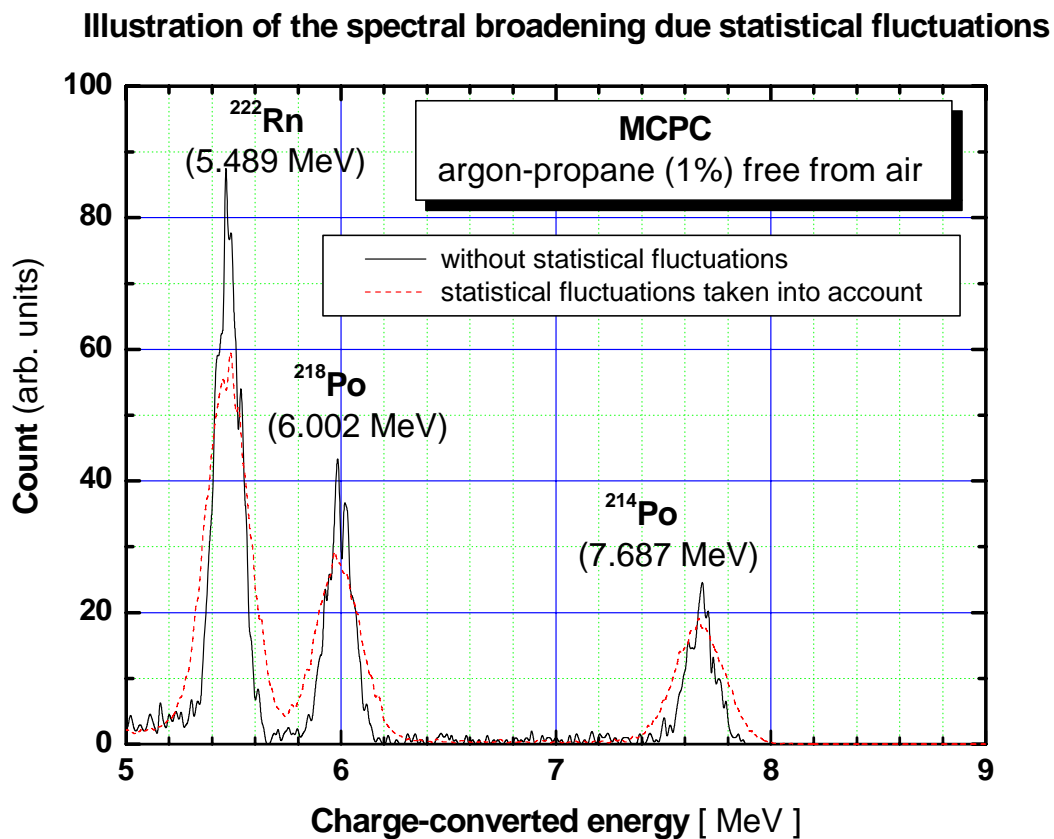


Figure 22 : *Illustration of the spectral broadening, taking into account the statistical fluctuations.*

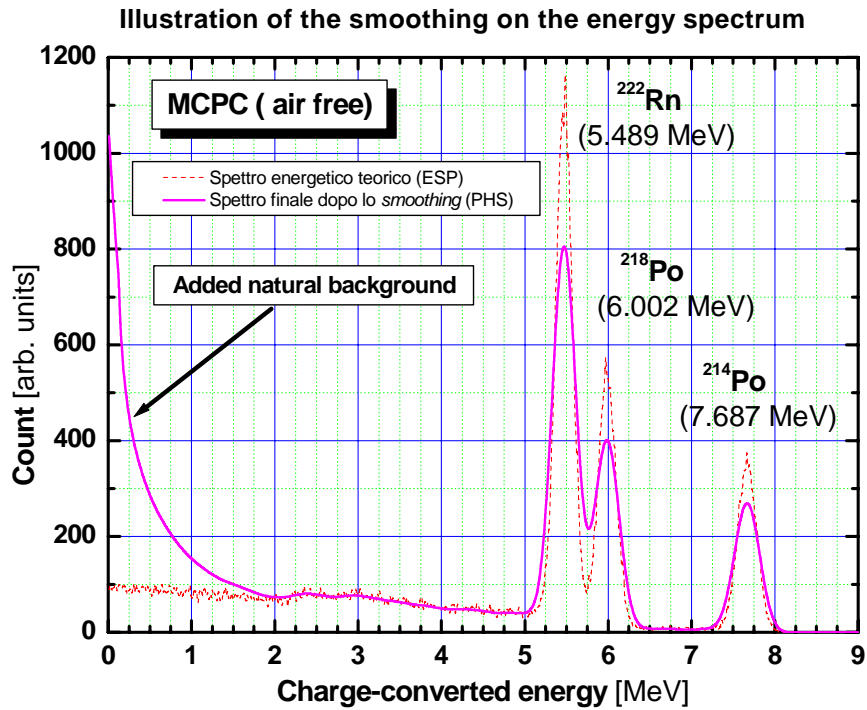


Figure 23 : Illustration of the effect of the smoothing routine on the obtained pulse height spectra. We show also the added natural background that depends upon the anode high voltage value.

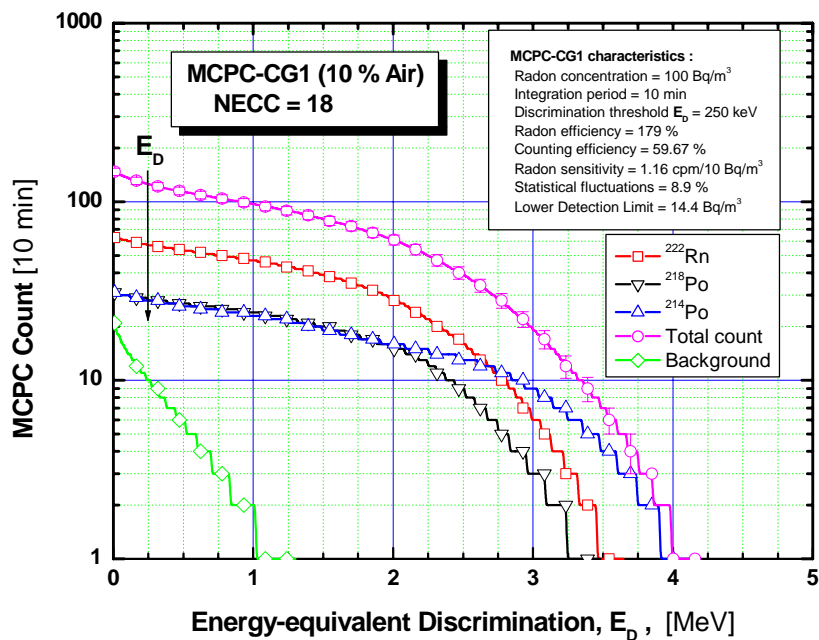


Figure 24 : An example of the deduced discrimination curve from the simulated pulse height spectrum. The assumed parameters and the deduced MCPC performances are also indicated.

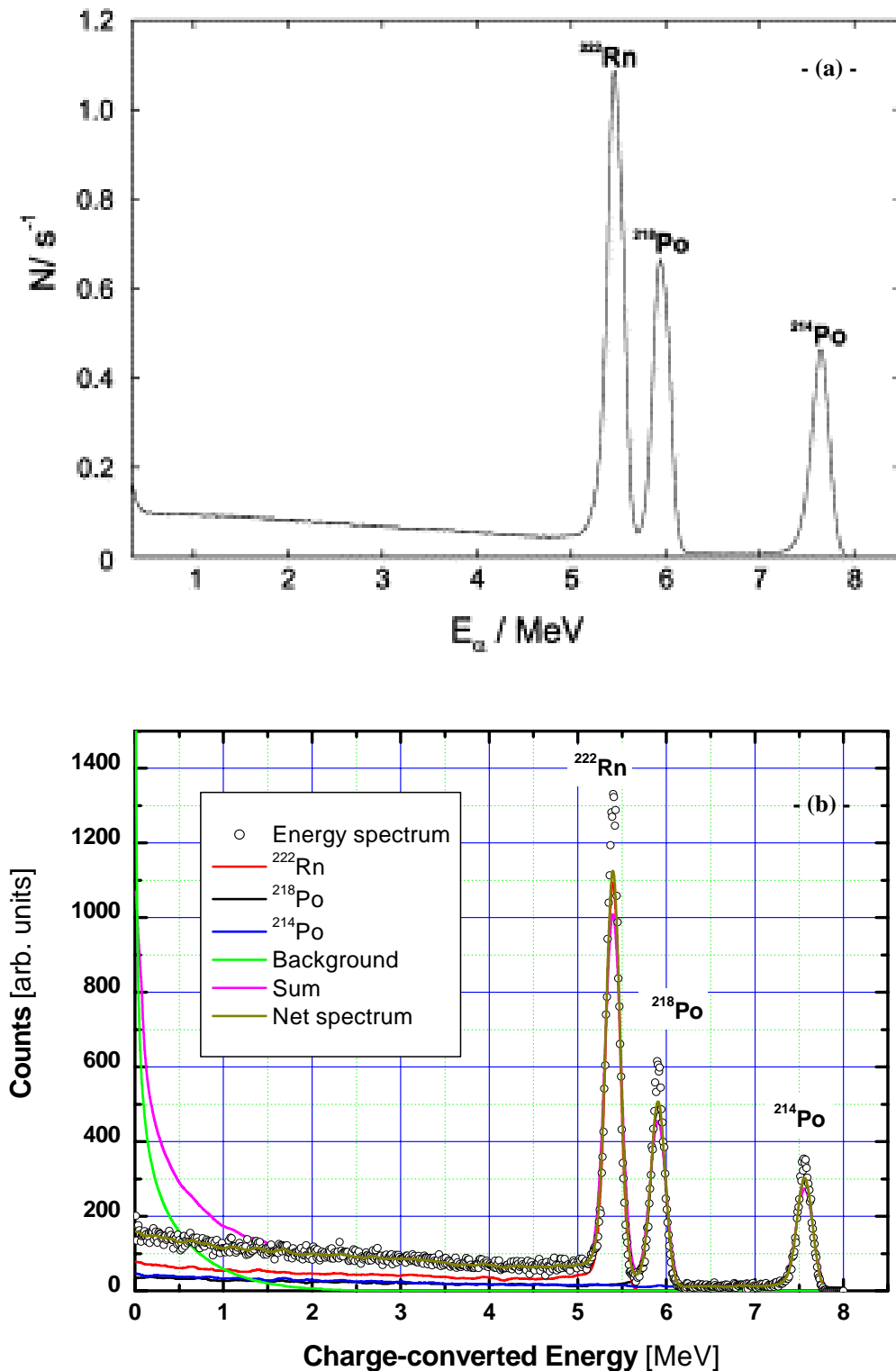


Figure 25 : Comparison between:(a) an α -spectrum recorded by Busch et al. [16] using their MEPC with P-10 gas mixture (gas pressure =1600 mbar) in radioactive equilibrium of ^{222}Rn with its short-lived decay products (^{218}Po and ^{214}Po) and (b) our MCPC (5 cells) simulated spectrum when mixing only 0.1 % air with argon-propane (1%) at a total pressure of 1atm. The resolution in both cases is sufficient to resolve the α -peaks of ^{222}Rn and its short-lived progenies (^{218}Po and ^{214}Po).

Once the expected alpha pulse height spectrum is obtained, RADON-MCPC code determines the integral counting curve, such that illustrated in figure 24, and deduces from it the net alpha counting rate, the counter sensitivity, the counter efficiency and the detection limit corresponding to the adopted MCPC configuration.

In order to check the consistency of the simulated alpha pulse height spectra, we have compared the delivered alpha pulse height spectrum, obtained for a 5-cells configuration with only 0.1% of air. The obtained spectrum features are rather consistent with those of that recorded by Busch *et al.* [16] using their MEPC with P-10 gas mixture (gas pressure =1600 mbar) in radioactive equilibrium of ^{222}Rn with its short-lived decay products (^{218}Po and ^{214}Po).

9. Convergence study of the Code

We have studied in great details the convergence criteria of the average values of the most determinant physical parameters (mean electron attachment coefficient, mean gas multiplication, mean electron drift distance, mean MCPC output pulse height, mean alpha efficiency of the counter) obtained through the simulation subroutines as a function of the number of alpha particles (alpha stories). For radon alpha events, it is found that the average values of electron attachment and gas gain, are approached within 0.025 % when the alpha stories number is greater than $2 \cdot 10^5$, as shown in figure 26.

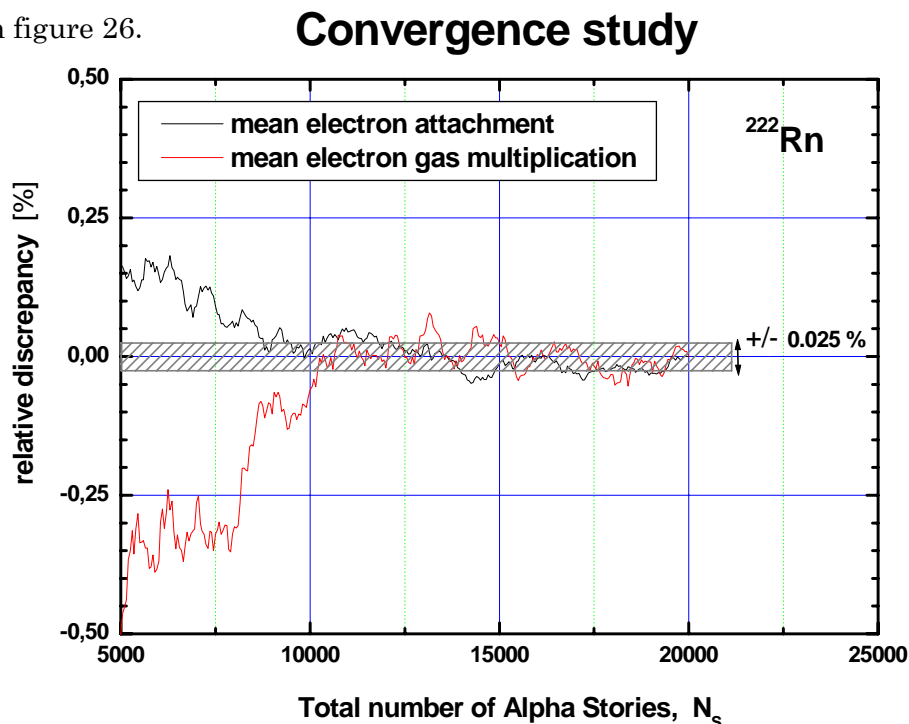


Figure 26: Convergence study of RADON-MCPC code for radon alpha particles (see text)

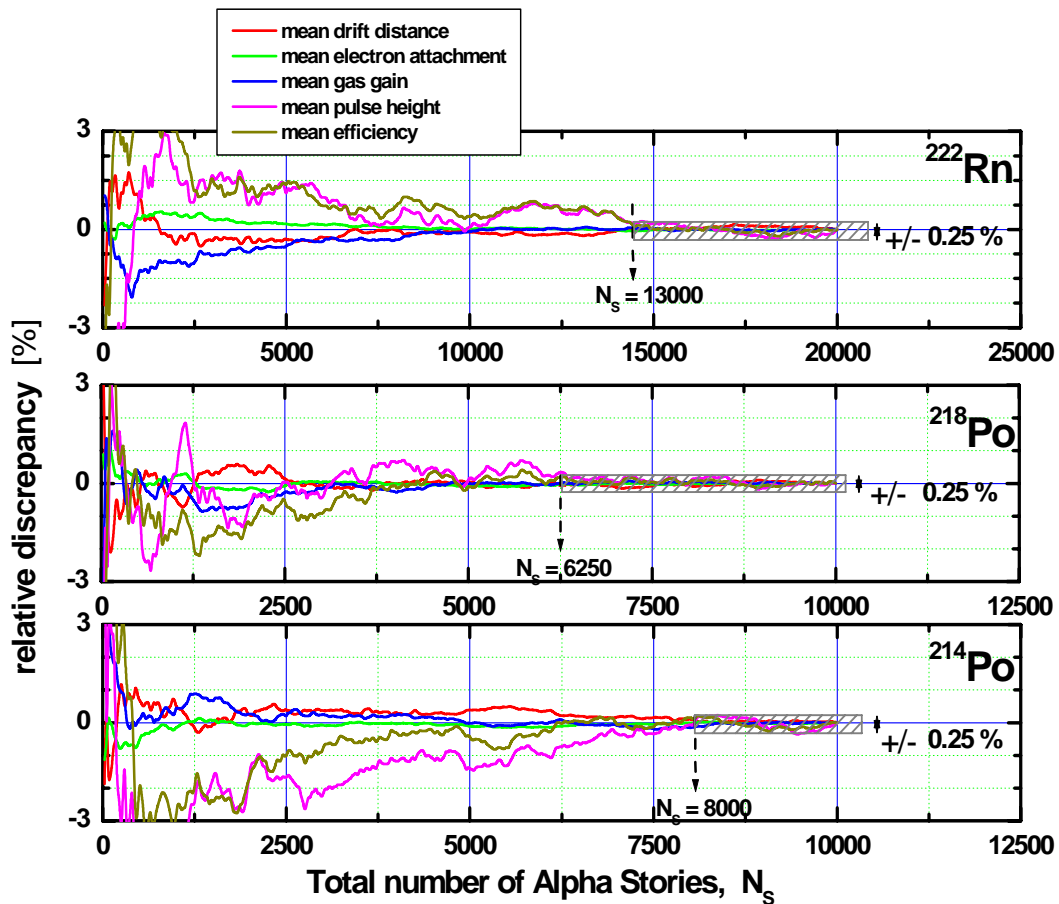


Figure 27: Convergence study of RADON-MCPC code, for radon and progenies events.

And, taking into account both of radon and progenies events, the convergence criteria are fulfilled within 0.25 % for radon stories number greater than 15000, as shown in figure 27, when radioactive equilibrium condition is assumed. This leads to conclude that the code subroutines are rather fast converging, thus, the simulation doesn't require excessive time cpu.

10. Conclusion

To achieve more reliable on-line measurements of airborne radon concentration using gas-filled detectors based on alpha counting technique, it is required to perform the measurement of the radon activity within the counter sensitive volume by counting the alpha particles emitted by decaying radon nuclides and progenies, especially, when the scope is to assess sudden radon concentration variations in time delays as short as possible. This implies the need to mix the counting gas with a small

fraction of the air sample to be monitored. Hence, the air sample becomes intrinsically a component of the sensitive gas mixture. The presence of oxygen, a highly electronegative gas, introduces serious problems related in particular to the electron attachment effect causing an excessive electron charge loss within the drift space. However, the electron attachment effect can be counterbalanced by subsequent gas amplification when using suitably designed proportional counters.

In this work, a Monte Carlo simulation code, baptized PADON-MCPC, has been developed and used to optimize the design of a Multiple Cell Proportional Counter (MCPC) prototype intended for airborne radon activity concentration on-line measurements. The MCPC uses an argon-propane (1%) gas mixture to which is admixed up to 10% of air, whose radon activity concentration has to be measured. The described Monte Carlo simulation code takes into account all the electrical and geometrical parameters and models the main physical processes that determine directly the detector performances, such as the electric field distribution, the alpha stopping and primary electron-ion pairs production, the wall effect, the gas amplification process, the electron attachment effect and also the Gaussian broadening of the collected alpha pulse height spectra.



References:

- [1] D. Mazed, « *Application de l'approximation des faibles seuils pour le calcul des coefficients de transport des électrons dans les mélanges de gaz* », Communication presented at the first Algerian Congress of Process Engineering, CAGeP'96, Pins Maritimes, Algiers, 24-26 December 1996, Proceedings of CAGeP'96, pp.481-484.
- [2] D. Mazed, « *Application P_2 de l'Equation de Boltzmann pour le Calcul des Coefficients de Transport des Electrons dans les Mélanges de Gaz* », Communication presented at the National Seminary on Lasers and their Applications, SENALAP'99, USTHB, Algiers, 14-16 June 1999, Published in the SENALAP'99 Proceedings, pp. 27-30.
- [3] S. Biagi, MAGBOLTZ: Transport of electrons in gas mixtures, CERN Program Library.
- [4] R. Veenhof, GARFIELD—Simulation of gaseous detectors, CERN Program Library W5050.

-
- [5] Nuclear Data, 1998. Decay Radiations. National Nuclear Data Center, Brookhaven National Laboratory Upton, NY, USA.
- [6] International Commission on Radiation Protection, 1987. ICRP Publication 50. *Ann. ICRP* **17**, pp. 1–60.
- [7] Allisy, et al., *Stopping Powers and Ranges for Protons and Alpha Particles.*, ICRU Report **49**, International Commission on Radiation Units and Measurements, ICRU (1993).
- [8] Dan. T.L. Jones, “*The W-value in air for proton therapy beams*”, Radiation Physics and Chemistry, Vol.75,n°5, (2006)541-550
- [9] *Average Energy Required to produce an Ion Pair*, ICRU Report 31, 1979. (see also I. B. Smirnov, « *Modeling of ionization produced by fast charged particles in gases* », Nucl. Instr. And Meth., **A554** (2005)474-493.
- [10] L.M. Chanin, A.V. Phelps and M.A. Biondi, *Measurement of the Attachment of Low-Energy Electrons to Oxygen Molecules*, Physical Review, vol.**128**, n.**1**, (1962)219-230
- [11] J.B. Freely and L.H. Fisher, *Ionization, Attachment, and Breakdown Studies in Oxygen*, Phys. Rev., vol.**133**, n.**1A**, (1964)A304-A310.
- [12] D. Mazed, M. Baaliouamer, “*A semi-microscopic derivation of gas gain formula for proportional counters*”, Nuclear Instruments and Methods, **A437** (1999) 381-392.
- [13] G. Curzio, D. Mazed, R. Ciolini, A. Del Gratta, A Gentili, “*Effect of air on gas amplification characteristics in argon-propane (1 %)-based proportional counters for airborne radon monitoring*”, Nucl. Instr. and Meth., **A 537** (2005)672-682.
- [14] G.F. Knoll, “*Radiation Detection and Measurement*”, John Wiley Ed. 2000.
- [15] P.J.B.M. Rachinhas et al., *Energy resolution of xenon proportional counters: Monte Carlo simulation and experimental results*, IEEE Transactions on Nuclear Science, vol. **43** (4) (1996)2399-2405.
- [16] I. Busch et al., *Absolute measurement of the activity of ^{222}Rn using a proportional counter*, NIM **A481** (2002)330-338



Section V

Simulation Results and Experimental tests the MCPC prototype

1. Introduction

In this section, the operation principle of the proposed active method for airborne radon activity concentration measurement is presented, the radon calibration method and the experimental tests the Multiple Cell Proportional Counter (MCPC) are described. On the other hand, RADON-MCPC code, presented in full details in the previous section, was used to determine the expected optimum operation conditions that permit to fulfil the required performances. The alpha pulse height spectra obtained through simulation are then compared to the recorded first experimental alpha pulse height spectra delivered by the constructed detector prototype.

2. Experimental setup and measurement procedures

2.1. Counter calibration procedure

Once all the MCPC parts are assembled and electrically tested, in order to perform the radon sensitivity calibration of the whole measurement system (counter and associated electronics), the MCPC counter was connected into a specially designed radon calibration loop as shown schematically in figure 1, and, in Figure 2, are shown some photographs of the whole apparatus manifold. The closed loop facility is built around a radon generation system based on a controlled heating of uranium containing rocks (autunite rocks), which necessitates also a proper and full characterization. Since, the standard radon sensitivity calibration procedure being more complex, it has not been yet fully effected within the framework of this thesis. We can thus only give some general features of its proceeding principle.

By referring to figure 1, the whole volume of the loop is first evacuated from air during some hours, it is then filled up with argon-propane (1%) gas mixture to a given pressure, P_m , below the atmospheric pressure, P_a , such that

$$P_m = (1 - f)P_a \quad (1)$$

where, f , is the desired air fraction mixed to the main counting gas mixture Argon-propane (1 %). The obtained gas mixture, containing a fraction f of air, is then pumped to flow through the radon generation system, which also could be put in by-pass mode at any time, in order to maintain a given radon activity concentration within the whole loop circuit. The radon activity concentration, the pressure, the humidity ratio and the temperature inside the loop are continuously monitored by an AlphaGUARD radon monitor (Genitron), defined as the reference measuring device. Just before letting the gas mixture to enter the MCPC, all the short-lived radon decay products are removed by a suitable membrane filter. Thus, using this loop, one can perform readily the calibration of the counter system in well defined environmental parameters (radon activity concentration, temperature, total pressure, relative humidity ratio as given by the adopted reference measuring device) and also well specified experimental measurement settings : the gas flow rate, Q , the applied high voltage value, V , the amplifier shaping time, τ , and the amplifier gain, G , the energy-equivalent discrimination threshold, E_D , counting time period, t_c .

Therefore, the counter calibration procedure permits us an experimental determination of the whole counting system parameters :

- The recommended counting electronics settings: operating high voltage value, amplifier gain and shaping time constant, discrimination threshold,
- The effective radon sensitivity, S_{Rn} , of the system.

Providing these calibration data, continuous measurement of airborne radon activity concentration, C_{Rn} , can be deduced from the periodical measurement of alpha integral counting, N_α , within the fixed operation conditions :

$$C_{Rn}(t) = \frac{1}{S_{Rn}} \frac{N_\alpha(t)}{t_c} \quad (2)$$

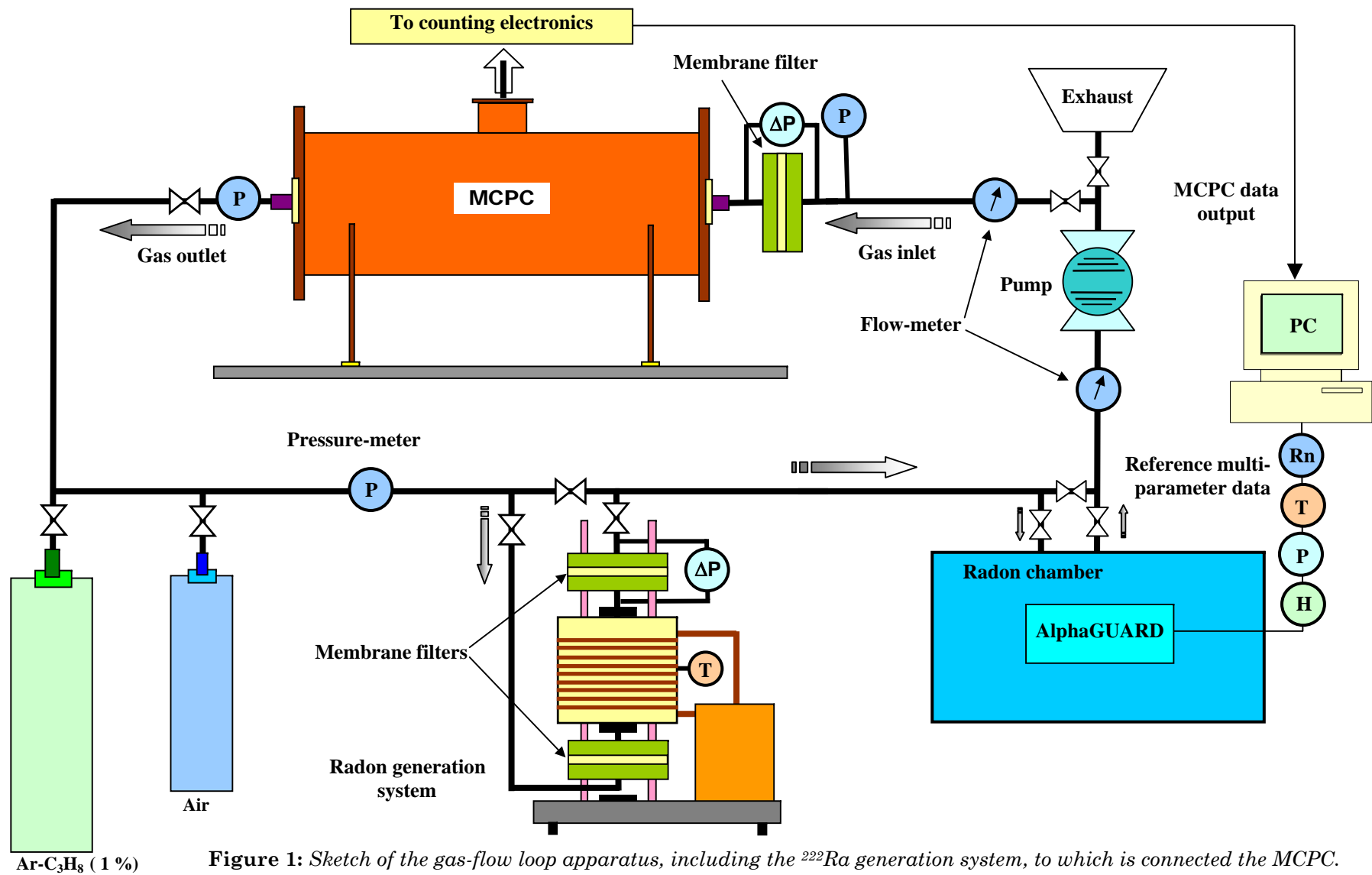


Figure 1: Sketch of the gas-flow loop apparatus, including the ²²²Ra generation system, to which is connected the MCPC.

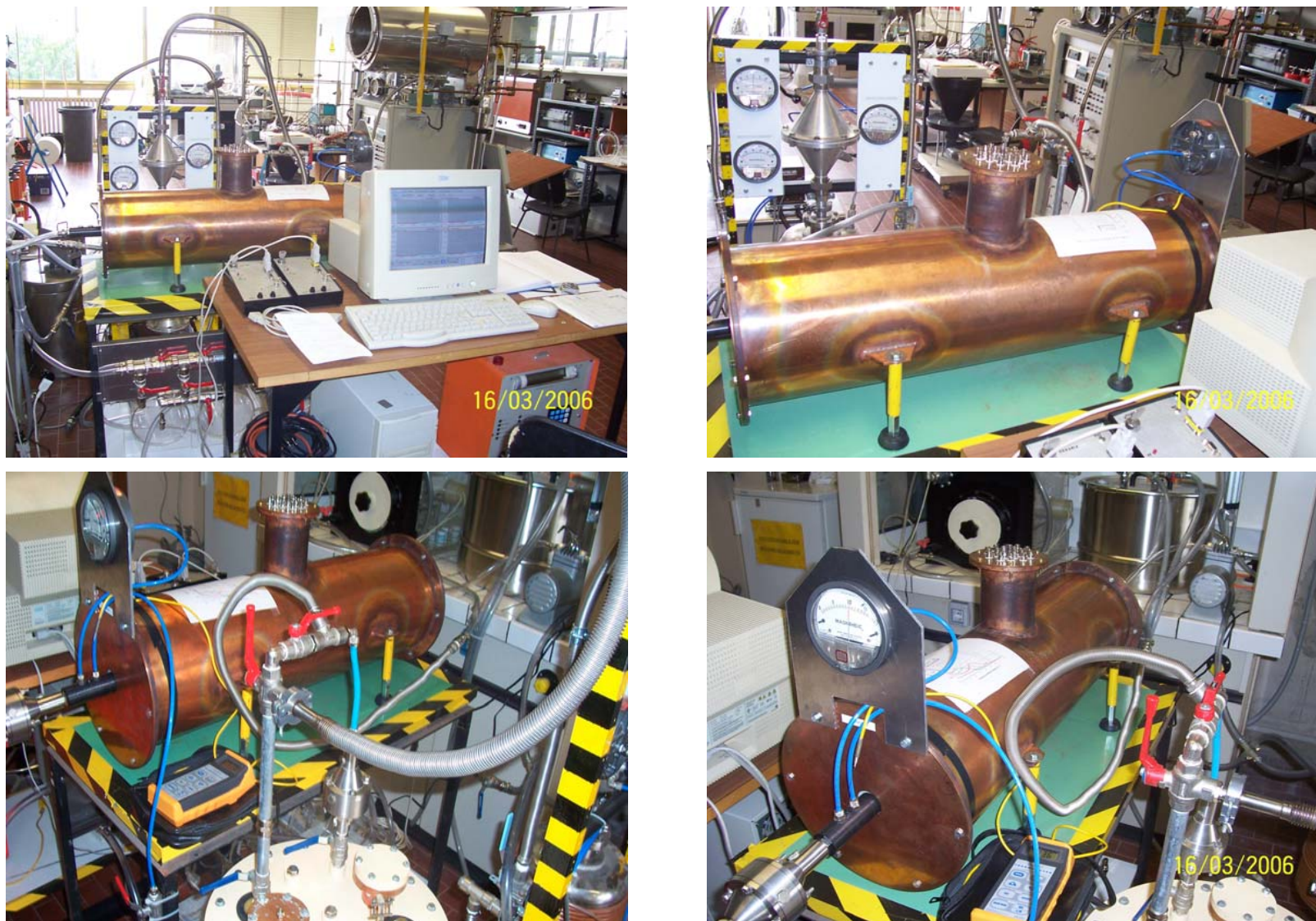


Figure 2: Some photographs of MCPC connected within the radon calibration loop manifold.

2.2. Associated electronics and data acquisition procedure

The electrical signals delivered by the MCPC are processed by an electronic chain shown in Figure 3. Since the effective counting cells operate within quasi the same physical and electrical conditions, all the cathode grids are polarised at the same negative value of high voltage. While, the generated electrical charge (electron collection) is drawn out through the anode wires in every cell. Each cell is then connected to its own low noise charge sensitive preamplifier as can be seen in figure 2, showing the block diagram of the data acquisition instrumentation. The main roles of the preamplifiers consist firstly in providing a correct impedance adaptation between the counter and the associated electronics and to convert the collected charge within each cell into a small voltage pulse with a preliminary slight electrical amplification, and finally signal filtering, insuring thus a better signal to noise ratio.

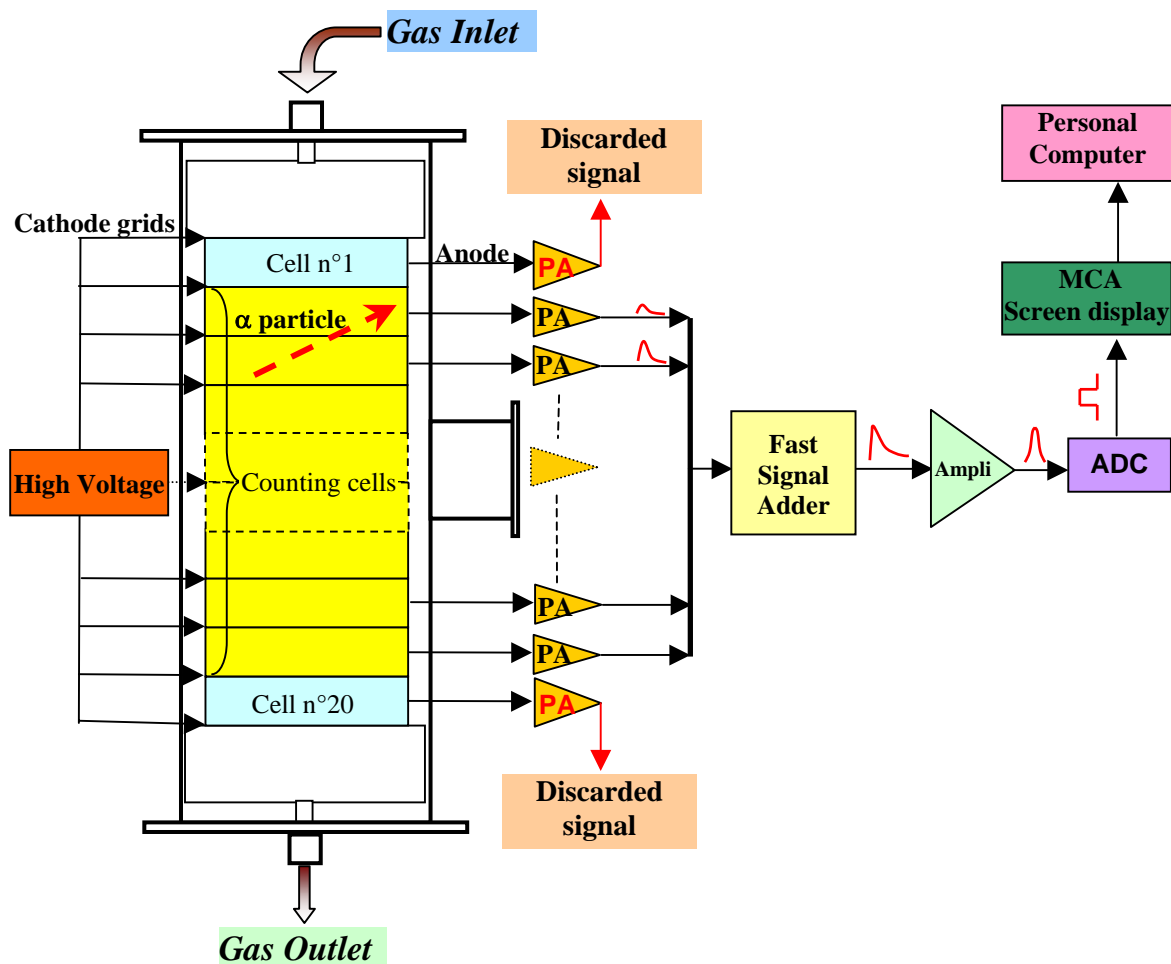


Figure 3: Block diagram of the spectrometry chain used to carry out the alpha pulse height distribution delivered by the MCPC. During the first experimental tests, only 5 effective counting cells are connected.

In order to insure a quasi identical operation condition of all the incorporated counting cells, the preamplifiers should be provided by a 0.5 – 1.5 potentiometer for fine gain adjusting. In this way, by setting the same high voltage value for each cell, eventual gas gain differences that could arise from one cell to another can be readily compensated, using the preamplifier fin gain adjusting, such that each cell should deliver an identical alpha pulse height spectrum, within the same conditions.

The charge sensitive preamplifier outputs are connected, through a fast signal adder module, to a common spectroscopy amplifier.

By this way, the voltage pulses due to the same alpha ionisation track, crossing two adjacent cells, are analogically summed, by the fast signal adder module, and the obtained pulse height remains always proportional to the useful energy expanded by the alpha particle within the sensitive volume. The amplifier output is connected to the ADC input of the MCA, where alpha pulse height spectra can be recorded periodically and saved in a personal computer. On-line data treatment allows to deduce from the recorded alpha pulse height spectra, the actual airborne activity concentration, C_{Rn} , as expressed by equation 2.

According to the simulation results, the full ranges of the alpha particles emitted by ^{222}Rn (5.489 MeV), ^{218}Po (6.002 MeV) and ^{214}Po (7.687 MeV) in the gas mixture, consisting of argon-propane (1%) with 10 % of air at a total pressure of 760 torr, are estimated to be about 44.2 ± 0.2 mm, 50.4 ± 0.2 mm and 73.4 ± 0.2 mm respectively. Therefore, in order to reduce the wall effect losses along the radial direction, the internal diameter of the cells should be at less greater than the largest alpha range: we designed the cells with 16 cm inner diameter. Since every cell is 3 cm height, to attenuate the wall effect also along the axial direction, one should pile-up at least 5 effective counting cells. Thus, to carry out preliminary experimental measurements of alpha pulse height spectra, we operate the MCPC in this minimal configuration as defined in the previous section : only 5 effective counting cells are incorporated.

3. Results and discussion

We show in figure 2 experimental alpha pulse height spectra recorded with the MCPC operated in the defined minimal configuration, when setting 3.0 kV and 3.3 kV high voltage values. The radioactive equilibrium within the counter is assumed to be well established: it is achieved after at least 240 min of continuous gas flushing, as was estimated by RADON-MCPC code.

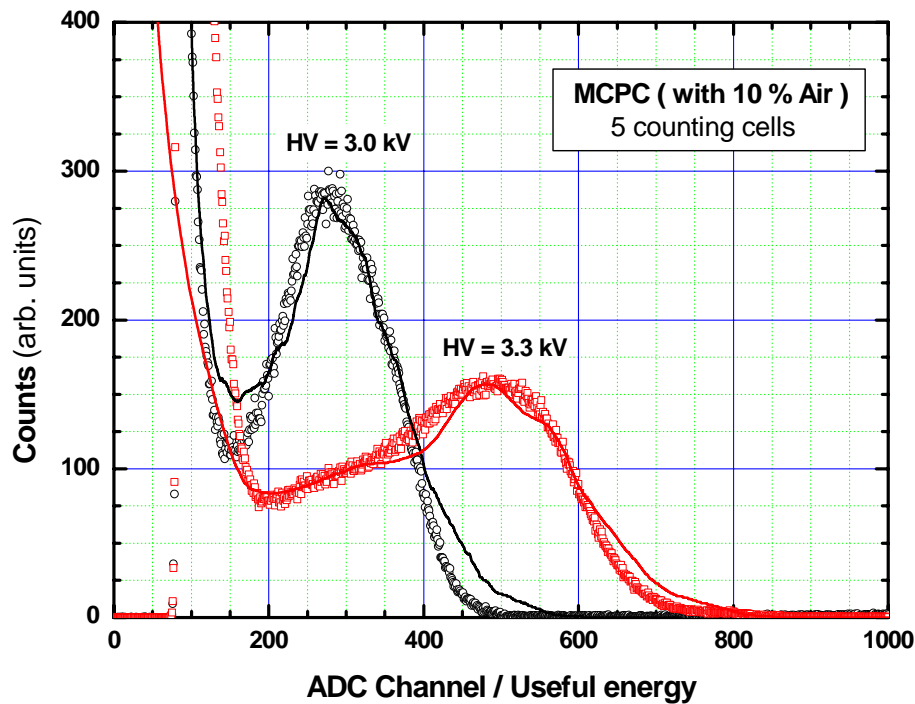


Figure 4: Experimental (symbols) and simulated (solid line) α pulse height spectra from the MCPC with 5 counting cells using an air fraction of 10%. The radon activity concentration was maintained at 1.1 kBq/m^3 , radon and its decay products were assumed in radioactive equilibrium within the MCPC. Increasing the high voltage value results in the broadening of the main alpha peak along with a marked flatness of the alpha spectrum features.

The radon activity concentration was maintained at a level of 1100 Bq/m^3 ($\pm 10 \text{ Bq/m}^3$) within the counter. The negative high voltage was applied on the cathode grids and using the semi-microscopic gas gain formula along with the previously obtained experimental data, the averaged gas gain values were estimated to be 26 (± 1) and 53 (± 2) for 3 kV and 3.3 kV high voltage values respectively. One can note a rapid evolution of the gas gain resulting in an important broadening of the common alpha peak along with a marked flatness of the whole spectrum features when the high voltage is increased by only 300 V .

Despite of the complexity of the mechanisms involved in the counter operation, we note that the simulated and the experimental alpha pulse height spectra are in a very good agreement. Indeed, the simulation program can not only predict the general shape of the spectrum but also gives a good estimation of the main spectrum parameters, such as the peak location, thus, the relative peak shift (due to electron

attachment) and the location of the spectrum valley, where one should fix the suitable value of discriminator threshold for performing integral alpha counting. However, we can notice an important intrinsic background due not only to natural radiation (such as cosmic rays) but probably inherent to the build-up of the long-lived decay products (especially ^{210}Po) on the inner walls of the MCPC. Another possible contribution to this background effect could be also assigned to the fact that polonium nuclides are produced by the decay of radon which has got into the counter volume by back diffusion from the material of the MCPC components, such as polyethylene, as pointed out by Busch *et al.* [10]. In any case, this problem requires further studies which are still in course. This excessive background could be ignored by setting the discriminator threshold close to the spectrum valley: in this case, however, the radon sensitivity decreases. Nevertheless, above an energy threshold of 250 keV the radon counting efficiency is estimated to be about 179%. Such efficiency can be achieved since there are three successive detectable α per ^{222}Rn decay event inside the MCPC.

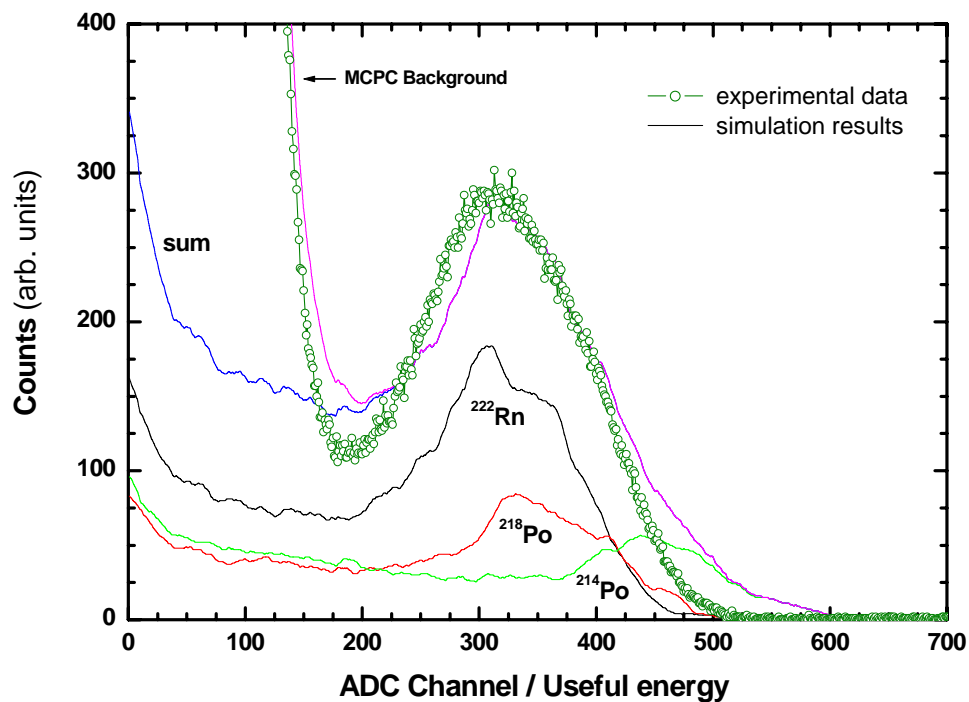


Figure 5: Illustration of the contribution to total alpha pulse height spectrum of the MCPC background and the alpha particles emitted by ^{222}Rn , ^{218}Po and ^{214}Po in radioactive equilibrium, as delivered by the MCPC (10 % air) in the minimal configuration (5 effective counting cells).

The alpha particles emitted by the grids-deposited ^{218}Po and ^{214}Po have a lower detection probability, almost half of the homogeneously distributed ^{222}Rn : this fact can be seen in figure 5, showing the separated alpha pulse height spectra as obtained through simulation, when comparing the total areas of the \square spectra from ^{222}Rn , ^{218}Po and ^{214}Po respectively, when prevailing the radioactive equilibrium. The simulated final spectrum is obtained by adding the three separated \square spectra due to ^{222}Rn , ^{218}Po and ^{214}Po with an assumed $1/E$ background. On the other hand, for ^{222}Rn , ^{218}Po and ^{214}Po \square spectra, the increase in the counting rate below approximately channel 50 (0.5 MeV) is due to several energy loss and/or electron capture mechanisms such as the Wall Effect Loss (WEL), the Attachment Effect Loss (AEL) and to the Grid Opacity Effect Loss (GOEL). The GOEL is due to the use of special grids characterized by a geometrical non-transparency for alpha particles due to the mesh pattern : however, the count loss ratio due to this effect is low compared to the WEL. Moreover, the GOEL and the AEL are compensated by counting the alpha particles generated within the two end cells and which penetrate through the grid back within the adjacent counting cell volume (End Cell Contribution, ECC). The end cells alpha pulse signals were discarded in order to define precisely the effective sensitive volume, avoiding those regions where the electric field is somewhat perturbed (see fig. 6, cells n°1 and n°20). Using RADON-MCPC code, we calculated the suitable value of the energy-equivalent pulse discriminator that allows to balance between AEL and GOEL on one hand, and the total counting excess due to ECC on the other hand. As an example, the optimum energy-equivalent discriminator is found to be $E_D \approx 80$ keV, as shown graphically in figure 6, which illustrates the dependence of AEL, GOEL and ECC on the energy-equivalent discriminator, when the MCPC constituted by 18 effective counting cells is polarized with a high voltage of 3.5 kV and uses argon-propane (1%) with 10 % of air. The compensation balance is thus verified for $E_D \approx 80$ keV, such that we have :

$$AEL + GOEL = ECC \approx 3.52\% \quad (3)$$

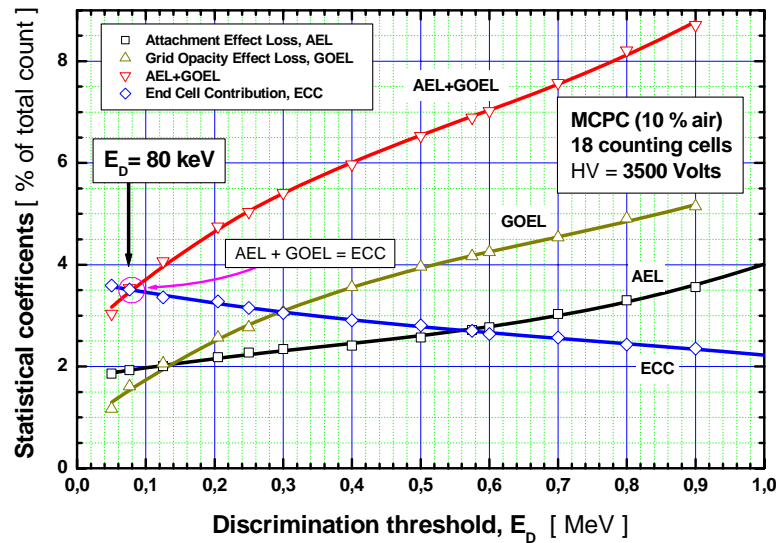


Figure 6: Evolution of the statistical coefficients (in % of the total count) with the energy equivalent discrimination threshold E_D during integral counting, when the MCPC (10 % air) operates in its full configuration (18 effective counting cells). The optimum value of the energy-equivalent discriminator threshold is found to be around 80 keV.

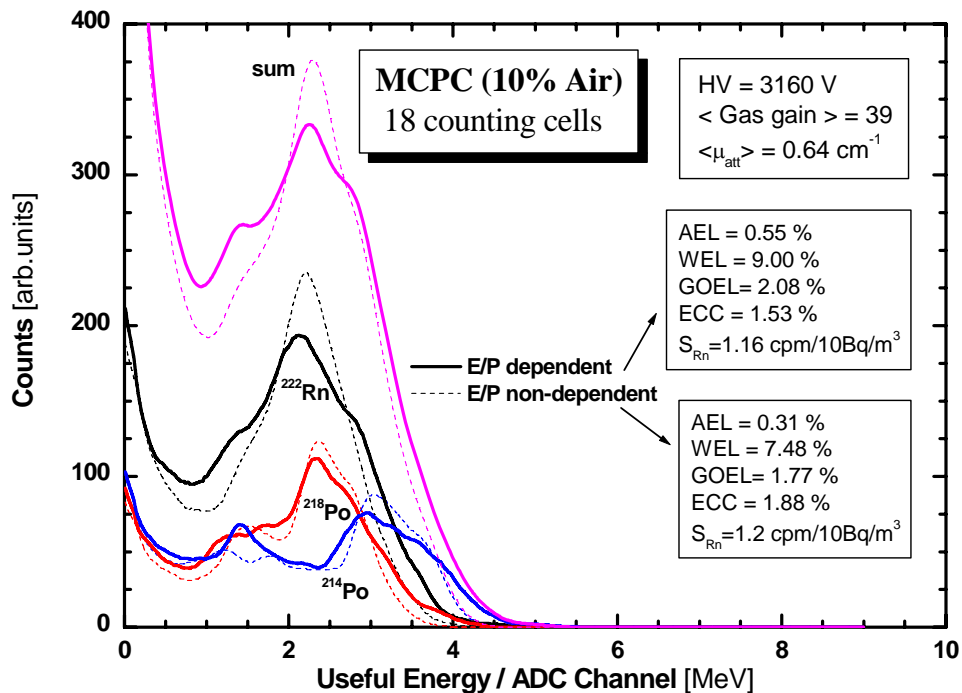


Figure 7: Study of the effect of the electric field to pressure ratio (E/P) dependence of the electron attachment coefficient upon the alpha pulse spectra delivered by the MCPC.

The effect of the particular dependence of the attachment coefficient on the electric field to pressure ratio, E/P , within the whole electron drift space and the avalanche region, is also studied with RADON-MCPC code. We show in figure 7 two computed alpha pulse height spectra simulated in the same counter conditions, assuming an electron attachment coefficient depending on E/P (solid lines) and constant (dashed lines), respectively. The constant value of the electron attachment coefficient in the latter case is chosen to have the same value of mean electron attachment coefficient in both cases. Since the computed values of the radon sensitivity in both cases differ by less than 4 % and the main alpha peak remains practically at the same energy position, it is possible to conclude that the particular analytical E/P dependence of the electron attachment coefficient has a negligible effect on the general shape of the α spectrum and the MCPC computed characteristics.

Finally, we shall underline that the important fact which leads us to use the proportional counter operation mode, where the electric pulse development is based on electron collection rather than on ion collection, as is the case in radon ionization chambers for example [17,18], is justified by the scope to design the MCPC providing a very large dynamic range (about 7 decades) of radon concentration measurement, namely from 15 Bq/m³ up to about $2 \cdot 10^8$ Bq/m³ with a fixed constant time delay of 10 minutes over the whole measurement range.

4. Comparison with other gas-filled measuring devices

In order to get an idea about the originality of the present contribution, it would be worthy to compare the MCPC expected and measured performances with those of previously reported laboratory prototypes and/or commercialized models of other gas-filled devices specifically devoted to continuous airborne radon activity concentration. Let's first recall briefly some of the most important devices.

4.1. Brief review of some developed airborne radon monitors

4.1.1. *The ATMOS (Gammadata MattekNIK) Radon gas monitor*

The ATMOS (Gammadata MattekNIK) radon gas monitor for indoor measurement is a pulse-counting ionization chamber with atmospheric air as filling gas [17]. It is constructed for the main purpose of measuring the radon concentration in air through its alpha activity. The problem with slow pulses due to the long collection times of the ions has been resolved with a combination of a specially designed electrode structure and pulse-shaping electronics optimized for highest energy resolution and count rate.

An energy resolution of 0.25 MeV FWHM has been achieved for the peaks associated with the alpha decay of radon and its daughters. This makes it possible e.g. to observe thoron (^{220}Rn) in the presence of radon (^{222}Rn). The instrument is portable and has a sensitivity of 1 cpm for a radon activity concentration of 50 Bq/m³. and covers a dynamical range extending from about 0.4 Bq/m³ up to 4.10⁴ Bq/m³.

4.1.2. *The PTB multiwire pulse ionization chamber MWPIC*

Since on-line determination of low and medium radon activity concentrations within the range from 1 to 10³ Bq/m is not possible with the detectors available so far, a large-volume multiwire pulse ionization chamber with an optimized electrode structure has been developed at the German PTB [18]. The position of the parallel electrode wires follows the shape of two archimedean spirals lying one inside the other. This ensures optimization of the electric field distribution, resulting in an improvement in the energy resolution. The laboratory prototype can therefore separate the events of the radon decay from those of its short-lived progenies, especially from ^{218}Po . This is achieved by α -spectrometry in air based on ionic collection of current pulses, under atmospheric pressure, without counting gas. Devices for continuous measurement of radon activity concentrations have to be of the on-line type (to resolve variations induced by the change of environmental parameters: temperature, humidity, pressure), and they must be operational in air under normal conditions. This means that α -spectrometry has to be performed in air under normal pressure. It is, therefore, not possible to use entrance windows, gas amplification or any kind of counting gas. Furthermore, electron collection (because electrons are captured by electronegative gases, e.g. oxygen) or small detector sizes (on-line low- and medium-activity concentration measurement is required) cannot be used. Since the electrons are captured by electronegative gases, only ions are suitable for being collected in pulses for the purpose of spectrometry. The solution is a multiwire pulse ionization chamber. The gas amplification is one, since the chamber must be run in a spectrometry mode. The energy of the α -particle is determined by the number of ions produced during its passage through air. The ions are collected by the multiwire array which is on a high electric potential. This results in a small current pulse. Due to ion collection, the pulse is quite long, of low amplitude of about 1 fA in 30 ms. These qualifications, are fulfilled by a radon monitor named Atmos. The active volume of this device is 0.6 l, resulting in a radon sensitivity of 3.57 cpm / 100 Bq/m³.

4.1.3 The Genitron Instruments GmbH AlphaGUARD radon monitor

It is a commercially model, widely used in applications involving continuous measurement of airborne radon activity concentration. Its principle is based on the use of an incorporated 0.56 l ionization chamber coupled to a specifically designed signal analysis board, built around Motorola 8-bit digital microcontroller chip, which performs subsequent digitalization and quantification of the chamber output signal. The AlphaGUARD radon monitor has a radon sensitivity of 4.5 cpm / 100 Bq/m³ within a measurement range extending from 2 up 2.10⁶ Bq/m³ [19].

4.1.4. The DurrIDGE RAD7 radon monitor

The commercialised instrument RAD7 has an internal sample cell of a 0.7 l hemisphere, with a solid state ion-implanted planar silicon alpha detector at the center. The inside of the hemisphere is coated with an electrical conductor which is charged to a potential of 2–5 kV relative to the detector, so that positively charged progeny decayed from ²²²Rn are driven by the electric field towards the detector. When a progeny atom reaches the detector and subsequently decays and emits an alpha particle, the alpha particle has a 50% probability of being detected by the detector. As a result, an electrical signal is generated with the strength being proportional to the alpha energy. RAD7 will then amplify and sort the signals according to their energies [20]. The ²²²Rn sensitivity is 6.75 cpm/100 Bq m⁻³, and measures the EPA action level of 148 Bq/m³ within 60 minutes with a deviation standard of 10 %. Its measurement range extends from 4 up 4.10⁵ Bq/m³.

4.2. Comparison of the MCPC performances to those of other devices

We have summarized in Table 1 some performances expected for the MCPC (10% air) compared to those of some devices devoted to on-line airborne radon activity concentration measurement. First of all, we can note the extremely rapid response time of the MCPC, since the signal development is based on the collection of electrons only. Except RAD7 device, based on a planar silicon detector, the remaining devices presented in table 1 are gas-filled detectors. Since all of these operate in the ionization chamber mode, both electrons and ions are collected to provide the measurable electrical signal. The MCPC, such as AlphaGUARD, being designed only for alpha counting do not allow spectrometry feature, whereas this feature is provided by MWPIC and RAD7 devices. The MCPC presents a very good radon sensitivity, over a widest dynamical range extending over 7 decades. However, the German MWPIC

TABLE 1 : Comparison of the MCPC prototype performances with those of commercially available devices devoted to on-line airborne radon activity concentration measurement: AlphaGUARD (Genitron Inc.), RAD7 (DurrIDGE Inc.) and those of laboratory developed prototypes : MWPIC(PTB, GmbH); ATMOS (Gammadata MattekNIK, Sweden)

Parameter	AlphaGUARD (Genitron)	RAD7 (DurrIDGE)	MWPIC (PTB, GmbH)	ATMOS (Gammadata MattekNIK)	MCPC (10% Air)
Effective sensitive volume (litre)	0.56	0.7	5	0.6	10.8
Air fraction in the sensitive volume	100 %	100 %	100 %	100 %	10 %
Air volume (litre)	0.56	0.7	5	0.6	1.08
Sensitive medium (material)	Pure air	Planar Silicon detector	Pure air	Pure air	Ar-propane (1%) (10% Air-mixed)
Nature of collected charges	ions and electrons (?)	Positive Radon decay products	ions only	ions only	electrons only
Signal time response	0.666 ms	0.222 ms	60 ms	75 ms	3 μ s
Radon sensitivity (cpm/100 Bq m ⁻³)	4.5	6.75	100	2.0	11.6
Maximum measurable activity	2.10 ⁶ Bq/m ³	4.10 ⁵ Bq/m ³	10 ³ Bq/m ³	4.10 ⁴ Bq/m ³	1.5 10 ⁸ Bq/m ³
Lower detectable activity (Bq/m ³)	2	4	1	0.4	15
Dynamical range length (decades)	6	6	3	5	7
Allows spectrometry feature	No	Yes	Yes	Yes	No
Time required for measuring a 150 Bq/m ³ radon level with 10 % s.d.	14.8 minutes	60 minutes	40 seconds	34 minutes	6 minutes

model is about 10 times more sensitive than the MCPC, but within a narrow dynamic range extending only over 3 decades. Therefore, we conclude that the MCPC can be most useful to carry out continuous radon activity concentration measurements, even at very high levels, enabling to reveal the occurrence of local very sharp and temporally narrow radon anomalies that could be correlated to geodynamic processes, such as in earthquakes prediction applications [21]. Indeed, a need of such instruments is felt to carry out experimental studies within the field of geology and seismicity, for example, to identify anomalous radon concentrations due to geodynamic processes by elimination of radon variations caused by other factors [22]. The use of the active method herein exposed, makes therefore possible to resolve very weak and sharp radon variations above any radon activity concentration level in the 7 decades dynamic range extending from 15 Bq/m³ up to 1.5 10⁵ kBq/m³. Other MCPC performances studies compared to those of commercially available specimens, are also reported [23], and the full radon calibration of the complete system, now in course, will be presented sooner [24].

5. Conclusion

A new proportional counter, called Multiple Cell Proportional Counter (MCPC), intended for continuous airborne radon activity concentration measurements, is constructed and its operation principle presented. By adopting this multiple cell pile-up design, it is possible to compensate for the electron attachment effect loss.

The radon sensitivity, the alpha counting efficiency, the operating high voltage value and the suitable pulse height discriminator threshold are therefore determined as a function of the air sample fraction in the gas mixture. Qualitative and quantitative analyses of the wall effect, the grid opacity effect, the electron attachment effect, the gas amplification mechanism were also carried out. The simulation results show that the admixture of 10 % of ambient air is sufficient to continuously assess radon concentration levels ranging from about 15 Bq/m³ up to 1.5 10⁵ kBq/m³ for an integral counting period of 10 minutes, when setting the energy discrimination at 250 keV. The expected radon sensitivity is about 11.6 cpm/100 Bq/m³. This configuration therefore allows further correlation studies of radon concentration variations related to inherent environmental, climatic and/or geological parameters variations.

Finally, the simulated alpha pulse height spectra are found in a very good agreement with those recorded experimentally when using the constructed MCPC in

minimal configuration, integrating only 5 effective counting cells. Subsequent experimental tests, such as the radon calibration of the complete system, and further development are foreseen as a future work.



References:

- [1] EPA Report 402-R-03-003, June 2003 (<http://www.unscear.org>).
- [2] H. Baysson, M. Tirmarche, G. Tymen, F. Ducloy, D. Laurier; “*Risk of lung cancer and Indoor Radon exposure in France*”, Proceedings of the 11th IRPA International Congress, Madrid, Spain, 23-28 May 2004.
- [3] S. Darby *et al.*, Biomed. J. **330** (2005) 223.
- [4] A.C. George, “*An overview of instrumentation for measuring environmental Radon and Radon progeny*”, IEEE Trans. on Nucl. Sci., Vol.37, n°2, (1990) 892-901.
- [5] G. Curzio, D. Mazed, R. Ciolini, A. Del Gratta, A. Gentili, “*Effect of air on gas amplification characteristics in argon-propane (1 %)-based proportional counters for airborne radon monitoring*”, Nucl. Instr. and Meth., **A 537** (2005) 672-682.
- [6] L. Zikovsky, “*Determination of radon-222 in gases by alpha counting of its decay products deposited on the inside walls of a proportional counter*”, Rad. Meas., **24** (1995) 315-317
- [7] A. Klett, W. Reuter, L. De Mey, “*Dynamical calibration of an aerosol monitor with natural and artificial alpha-emitters*”, IEEE Nucl. Symp., **2** (1996) 875-876.
- [8] W.R. Russ, D.O. Stuenkel, J.D. Valentine, K.C. Gross, “*Improved radon detection techniques for use with fluid-based concentration*”, IEEE Trans. on Nucl. Sci., **47** (2000) 908-913.
- [9] G. Heusser, W. Rau, B. Freudiger, M. Laubenstein, M. Balata and T. Kirsten, “*²²²Rn detection at the $\mu\text{Bq}/\text{m}^3$ range in nitrogen gas and a new Rn purification technique for liquid nitrogen*”, Appl. Rad. And Isot., **52** (2000) 691-695.
- [10] I. Busch, H. Greupner, U. Keyser, “*Absolute measurement of the activity of ²²²Rn using a proportional counter*”, Nucl. Instr. and Meth. A **481** (2002) 330-338.
- [11] G. Zuzel, *Highly sensitive measurements of ²²²Rn diffusion and emanation*, in AIP Conference Proceedings, **785** (2005) 142-149

-
- [12] D. Mazed, G. Curzio, R. Ciolini, “*Monte Carlo simulation of a new air-mixed gas-flow proportional counter for on-line airborne radon activity measurements*”, Proceedings of the 4th European Conference on Protection Against Radon at Home and at Work, June 28-July 2, 2004, Prague, Czech Republic [Ed. Czech Technical University in Prague, ISBN/ISSN:80-01-03009-1].
- [13] D. Mazed, R. Ciolini, G. Curzio, “*Monte Carlo Simulation and Modelling of a Radon Multiple Cell Proportional Counter (MCPC)*”, submitted for publication to *Radiation Measurements*.
- [14] D. Mazed, G. Curzio, R. Ciolini, “*Conception Optimisée par Simulation Monte Carlo d’un Compteur Proportionnel Multiélément Destiné à la Mesure du Radon dans l’Air*”, Communication presented at the SFRP National Radiation Protection Congress, Nantes (France) 14-16 June 2005.
- [15] D. Mazed, R. Ciolini, G. Curzio, “*Realizzazione di un Contatore Proporzionale Multicellulare per Misure in Continuo di Radon nell’Aria Ambiente*”, Communication presented at the AIRP XXXIII National Radiation Protection Congress, Torino, (Italy) 20-23 September 2006, ISBN 88-88648-05-4.
- [16] D. Mazed, M. Baaliouamer, “*A Semi-Microscopic Derivation of Gas Gain Formula for Proportional Counters*”, Nucl. Instr. and Meth., **A 437** (1999) 381-392.
- [17] P. Baltzer, K. G. Görsten, A. Bäcklin, “*A pulse-counting ionization chamber for measuring the radon concentration in air*”, Nucl. Instr. and Meth., **A 317** (1992) 357-364.
- [18] S. Rottger, A. Paul, A. Honig, U. Keyser, “*On-line low- and medium-level measurements of the radon activity concentration*”, Nucl. Instr. and Meth. **A 466** (2001) 475-481.
- [19] AlphaGUARD Radon meter PQ2000 user manual, see also web page :
<http://www.genitron.de/products/slides/alphaslide01.html>
- [20] DurrIDGE Company Inc., RAD7 Manual, V 6.0.1, 2000.
- [21] R.G.M. Crockett, G.K. Gillmore, P.S. Phillips, A.R. Denman, C.J. Groves-Kirkby; “*Radon anomalies preceding earthquakes which occurred in the UK, in summer and autumn 2002*”, Sci. of the Tot. Env., **364**(2006)138-148.
- [22] M. Finkelstein, S. Brenner, L. Eppelbaum and E. Ne’eman; “*Identification of anomalous radon concentrations due to geodynamic processes by elimination of Rn variations caused by other factors*”, Geophys. J. Int. , **133**(1998)407-412.

-
- [23] D. Mazed, R. Ciolini, G. Curzio, A. Del Gratta; “*A new active method for continuous radon measurements based on a multiple cell proportional counter*”, accepted for publication in Nucl. Instr. and Meth., (Review process in course)
- [24] D. Mazed, R. Ciolini, G. Curzio, A. Del Gratta; “*Mise au point d’une nouvelle méthode de mesure en continu du radon dans l’air ambiant*”, communication accepted for presentation at the National Radiation Protection Congress to be organized by the French Society of Radiation Protection (SFRP) 19-21 June 2007, at Reims (France).



CONCLUDING SUMMARY

From a health viewpoint, ^{222}Rn is the most important radon isotope since its decay products, especially ^{218}Po and ^{214}Po , can get a so pronounced adverse effect on lung tissues, leading to lung cancer in many cases as reported recently by many epidemiologists. Radon is thus a very inescapable radiation exposure source both at home and at work. Consequently, to prevent from its incidental accumulation in human living and working areas, several detection systems and various measurement methods aiming for an accurate assessment of radon activity concentration in the ambient air, were developed in the past. In particular, continuous measurements methods (active methods) are of a fundamental relevance for the study of the time variation of radon activity concentration and related equilibrium factors, especially when correlation studies with varying environmental parameters are dealt.

Up to now, the active methods so far developed for airborne radon monitoring and based on the use of air-filled gaseous detector, are based on specially designed ionization chambers having a sensitive volume ranges from 0.5 l up to 13 litres or more. The electrical signal development is founded essentially on ionic charges collection, since the electrons realeazed within the sensitive volume are almost captured by oxygen molecules. Therefore the electron attachment effect is responsible of the observed systematic limitations. To enable the device with a spectrometry feature (separation of the alpha energy peaks) and to resolve sharp radon variations, one has to narrow drastically the dynamic range of the instrument. Extending the measurement dynamic range, does not allow to individuates such radon pulses even if they were very strong.

In the present work, we propose a new active method, based on the use of a specially designed multiple cell proportional counter which enables to resolve such strong radon pulses above mean radon levels extending within a 7 decades dynamic range.

The design study of such an instrument is initiated with experimental investigations of the effect of air in gas-filled detectors.

First of all, we reported in this thesis about an experimental study of the influence of the air fraction admixed to a counting gas in a specially designed gas-flow proportional counter intended for a new continuous measurement method of airborne radon activity concentration. That study has also permitted to show the feasibility of a new continuous measurement method as will be expounded. A preliminary design study of a so-called Multiple Cell Proportional Counter (MCPC) prototype are then fully described. The device is designed to use an argon-propane (1%) gas mixture to which should be admixed an appropriate fraction of ambient air, whose radon activity concentration has to be measured. In order to perform a consistent optimization of the measuring device performances, a Monte Carlo simulation program, baptized RADON-MCPC, has been written. The program takes into account all the electrical and geometrical parameters and models rather in a simple way the main physical processes that determine directly the detector performances. Using RADON-MCPC code, the main design parameters of the MCPC prototype were thus studied and optimized in order to achieve the highest possible alpha detection efficiency and a detection limit of about 15 Bq/m³ or less.

Therefore, a new proportional counter, called Multiple Cell Proportional Counter (MCPC), intended for continuous airborne radon activity concentration measurements is constructed and its operation principle presented. An appropriate fraction of ambient air is admixed to the counting gas mixture: its radon activity concentration is continuously measured through a periodic counting of the α particles emitted by ²²²Rn and its short-lived decay products within the well defined sensitive volume of the counter. By adopting this multiple cell pile-up design, it is possible to compensate for the electron attachment effect loss.

RADON-MCPC code has been used for improving the design optimization purposes. The radon sensitivity, the alpha counting efficiency, the operating high voltage value and the suitable pulse height discriminator threshold are therefore determined as a function of the air sample fraction in the gas mixture. Qualitative and quantitative

analyses of the wall effect, the grid opacity effect, the electron attachment effect, the gas amplification mechanism were also carried out. The simulation results show that the admixture of 10 % of ambient air is sufficient to continuously assess radon concentration levels ranging from about 15 Bq/m³ up to 1.5 10⁵ kBq/m³ for an integral counting period of 10 minutes, when setting the energy discrimination at 250 keV. The expected radon sensitivity is about 11.6 cpm / 100 Bq·m⁻³. This configuration therefore allows further correlation studies of radon concentration variations related to inherent environmental, climatic and/or geological parameters variations.

Finally, the simulated alpha pulse height spectra are found in a very good agreement with those recorded experimentally when using the constructed MCPC in minimal configuration, integrating only 5 effective counting cells.

Using the written simulation code, MCPC-RADON, it is possible to find out other more advantageous MCPC configurations, improving the time autonomy, regarding the necessity to reduce counting gas consuming, and thus, the economical cost of the method. Working always towards this insight subsequent experimental tests are still in course.



A P P E N D I X - A

The **RADON-MCPC source file** (containing 49 pages) is available on request from the author; just ask for.

The author's e-mail address is : d.mazed@ing.unipi.it

❧❧❧❧

A P P E N D I X - B

RADON – MCPC

Structure of input data file

1.000e-01	fr3 : air fraction in the mixture
7.6e+02	P : total pressure in torr
2.98e+02	T : temperature in K
1.000e+02	co : airborne radon activity concentration (Bq/m ³)
1.5e+01	rpa :relative amplitude (%) of the gaussian-shaped airborne radon pulse
1.70	gam1 : 1st radon ramp (increment) to stationnary value ratio
4.30	gam2 : 2nd radon ramp (increment) to stationnary value ratio
6.90	gam3 : 3rd radon ramp (increment) to stationnary value ratio
18.0	gam4 : 4th radon ramp (increment) to stationnary value ratio
11.0	gam5 : 5th radon ramp (increment) to stationnary value ratio
8.10	gam6 : 6th radon ramp (increment) to stationnary value ratio
-8.1	gam7 : 7th radon ramp (increment) to stationnary value ratio
-11.0	gam8 : 8th radon ramp (increment) to stationnary value ratio
-18.0	gam9 : 9th radon ramp (increment) to stationnary value ratio
-6.90	gam10 : 10th radon ramp (increment) to stationnary value ratio
-4.30	gam11 : 11th radon ramp (increment) to stationnary value ratio
-1.70	gam12 : 12th radon ramp (increment) to stationnary value ratio
3.0e+01	rpd :time duration (in min) of the gaussian-shaped airborne radon pulse
452	ip1 : time of the 1st radon increment in minutes
454	ip2 : time of the 2nd radon increment in minutes
456	ip3 : time of the 3rd radon increment in minutes
459	ip4 : time of the 4th radon increment in minutes
461	ip5 : time of the 5th radon increment in minutes
464	ip6 : time of the 6th radon increment in minutes
470	ip7 : time of the 7th radon increment in minutes
473	ip8 : time of the 8th radon increment in minutes
475	ip9 : time of the 9th radon increment in minutes
478	ip10 : time of the 10th radon increment in minutes
480	ip11: time of the 11th radon increment in minutes
482	ip12: time of the 12th radon increment in minutes
440	440 ii0 : start time of measurement (spectrum acquisition & counting)in minutes
10	io : time duration of the measurement (acquisition & counting) in minutes
1.0e+01	q : gas flow rate in liters/min
8.000e+00	rmaxin : internal radius of cell element in cm
20	ncelt : total number of incorporated element cells
18	necc : total number of operating (counting) cell elements
3.0000e+00	Hcel : height of the element cells in cm
5.0000e+01	ranode : anode radius in microns
2.000e+00	pad : anode pad in a cell in cm

100000	IMAX : number of stories (alpha particles from radon alone)
4.000e+03	HV,anode high voltage in volts
1.00e-01	eb : energy equivalent of the basic total electronic noise in MeV
1.0e+00	bcr : the background count rate in count per min (cpm) [assufor Ed = 0.250 MeV]
1.2000e+04	epch (1.537) : the MCA conversion gain in electrons per channel
1800	ntchn : the total channel number
3.08943e+05	edisc : the electron equivalent discrimination bias (threshold level for alpha counting)
0.8140e0	cgsp : probability of an alpha particle to pass through the grid array material
1.0e+00	TFano : Total fano fitting factor
0.00e-00	ggnu : The gas gain non-uniformity factor
1.00e+00	Fatt : Electron attachment fitting factor
1.00e+00	Fion : Ionization coefficient fitting factor
0.00e-00	Defg : Random default in the wire GAP uniformity
0.00e-00	Defh : Random default in the cell height HCEL uniformity



A P P E N D I X - C

RADON – MCPC

Structure of output data file

La frazione di ARIA = 1.000000E-01
La pressione del gas in torr = 760.000000
La temperatura in gradi KELVIN = 298.000000
La concentrazione di attivita di Rn222 (in Bq/m3) : 100.000000
La portata Q del flusso di aspirazione del gas (l/min): 10.000000
La durata della misura (in minuti) : 10
Il raggio del contatore proporzionale MCPC (in cm) : 8.000000
Il numero totale degli elementi (NCELT) del MCPC : 20
Il numero degli elementi MCPC operativi (NECC) : 18
Hcel,l'altezza di ogni elemento (in cm) : 3.000000
Il raggio dell'anodo (in micron) : 5.000000E-03
Lo spazio tra i fili anodi (in cm) : 2.000000
IMAX,il numero delle storie per solo ARGO = 250000
Il valore dell'Alta Tensione, HV = 4000.000000
Il guadagno medio nel gas GasGain = 40.095730
Electron attachment medio = 6.012651E-01 1/cm
Il valore del fattore di fano totale : 1.000000
Wg (/1 paio di cariche) della miscela (eV): 26.660020
RMS del rumore elettronico= 5632 elettroni
Valore corrispondente a = 15 canali
energia eb = 1.501914E-01 MeV
Il fattore di conversione MeV/channel = 9.979001E-03
Il numero totale canali del MCA = 901
La soglia di discriminazione (Mev) = 2.528014E-01

***** I PARAMETRI DI CALCOLO *****

R (cm) = 8.000000
H (cm) = 60.000000
N. Cells = 20
C. Cells = 18
Hcel = 3.000000
Anode gap = 2.000000
fr. ARGO = 8.910000E-01
fr. PROPANO = 9.000000E-03
fr. ARIA = 1.000000E-01
W del gas(eV) = 26.660020
Portata (l/min) = 10.000000
C0 (Bq/m3) = 100.000000
t0(inizio, min) = 440
n. Storie = 750000
n. Rn222 = 250000
n. Po218 = 250000
n. Po214 = 250000

I R I S U L T A T I

Numero totale delle particelle alfa emesse = 750000
N. part. alfa assorbite nel gas :
* Rn222 = 212265 * Po218 = 106003 * Po214 = 104042
N. part. alfa fermate dalle pareti non contate :
* Rn222 = 28654 * Po218 = 16305 * Po214 = 19266
N. part.alfa fermate dalla griglia non contate :

A P P E N D I X - D

□ List of publications (Articles)

Published papers and/or still in course (review process)

- 1° - G. Curzio, D. Mazed, R. Ciolini, A. Del Gratta, A. Gentili, "*Effect of air on Gas Amplification Characteristics in Argon-Propane(1%) -based proportional counters*", a publication in "*Nuclear Instruments and Methods in Physics Research, Section A*", NIM A537 (2005) 672-682, edited by ELSEVIER Science, North-Holland.
- 2° - Dahmane Mazed, « *Experimental Gas Amplification Study in Boron-lined Proportional Counters for Thermal Neutron Detection* », published in "*Radiation Measurements*", ELSEVIER , North-Holland. (in press, already available on-line).
- 3° - D. Mazed, R. Ciolini, G. Curzio, "*Monte Carlo Simulation and Modelling of a Radon Multiple Cell Proportional Counter (MCPC)*", submitted for publication to *Radiation Measurements*. (review process in course).
- 4° - D. Mazed, R. Ciolini, G. Curzio, A. Del Gratta, "A new active method for continuous radon concentration measurements based in a Multiple Cell Proportional Counter (MCPC)", submitted for publication to *Nuclear Instruments and Methods in Physics Research*,(review process in course NIMA-D-06-00783).

□ List of presented communications

Communications presented (published in proceedings) :

- 1° - D. Mazed, R. Ciolini "*Gas gain in air-mixed argon-propane (1%)-based proportional counters*", Communication presented at the 11th International Congress of the IRPA, Madrid, 23-28th May 2004
- 2° - D. Mazed, G. Curzio, R. Ciolini, "*Monte Carlo simulation of a new air-mixed gas-flow proportional counter for on-line airborne radon activity measurements*", Proceedings of the 4th European Conference on Protection Against Radon at Home and at Work, June 28-July 2, 2004, Prague, Czech Republic [Ed.Czech Technical University in Prague,ISBN/ISSN:80-01-03009-1]

- 3° - D. Mazed, G. Curzio, R. Ciolini "*Conception Optimisée par Simulation Monte Carlo d'un Compteur proportionnel Multiélément Destiné à la mesure du radon dans l'Air*", Communication presented at the SFRP'2005 Radiation Protection National Congress, Nantes (France), 14-16 June 2005.
- 4° - D. Mazed, R. Ciolini, G. Curzio "*Design and Monte Carlo Simulation of a Multiple Cell Proportional Counter (MCPC) for Continuous Airborne ²²²Rn Activity Measurements*", Communication presented at the second European IRPA Congress on Radiation Protection, 15-19 May 2006, Paris, France.
- 5° - D. Mazed, R. Ciolini, G. Curzio, "*Realizzazione di un Contatore Proporzionale Multicellulare per Misure in Continuo di Radon nell'Aria Ambiente*", Communication presented at the AIRP XXXIII National Radiation Protection Congress, Torino, (Italy) 20-23 September 2006, ISBN 88-88648-05-4.
- 6° - D. Mazed, G. Curzio, R. Ciolini, A. Del Gratta, "*Mise au point d'une nouvelle méthode active pour la mesure en continu du radon dans l'air ambient*", communication accepted for oral presentation at the SFRP National Congress of Radiation Protection, at Reims (France), 19-21 June 2007.



A Multiple Cell Proportional Counter for Continuous Airborne Radon Assessment



Table of Content

INTRODUCTION	5
References	8
Section I : The NORM/TENORM Problem and Radon Assessment	10
1. Introduction	10
2. About the NORM-TENORM problem	11
3. Activities that lead to the technological enhancement of NORM	11
4. Analysis of Pathways Associated with NORM	12
5. The regulatory and normative policies in radiation protection	13
6. Radon Concentration Measurement	13
6.1. A short history of Radon	13
6.2. Radon and its progeny	14
6.3. Special quantities and units	14
6.3.1. Potential alpha energy	14
6.3.2. Concentration in air	15
6.3.3 The equilibrium equivalent concentration in air	15
6.3.4 The equilibrium factor F	15
6.3.5 Inhalation exposure of individuals (The Working level month)	16
7. Radon gas measurement methods	17
7.1. Activated Charcoal Adsorption	17
7.2. Alpha Track Detection (filtered)	17
7.3. Unfiltered Track Detection	17
7.4. Charcoal Liquid Scintillation	18
7.5. Continuous Radon Monitoring	18
7.6 Electret Ion Chamber: Long-Term	18
7.7. Electret Ion Chamber: Short-Term	19
7.8. Grab Radon/Activated Charcoal	19

7.9. Grab Radon/Pump-Collapsible Bag	19
7.10. Grab Radon/Scintillation Cell	19
7.11. Three-Day Integrating Evacuated Scintillation Cell	20
7.12. Pump-Collapsible Bag (1-day)	20
8. Radon decay products measurement techniques	20
8.1 Continuous Working Level Monitoring	20
8.2 Grab Working Level	20
8.3 Radon Progeny (Decay Product) Integrating Sampling Unit	21
9. Conclusion and the special orientation of our contribution	21
References	22
Section II : The use of gas-filled detectors for radon activity concentration measurement	24
1. Introduction	24
2. Application to airborne radon monitoring	25
3. The use of gas-filled detectors for radon measurement in air	27
4. The electron attachment effect in air-mixed counting gases	29
5. The gas amplification compensation	29
6. Experimental set-up and procedure	32
7. Experimental results and discussion	35
8. Applicability for radon measurements and achievable sensitivity	40
9. Conclusions	41
References	42
Section III : Design and construction of the Multiple Cell Proportional Counter (MCPC)	45
1. Introduction	45
2. Design criteria and description of the MCPC	47
2.1. General Features	47
2.2. The designed MCPC	51
2.3. The operation principle of the MCPC	52
3. The MCPC characteristics and parameters definition	54
3.1. Alpha counting efficiency	54
3.2. Radon counting efficiency	54
3.3. The minimum detectable activity concentration of radon	54

3.4. Radon sensitivity	55
3.5. The wall effect loss, <i>WEL</i>	55
3.6. The attachment effect loss, <i>AEL</i>	55
3.7. The grid opacity effect loss, <i>GOEL</i>	56
3.8. The end cell contribution, <i>ECC</i>	56
3.9. The spectrometric and counting quality factors	56
4. The Monte Carlo simulation code RADON-MCPC	57
5. Design optimization and performance requirements	58
5.1 Maximum air fraction allowed	58
5.2 Cell inner radius selection	60
5.3 Selection of the number of effective counting cells, NECC	62
6. Operating high voltage	62
7. Selection of the optimum discrimination level	67
8. Selection of the suitable gas flow rate	67
9. Response to a short duration varying radon pulse	69
10. Conclusion	70
References	71
Section IV : The Monte Carlo Simulation code RADON-MCPC	73
1. Simulation of gas-filled detectors	73
2. Description of the Monte Carlo simulation code RADON-MCPC	75
3. The ^{222}Rn and progenies activity evolution inside the counter	77
3.1. The radioactive equilibrium inside the counter	79
3.2. Response to a stepwise variation of radon activity concentration	81
3.3. Response to a Gaussian-shaped radon pulse transient	83
4. The derivation of the electric field distribution	84
5. Random alpha particles emission and the stopping process	89
6. Modeling of the wall effect and the grid opacity effect	95
7. The electron attachment effect and gas amplification mechanism	97
7.1 The electron attachment coefficient distribution	98
7.2 The gas amplification mechanism	101
8. The alpha pulse height spectra	103
9. Convergence study of the code	107
10. Conclusion	108

References	109
Section V : Simulation results and experimental tests the MCPC prototype	111
1. Introduction	111
2. Experimental setup and measurement procedures	111
2.1. Counter calibration procedure	111
2.2. Associated electronics and data acquisition procedure	115
3. Results and discussion	116
4. Comparison with other gas-filled measuring devices	121
4.1. Brief review of some developed airborne radon monitors	121
4.1.1. The ATMOS (Gammadata Metteknik) Radon gas monitor	121
4.1.2. The PTB MultiWire Pulse Ionization Chamber (MWPIC)	122
4.1.3. The Genitron Instruments GmbH AlphaGUARD radon monitor	123
4.1.4. The DurrIDGE Inc. RAD7 radon monitor	123
4.2. Comparison of the MCPC performances to those of other devices	123
5. Conclusion	125
References	126
CONCLUDING SUMMARY	129
Appendix – A : RADON-MCPC , source file (ultimate version)	132
Appendix – B : RADON-MCPC , structure of input data file	181
Appendix – C : RADON-MCPC , structure of output data file	183
Appendix – D : List of Publications and communications	185

